

# **LOCALISATION OF PARTIAL DISCHARGE SOURCE IN OIL INSULATION USING ACOUSTIC EMISSION TECHNIQUE: NON-ITERATIVE METHOD, NEWTON'S METHOD AND GENETIC ALGORITHM**

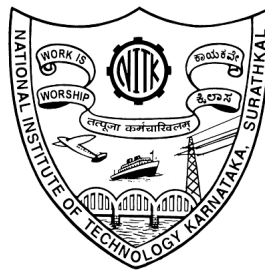
Thesis

Submitted in partial fulfillment of the requirements for the degree of

DOCTOR OF PHILOSOPHY

by

DEEPTHI ANTONY



DEPARTMENT OF ELECTRICAL & ELECTRONICS ENGINEERING

NATIONAL INSTITUTE OF TECHNOLOGY KARNATAKA

SURATHKAL, MANGALORE - 575025

DECEMBER, 2018

## **DECLARATION**

*By the Ph.D. Research Scholar*

I hereby *declare* that the Research Thesis entitled **LOCALISATION OF PARTIAL DISCHARGE SOURCE IN OIL INSULATION USING ACOUSTIC EMISSION TECHNIQUE: NON-ITERATIVE METHOD, NEWTON'S METHOD AND GENETIC ALGORITHM** which is being submitted to the **National Institute of Technology Karnataka, Surathkal** in partial fulfillment of the requirements for the award of the Degree of **Doctor of Philosophy** in **Electrical and Electronics Engineering** is a *bonafide report of the research work carried out by me*. The material contained in this Research Thesis has not been submitted to any University or Institution for the award of any degree.

Deepthi Antony

Reg. No.: 148025 EE14F06

Department of Electrical and Electronics Engineering

Place: NITK, Surathkal.

Date:

## **CERTIFICATE**

This is to *certify* that the Research Thesis entitled **LOCALISATION OF PARTIAL DISCHARGE SOURCE IN OIL INSULATION USING ACOUSTIC EMISSION TECHNIQUE: NON-ITERATIVE METHOD, NEWTON'S METHOD AND GENETIC ALGORITHM** submitted by **Deepthi Antony**, (Reg. No.: 148025 EE14F06) as the record of the research work carried out by her, is *accepted as the Research Thesis submission* in partial fulfillment of the requirements for the award of degree of **Doctor of Philosophy**.

(Dr. G. S. Punekar)

Research Supervisor

Chairman - DRPC

# ACKNOWLEDGEMENT

First and foremost, I would like to thank God Almighty for his blessings, giving me the opportunity, knowledge and strength to undertake this research study and to persevere and complete it satisfactorily.

I offer my sincere gratitude to my research supervisor Dr. Gururaj S. Punekar, who brilliantly guided me throughout, patiently sharing his knowledge and experience whilst providing me enough room for pursuing the work independently. His timely advices and assistance ensured that my work progressed on schedule. I am profoundly indebted to him for giving invaluable life lessons as a teacher and mentor.

A special word of gratitude to Dr. Venkatesa Perumal, Head of the Department, Department of Electrical and Electronics Engineering for his administrative support and his invaluable advice as my RPAC member . My heartfelt thanks to Dr. Basavaraj Talwar (Dept. of CS), RPAC member, for his encouragement and useful guidance.

I express my sincere thanks to Mr. Naik, Foreman, and to the supporting staff of Electrical Machines Lab, EED, for their cooperation during the project work. I am particularly grateful for the assistance given by all teaching and non-teaching faculty of EE department, NITK.

I thank all my fellow research scholars at NITK for their friendship, motivation and support. I am immensely thankful to my friend Mr. Harimurugan for his help, discussions, and useful suggestions. I wish to thank my friend Ms. Biji for being so understanding and standing by me throughout this entire journey. I also thank Ms. Aiswarya, Ms. Soumya, Ms. Remya and Ms. Manju for their love and support.

Nobody has been more important to me in the pursuit of this research work than the members of my family. I am deeply indebted to my parents, whose love, care and words of encouragement kept my spirits high throughout. I wish to thank my loving and supportive sister Mrs. Deepa Jebin and my brother-in-law Mr. Jebin Jacob for being so understanding and standing by me throughout this entire journey. I also express my love and thanks to my niece Jianna Jacob, for being my constant source of smile and happiness. I thank my whole family for providing me with unfailing support and continuous encouragement throughout the entire tenure of study and researching.

**Deepthi Antony**

# ABSTRACT

The power transformers are a vital component of power systems. The condition assessment of transformers is of utmost importance to ensure the reliable operation of the power system. The partial discharges (PD) originating from defects in operating transformers should be detected as early as possible. In large power apparatus like transformers, locating the source of PD is as important as identifying it. The PD source localisation helps in risk assessment and in planning of maintenance activities.

The acoustic emission (AE) technique is one of the on-line non-destructive testing (NDT) techniques for PD source localisation in power transformers. The PD source is located by solving a system of non-linear sphere equations obtained by modeling the acoustic emission partial discharge (AEPD) location system mathematically. The algorithms that have been developed to solve the mathematical model of AEPD location system need to be improved due to the various limitations. Hence, the current research proposal aims to address this existing research gap by suggesting new algorithms/modifications in the existing algorithms. Further, the factors which affect the accuracy of PD source localisation will be studied and analysed.

According to IEEE standard C.57.127-2007, there are two AEPD location systems: (i) all-acoustic system; and (ii) combined acoustic-electrical system. When AE technique is used for PD source localisation in power transformers, the error in PD localisation can occur mainly due to two reasons: (i) the inefficacy of the algorithm used for solving the mathematical model; and (ii) the error in measurement of acoustic signal arrival time from the PD source to various sensors.

For an all-acoustic system, a hybrid method combining the advantages of both the iterative and random search algorithms is developed to solve the mathematical model of AEPD location system. The existing non-iterative algorithm is modified/extended so that it works for cases with zero time-differences. The PD localisation experiments in an all-acoustic system are conducted in the diagnostic laboratory of Central Power Research Institute (CPRI), Bangalore. The proposed algorithms are verified using data from laboratory experiments.

For the combined acoustic-electrical PD-locator-system, a non-iterative algorithm is devised for the first time. The effect of the sensor positioning on the performance of the method is studied, and some guidelines for the sensor placement on the transformer's tank wall are suggested. The efficacy of the proposed algorithm is verified by applying to data from published literature.

The error in estimating the acoustic signal arrival time from the PD source to the multiple AE sensors results in false localisation of the PD source, irrespective of the algorithm used for the AEPD source localisation in transformers. Two mathematical methods for the identification of such erroneous time measurements are proposed: (i) using discriminant; and (ii) using Jacobian-determinant. The verification of the proposed methods are carried out by applying to published data in literature.

**Key Words**— Absolute time, Acoustic emission (AE), Acoustic emission partial discharge (AEPD), All-acoustic, Combined acoustic-electrical, Discriminant, Genetic algorithm (GA), Jacobian-determinant, Newton's method, Non-iterative method, Partial discharge (PD), Time-delay.



# Contents

Abstract . . . . .	i
List of Figures . . . . .	vii
List of Tables . . . . .	ix
List of Abbreviations . . . . .	xv
List of Symbols . . . . .	xvii
<b>1 Introduction</b>	<b>1</b>
1.1 General . . . . .	1
1.2 Literature survey . . . . .	2
1.2.1 Condition assessment of transformers . . . . .	3
1.2.2 Partial discharges . . . . .	6
1.2.3 Acoustic emission technique . . . . .	12
1.3 Motivation . . . . .	27
1.4 Objectives . . . . .	27
1.5 Organisation of the thesis . . . . .	28
<b>2 Algorithms for PD source localisation: All-acoustic system</b>	<b>31</b>
2.1 Introduction . . . . .	31
2.2 Mathematical model of an all-acoustic system . . . . .	33
2.3 Newton's method for PD source localisation . . . . .	34
2.3.1 Implementation of Newton's method . . . . .	34
2.3.2 Challenges faced when implementing Newton's method . . . . .	35
2.3.3 Proposed improvements of Newton's method for PD source localisation . . . . .	35
2.4 Non-iterative method for PD source localisation . . . . .	41
2.4.1 Implementation of non-iterative method . . . . .	41

2.4.2	Challenges faced when implementing non-iterative method . . .	47
2.4.3	Proposed improvement of non-iterative method for PD source localisation . . . . .	49
2.5	Performance verification of algorithms: numerical experiments . . . . .	56
2.5.1	Data for numerical experiments . . . . .	56
2.5.2	Procedure for numerical experiments . . . . .	56
2.5.3	Results and Discussion . . . . .	57
2.6	Verification of the algorithms: laboratory experiments . . . . .	65
2.6.1	Experimental Set-up . . . . .	65
2.6.2	Experimental Procedure . . . . .	67
2.6.3	Results and Discussion . . . . .	68
2.7	Summary . . . . .	76
<b>3</b>	<b>Algorithms for PD source localisation: Combined acoustic-electrical system</b>	<b>79</b>
3.1	Introduction . . . . .	79
3.2	Mathematical model of a combined acoustic-electrical system . . . . .	81
3.3	Proposed non-iterative PD source localisation method . . . . .	82
3.4	Performance verification of the proposed method . . . . .	84
3.4.1	Effect of the sensor positioning . . . . .	86
3.4.2	Effect of the PD source position . . . . .	88
3.5	Application of proposed method to the published data . . . . .	92
3.6	Summary . . . . .	95
<b>4</b>	<b>Effect of error in time measurement on PD source localisation</b>	<b>97</b>
4.1	Introduction . . . . .	97
4.2	Effect of error in time-delay measurement on all-acoustic system . . . . .	100
4.2.1	Numerical experiments to study the effect of error in time-delay measurement . . . . .	100
4.2.2	Proposed methods for identification of invalid time-delay-groups	105
4.2.3	Verification of the proposed methods using numerical experiments	108
4.2.4	Application of proposed method to published literature . . . . .	111



4.3	Effect of error in absolute-time measurement on combined acoustic-electrical system . . . . .	113
4.3.1	Numerical experiments to study the effect of error in absolute-time measurement . . . . .	114
4.3.2	Proposed method for identification of invalid absolute-time-groups	119
4.3.3	Verification of the proposed method using numerical experiments	120
4.3.4	Application of proposed method to published literature . . . . .	122
4.4	Summary . . . . .	125
<b>5</b>	<b>Conclusions and scope for further study</b>	<b>129</b>
5.1	Summary of the work . . . . .	129
5.1.1	Algorithms for PD localisation using all-acoustic system . . . . .	129
5.1.2	Algorithms for PD localisation using combined acoustic-electrical system . . . . .	130
5.1.3	Effect of error in time measurement on PD source localisation .	130
5.2	Important conclusions of the present study . . . . .	130
5.2.1	Conclusions from the study of algorithms used for an all-acoustic system . . . . .	130
5.2.2	Conclusions from the study of proposed non-iterative algorithm used for a combined acoustic-electrical system . . . . .	132
5.2.3	Conclusions from the study of effect of error in time measurement	133
5.3	Contributions . . . . .	133
5.4	Scope for further study . . . . .	134
	<b>References</b>	<b>135</b>
	<b>List of publications based on research work</b>	<b>A</b>
	<b>Biodata</b>	<b>C</b>



# List of Figures

1.1	Skeleton of the literature survey. . . . .	2
1.2	A block schematic depicting the literature review, showing the published literature, on related sub-areas of research. . . . .	3
1.3	Typical block schematic of acoustic detection system. . . . .	14
1.4	Typical AE burst and its parameters. . . . .	15
1.5	The block digram for (a) all-acoustic system and (b) combined acoustic-electrical system. . . . .	20
1.6	Schematic visualisation of absolute-time approach for a combined acoustic-electrical system. . . . .	21
1.7	Schematic visualisation of time-difference approach for an all-acoustic system. . . . .	22
1.8	Overview of the research work. . . . .	30
2.1	Generalised flowchart for PD source localisation in power transformers using the Newton's method. . . . .	36
2.2	Generalised flowchart for PD source localisation in power transformers using the existing non-iterative method. . . . .	47
2.3	Generalised flowchart for PD source localisation in power transformers using the proposed non-iterative method (the highlighted portion shows the proposed extension of the existing non-iterative method). . . . .	55
2.4	The distance error calculated for the estimated PD source position PD-3, for 100 trials, for Newton method and hybrid method. NaN are the errors of divergent trials, which occurred only in the case of Newton's method. . . . .	64

2.5	The oil test tank with the point-to-plane electrode arrangement to simulate the PD (all dimensions are in m). . . . .	66
2.6	Components of AE workstation at CPRI; (a) AE sensor with integrated pre-amplifier (b) AE-DSP board (c) 16-channel AE workstation (source: M/s. Physical acoustics corporation, USA. . . . .	67
2.7	The screen-shot of the event display captured from the AE workstation for the sensor arrangement $SA_1$ . The AEPD signals detected by the four sensors and the time-delay in signal reception of the sensors $S_2$ (channel 4), $S_3$ (channel 2), and $S_4$ (channel 1) with respect to the sensor $S_1$ (channel 3) are seen. . . . .	70
2.8	The screen-shot of the event display captured from the AE workstation for the sensor arrangement $SA_2$ . The AEPD signals detected by the four sensors and the time-delay in signal reception of the sensors $S_2$ (channel 3), $S_3$ (channel 4), and $S_4$ (channel 1) with respect to the sensor $S_1$ (channel 2) are seen. The time-delay ( $t_{12}$ ) between the signal reception of $S_1$ and $S_2$ is zero. . . . .	71
3.1	Generalised flowchart for PD source localisation in power transformers using the newly devised non-iterative method for the combined acoustic-electrical system. . . . .	85
3.2	The sensor layout (similar to layout suggested in IEEE Std C57.127 (2007)) used for the numerical experiment. . . . .	88
4.1	Flowchart for identification of invalid time-delay-group by using Newton's method (The highlighted portion is the proposed extension of Newton's method for the identification of invalid time-delay-group). . .	110

# List of Tables

1.1	Different techniques for condition assessment of transformer insulation	7
1.2	The acoustic wave velocity (at various temperatures) used for PD source localisation in published literature . . . . .	24
2.1	The numerical examples of sensor arrangements (Set-1 to Set-5) with the corresponding PD source locations and the initial guesses that results in a singular Jacobian matrix . . . . .	40
2.2	The generalised conditions for which the Jacobian matrix becomes singular and the suggested remedy via sensor re-positioning . . . . .	42
2.3	Conditions for which the existing non-iterative method fails to locate the PD source . . . . .	48
2.4	Coordinates of the sensors used for the numerical experiment (conforming to the guidelines given in sub-sections 2.3.3.2 and 2.4.3.5) . . . . .	56
2.5	Coordinates of the PD source used for the numerical experiment, sensor sequence based on signal arrival time, and the corresponding time-delays	57
2.6	The comparison of PD source localisation result of Newton’s method and hybrid method based on 100 trials for each PD source position . . .	58
2.7	The PD source localisation results of the diverged trials or the trials with high distance error (greater than 10%) when using Newton’s method for localising PD-1 . . . . .	59
2.8	The PD source localisation results of the diverged trials or the trials with high distance error (greater than 10%) when using Newton’s method for localising PD-2 . . . . .	60

2.9	The PD source localisation results of the diverged trials or the trials with high distance error (greater than 10%) when using Newton’s method for localising PD-3 . . . . .	61
2.10	The PD source localisation results of the diverged trials or the trials with high distance error (greater than 10%) when using Newton’s method for localising PD-4 . . . . .	62
2.11	Estimated PD source coordinates, acoustic signal arrival time, distance percentage error, and computational time: comparison of different methods for the four PD source positions . . . . .	63
2.12	Coordinates of the sensors used for the experimental studies and the sensor sequence based on signal arrival time for the sensor arrangement $SA_1$ . . . . .	69
2.13	Coordinates of the sensors used for the experimental studies and the sensor sequence based on signal arrival time for the sensor arrangement $SA_2$ . . . . .	69
2.14	Measured time-delays for the two sensor arrangements $SA_1$ and $SA_2$ . . .	69
2.15	The comparison of PD source localisation result of Newton’s method and hybrid method based on 100 trials for each sensor arrangement . . .	72
2.16	The PD source localisation results of the diverged trials or the trials with high distance error (greater than 10%) when using Newton’s method for PD source localisation with sensor arrangement $SA_1$ . . . . .	73
2.17	The PD source localisation results of the diverged trials or the trials with high distance error (greater than 10%) when using Newton’s method for PD source localisation with sensor arrangement $SA_2$ . . . . .	74
2.18	Estimated PD source coordinates, acoustic signal arrival time, distance percentage error, and computational time: comparison of the different methods for each sensor arrangement . . . . .	75
3.1	Coordinates of the sensor conferring to the layout given in IEEE Std C57.127 (2007) on the $z = 0$ plane . . . . .	88

3.2	The conditions for which the proposed non-iterative method fails to locate the PD source for the layout given in Figure 3.2 . . . . .	89
3.3	Coordinates of the sensors used for numerical experiment conforming to proposed guidelines for sensor positioning . . . . .	90
3.4	Five sample PD source positions (PD-1 to PD-5), with equal absolute signal arrival time from the PD source to any two sensors in the sensor combination, that can be located using the proposed method . . . . .	91
3.5	Absolute arrival time reported (Al-Masri <i>et al.</i> 2016a), and calculated for a known PD location (Al-Masri <i>et al.</i> 2016a) with the velocity of acoustic signal taken from IEEE Std C57.127 (2007) . . . . .	92
3.6	The initial guess used for Newton’s method and hybrid method for each group of absolute signal arrival times (AT-1 to AT-6) . . . . .	94
3.7	The PD source localization results of Newton’s method, hybrid method, and proposed non-iterative method . . . . .	95
4.1	Coordinates of the sensors used for the numerical experiment . . . . .	101
4.2	Coordinates of the PD source used for the numerical experiment, sensor sequence based on signal arrival time, and the corresponding time-delays	101
4.3	The six time-delay-groups (TD-1 to TD-6) for the PD source position PD-1 . . . . .	103
4.4	The six time-delay-groups (TD-1 to TD-6) for the PD source position PD-2 . . . . .	103
4.5	The six time-delay-groups (TD-1 to TD-6) for the PD source position PD-3 . . . . .	103
4.6	The six time-delay-groups (TD-1 to TD-6) for the PD source position PD-4 . . . . .	104
4.7	The PD source localisation results for the PD source position PD-1 with six time-delay-groups . . . . .	105
4.8	The PD source localisation results for the PD source position PD-2 with six time-delay-groups . . . . .	105

4.9	The PD source localisation results for the PD source position PD-3 with six time-delay-groups . . . . .	106
4.10	The PD source localisation results for the PD source position PD-4 with six time-delay-groups . . . . .	106
4.11	The discriminant value computed for the PD source position PD-4 with each time-delay-group . . . . .	109
4.12	Jacobian-determinants calculated for ten iterations in Newton's method for the PD source position PD-1 with each time-delay-group (TD-1 to TD-6) . . . . .	111
4.13	Jacobian-determinants calculated for ten iterations in Newton's method for the PD source position PD-2 with each time-delay-group (TD-1 to TD-6) . . . . .	112
4.14	Jacobian-determinants calculated for ten iterations in Newton's method for the PD source position PD-3 with each time-delay-group (TD-1 to TD-6) . . . . .	113
4.15	Jacobian-determinants calculated for ten iterations in Newton's method for the PD source position PD-4 with each time-delay-group (TD-1 to TD-6) . . . . .	114
4.16	(A) Five groups of time-delays given in reference Lu <i>et al.</i> (2000) (B) Discriminant value ( $m^2$ ) for each group of time-delays (C) Jacobian-determinants calculated for 10 iterations in Newton's method for each group of time-delays . . . . .	115
4.17	Percentage error in time-delay-groups TD-3 and TD-4 . . . . .	116
4.18	PD source located using different algorithms with time-delay-groups TD-3 and TD-4 . . . . .	116
4.19	Coordinates of the sensors used for numerical experiment . . . . .	116
4.20	PD source coordinates used for numerical experiment . . . . .	116
4.21	The six absolute-time-groups (AT-1 to AT-6) for the PD source position PD-1 . . . . .	118



4.22	The six absolute-time-groups (AT-1 to AT-6) for the PD source position PD-2 . . . . .	118
4.23	The six absolute-time-groups (AT-1 to AT-6) for the PD source position PD-3 . . . . .	119
4.24	The PD source localisation results for the PD source position PD-1 with six absolute-time-groups . . . . .	120
4.25	The PD source localisation results for the PD source position PD-2 with six absolute-time-groups . . . . .	121
4.26	The PD source localisation results for the PD source position PD-3 with six absolute-time-groups . . . . .	121
4.27	Discriminant value computed for the PD source position with all the absolute-time-groups . . . . .	122
4.28	Absolute signal arrival time given in Phung <i>et al.</i> (2001) with the corresponding discriminant value computed and PD source coordinates estimated for each absolute-time group . . . . .	124



# List of Abbreviations

AE	Acoustic Emission
AEPD	Acoustic Emission Partial Discharge
CBM	Condition Based Maintenance
CPRI	Central Power Research Institute
DGA	Dissolved Gas Analysis
DSP	Digital Signal Processing
DWT	Discrete Wavelet Transform
FFT	Fast Fourier Transform
GA	Genetic Algorithm
GPS	Global Positioning System
HV	High Voltage
NaN	Not a Number
OLTC	On Load Tap Changer
PD	Partial Discharge
PSO	Particle Swarm Optimisation
TDOA	Time Difference of Arrival
TOA	Time of Arrival
UHF	Ultra High Frequency



# List of Symbols

$x$	x-coordinate of the PD source
$y$	y-coordinate of the PD source
$z$	z-coordinate of the PD source
$S_n$	$n^{th}$ AE sensor
$x_n$	x-coordinate of the $n^{th}$ AE sensor
$y_n$	y-coordinate of the $n^{th}$ AE sensor
$z_n$	z-coordinate of the $n^{th}$ AE sensor
$T_n$	Acoustic signal arrival time from PD source to the $n^{th}$ sensor
$t_{1n}$	Time-delay in acoustic signal detection of $n^{th}$ sensor with respect to the nearest sensor
$v$	Acoustic wave velocity in transformer oil
$\sigma_1$ to $\sigma_{22}$	Intermediate constants used in estimating PD source location, for an all-acoustic system, when none of the time-delays are zero
$\alpha_1$ to $\alpha_{17}$	Intermediate constants used in estimating PD source location, for an all-acoustic system, when all the time-delays are zero
$\beta_1$ to $\beta_{18}$	Intermediate constants used in estimating PD source location, for an all-acoustic system, when two of the time-delays are zero
$\gamma_1$ to $\gamma_{19}$	Intermediate constants used in estimating PD source location, for an all-acoustic system, when one of the time-delay is zero
$k_1$ to $k_{16}$	Intermediate constants used in estimating PD source location for a combined acoustic-electrical system



# Chapter 1

## Introduction

### 1.1 General

Transformers are one of the most expensive equipment in the power network. There is an increasing focus on maintenance and life extension of existing transformers to maximise the return on investment. The integrity of a power transformer depends upon the condition of its major components. The main components of a transformer are the insulation system, winding, core, main tank, and cooling system (at times on load tap changer (OLTC)) (Han and Song 2003). The normal operation of these components ensure the health of the transformer. The objective of any maintenance program should be to prevent unplanned outages and to extend the life of the transformer. Traditionally, time-based maintenance was used to examine and repair the machine off-line at regular intervals of time. The disadvantage of this kind of maintenance is that many unnecessary shutdowns and unexpected accidents can still occur in the intervals. Hence, there is a trend in the industry to move from traditional time-based maintenance to condition-based maintenance (CBM). In CBM, the maintenance is carried out if the condition of the equipment requires it (Wang *et al.* 2002).

The CBM will be an optimal maintenance service under the help of a condition monitoring system to provide correct and useful information of the machine condition. The important functions of the transformer are monitored to detect developing faults. This helps in preventing a catastrophic failure. The condition monitoring can be defined as a process of monitoring the operating characteristics of a machine in such a way that, the changes and trends of the monitored characteristics can be used to pre-

dict the need for maintenance before serious deterioration or breakdown occurs. The condition monitoring has the potential to reduce operating costs, enhance the reliability of operation, and provide improved service to customers. It is important to define the terms ‘monitoring and diagnostics’. The ‘monitoring’ implies the on-line collection of data and it includes sensor development, measurement techniques for on-line application, and data acquisition. The ‘diagnostics’ contains all interpretation of data, as well as sophisticated off-line measurements (Bengtsson 1996). The access to relevant data can be obtained using monitoring equipment, but one should also have well developed methods for interpreting this data. It is important to interpret the data to make reliable recommendations. Hence, the diagnostics capabilities must be developed along with monitoring technologies. The monitoring and diagnostics together constitute transformer ‘condition assessment’.

## 1.2 Literature survey

An attempt has been made to survey the literature available in the area of condition assessment of transformers. Skeleton of the literature survey is as presented in Figure 1.1. The different sub-areas which are of importance, in the present research, are highlighted in Figure 1.1. A block schematic depicting the literature review, showing the prominent published literature, on related sub-areas of research, are given in Figure 1.2.

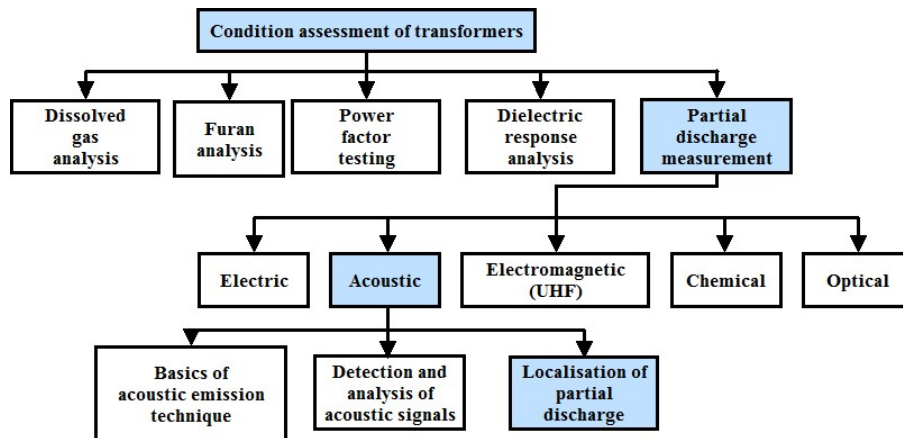


Figure 1.1 Skeleton of the literature survey.



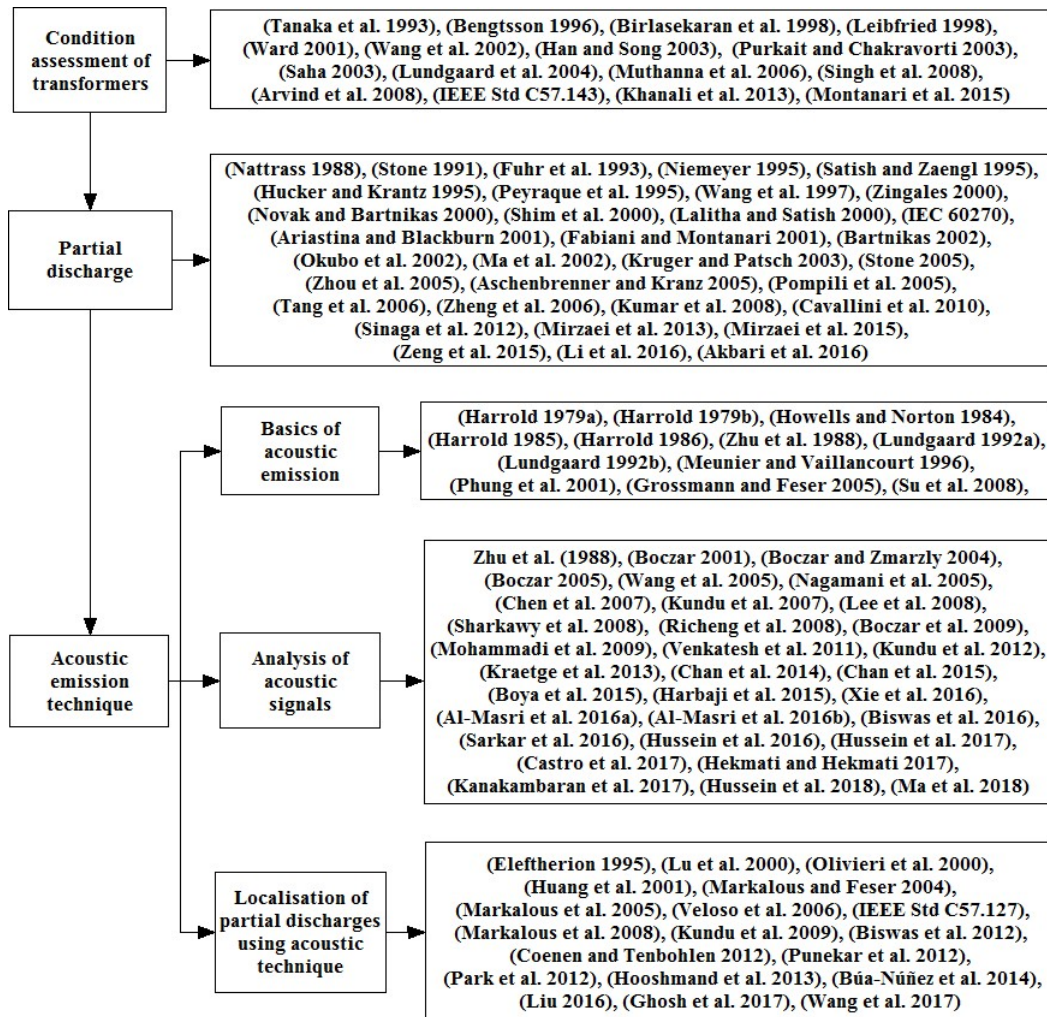


Figure 1.2 A block schematic depicting the literature review, showing the published literature, on related sub-areas of research.

### 1.2.1 Condition assessment of transformers

The operating reliability of transformers mainly depends on their insulation status. According to statistics, insulation faults accounted for 80% of the total transformer faults. Therefore, it is necessary to carry out condition monitoring which can reflect the insulation status of transformers, timely. The major indicators of the insulation problems in transformers are temperature, gas-in-oil, partial discharge (PD), and moisture (Han and Song 2003). Tanaka *et al.* (1993) suggests that the ageing processes are due to tree formation, PDs, electro-chemical processes, and thermo-chemical processes.

An extensive review on different techniques for transformer condition assessment

are available in published literature. Some of the prominent literature that explains the different aspects of transformer condition assessment are as follows.

Leibfried (1998) reviews the different on-line monitors used for in-service transformers. The R&D work in the field of transformer condition assessment and the readily available commercial instrumentation based on electrical, chemical, and mechanical methods are presented in Birlasekaran *et al.* (1998). Saha (2003) describes analysis and interpretation of techniques like polarisation/depolarisation current measurement, return voltage measurement, and frequency domain dielectric spectroscopy at low frequencies for transformer insulation condition assessment. Purkait and Chakravorti (2003) applies the concept of fractal geometry to analyse the properties of fault currents in transformers. The pattern of the fault currents in a transformer depends on the type of fault and its location along the length of the winding. Lundgaard *et al.* (2004) studies in detail, the effects of moisture, oxygen, and acidity upon the aging of Kraft and thermally upgraded papers. In Muthanna *et al.* (2006), the consumed life of insulation is assessed using the hourly load and ambient temperatures obtained through condition monitoring. The estimated load factors and ambient temperatures are then given as input to the IEEE life consumption models. Different methodologies adopted for on-line monitoring of power transformers are reviewed in Arvind *et al.* (2008). The changes that occur in transformer insulation properties when voltages with steep fronts and high-frequency contents are applied is studied in Khanali *et al.* (2013). Montanari *et al.* (2015) presents the on-line monitoring of high voltage (HV) power transformers using techniques such as PD analysis, dissolved gas analysis (DGA), and capacitance and loss tangent measurements. Singh *et al.* (2008) lists relevant references grouped according to the various sub-topics in condition monitoring of power transformers. A brief description on the various techniques for power transformer condition assessment, taken from the literature listed in Figure 1.2, are given in the following sub-sections.

#### **1.2.1.1 Dissolved gas analysis**

The abnormal electrical or thermal stresses leads to breakdown of insulating oils to liberate small quantities of gases. The regular monitoring of dissolved gases can provide useful information about the condition of the transformer and prior information of the

faults. The DGA test commonly evaluate the concentration of hydrogen ( $H_2$ ), methane ( $CH_4$ ), ethane ( $C_2H_6$ ), acetylene ( $C_2H_2$ ), ethylene ( $C_2H_4$ ), carbon monoxide ( $CO$ ), carbon dioxide ( $CO_2$ ), nitrogen ( $N_2$ ), and oxygen ( $O_2$ ) (Wang *et al.* 2002). For off-line DGA, the gases are extracted from oil samples taken manually at regular intervals, every one or two years, depending on the importance of the transformer (Bengtsson 1996). The periodic sampling and testing in the laboratory have been successful in diagnosing incipient faults. However, there are many problems associated with off-line DGA test. The on-line gas analysis offers the potential for doing a much more revealing assessment of the dynamic conditions inside transformers, than possible through laboratory DGA (Ward 2001). The infrared based analysers such as Fourier transform infrared spectroscopy and photo acoustic spectroscopy cannot measure the gases (hydrogen, oxygen, and nitrogen) on-line. The multi-gas on-line DGA monitors based on gas chromatography can detect all key gases. These are designed to provide sufficient dissolved gas data ensuring that analysis and interpretation of faults could take place on-line (IEEE Std C57.143 2012). IEEE Std C57.104 (2009) gives the guidelines for the interpretation of gases generated in oil-immersed transformers.

#### **1.2.1.2 Furan analysis**

The Furan analysis is a diagnostic tool to evaluate the health of transformer paper insulation. Furans are generated only when insulation paper degrades due to ageing of cellulose materials as a result of thermal stress. These compounds, which are dissolved in oil, can be detected using standard analytical method. The degree of polymerisation and concentration of furanic compounds are interrelated which helps in indirect measurement of the degree of ageing of the cellulose (Bengtsson 1996). The degree of polymerisation estimated from Furan analysis gives an average value. There will be areas in transformer paper insulation where degradation is more severe. This is because, the paper does not age uniformly (Wang *et al.* 2002).

#### **1.2.1.3 Power factor testing**

Power factor testing of transformer insulation helps in identifying weakness which develops in bushing or winding insulation. The insulation power factor is the ratio of

resistive current component to the total leakage current under an applied voltage. The condition of insulation is also assessed based on the history of change in power factor. The test requires an outage and isolation of the transformer (Wang *et al.* 2002).

#### **1.2.1.4 Dielectric response analysis**

The dielectric response methods are used to determine moisture content and ageing of the press board and paper by measuring the effects of moisture on electrical properties (Bengtsson 1996). Dielectric response measurements analyse the response of the dielectric system across multiple frequencies. The mathematical property that the current is proportional to the capacitance is the basis for dielectric response measurements. The three important techniques for measuring the various dielectric response parameters are: (a) recovery voltage measurement; (b) dielectric spectroscopy in time domain, i.e., measurement of polarisation and depolarisation currents; and (c) dielectric spectroscopy in frequency domain, i.e., measurement of electric capacitance and loss factor ( $\tan\delta$ ) (Ward 2001).

#### **1.2.1.5 Partial discharge measurement**

The PDs originating from defects in operating transformers can cause permanent insulation failure. The PD is a localised electric discharge that partially bridges the insulation between conductors. These are consequence of local electrical stress concentrations in the insulation (IEC 60270 2000). The two commonly used PD detection methods are using acoustic signals and electrical signals produced by the PD. The PD can also be detected indirectly using chemical techniques such as measuring the degradation products produced by the PD and also using the optical method. The acceptable PD limits for new transformers are dependent on the voltage rating and size of the transformers. It ranges from  $>100$  pC to  $<500$  pC (Wang *et al.* 2002).

Based on the above discussion, the applicability of different techniques for the condition assessment of transformer insulation are summarised in Table 1.1.

Table 1.1 Different techniques for condition assessment of transformer insulation

Sl.No	Technique	Information	On-line/Off-line
1	Dissolved gas analysis	Different fault condition	On-line and off-line
2	Furan analysis	Health of transformer paper insulation	Off-line
3	Power factor testing	Weakness in winding and bushing insulation	Off-line and on-line (Only for bushing)
4	Dielectric response analysis	Moisture content and aging of the press board and paper	Off-line
5	Partial discharge measurement	Detection of incipient faults	On-line and off-line

### 1.2.2 Partial discharges

The PDs are defined as localised electrical discharge that partially bridges the insulation between conductors and which can or cannot occur adjacent to a conductor (IEC 60270 2000). In electrical insulation, PDs are both a symptom and cause of deterioration (Stone 1991). The voids are the most likely sources of PD. The void region has a lower dielectric constant than the surrounding material. The PD occurs when the electric field in the void exceeds minimum breakdown strength (intrinsic strength) of the void. For a PD to occur, a free electron must be present within the electrically stressed volume. The electric field strength should be high enough to cause an avalanche of electrons from a single free electron. The probability of having free electrons makes the occurrence of PD unpredictable (Mohammadi *et al.* 2009).

There is an extensive study in the literature on PD phenomenon. The PD can occur in the insulation system of any electrical apparatus (generators, motors, transformers, etc.). The available literature on: (i) the PD phenomenon in general and (ii) PD detection for the condition assessment of transformer in particular, are given in the sequel.

The overview of PD patterns, their evaluation and determination of origin are pre-

sented in Nattrass (1988). Niemeyer (1995) presents a concept which merges the available physical knowledge about various PD types into a generalised model which can be applied to arbitrary insulation defects. The consequences of static electrification on the dielectric strength and the conditions of PD occurrence are studied in Peyraque *et al.* (1995). The PD pattern shapes and underlying defects causing PD have a 1:1 correspondence. Satish and Zaengl (1995) explores the methods to describe and quantify the PD pattern shapes. The 3-dimensional PD pattern surface was considered to be a fractal, and the computed fractal features were analysed and found to possess fairly reasonable pattern discriminating abilities. Hucker and Krantz (1995) investigates the quality of the PD fingerprint extraction methods. The potential of every pattern recognition in PD diagnosis is influenced predominantly by the quality of the PD fingerprint. Wang *et al.* (1997) develops a multi-band-pass digital filter based on fast fourier transform (FFT) for the purpose of suppressing continuous periodic interference in case of on-line PD monitoring. Lalitha and Satish (2000) suggests that the multi-resolution signal decomposition technique of wavelet transforms has interesting properties of capturing the embedded horizontal, vertical, and diagonal variations within an image in a separable form. This helps in identifying individual PD sources present in multi-source PD patterns. Shim *et al.* (2000) gives an overview of the digital signal processing (DSP) applied to the detection of PDs. Zingales (2000) suggests that the PD measuring system should be designed with an appropriate resolution-time. It is to be calibrated with a current pulse having a shape and duration appropriate to the PD pulse to be measured. Novak and Bartnikas (2000) examines the nature of the initiating discharge on the dielectric surface of a dielectric/metallic electrode gap employing a mathematical model. The effect of voltage distortion on ageing acceleration of insulation systems under PD activity is studied in Fabiani and Montanari (2001). In Okubo *et al.* (2002), the PD characteristics and extension of PD were discussed from the viewpoint of critical electric field of each gas or gas mixtures. Ma *et al.* (2002) proposes a method to select optimally the wavelet corresponding to the representative forms of PD pulse. Kruger and Patsch (2003) suggests that removing the high-energy spectral lines removes most of the noise. This can be carried out in real-time using the frequency domain analysis

and the DSP. Zhou *et al.* (2005) presents an improved methodology to apply the discrete wavelet transform in conjunction with an algorithms to select optimal mother wavelet and threshold values. The proposed methodology results in significant improvement in de-noising effect. Zheng *et al.* (2006) constructs an improved wavelet neural network by principle of the temporal-scaling approach. The improved wavelet neural network has better identifying ability and the PD pattern features could be automatically extracted. Cavallini *et al.* (2010) provides the details of the hardware and software tools to remove disturbance, noise, separate contributions from different sources, and eventually identify PD sources. The on-line PD measurement performed on an HVDC converter transformer and an HVDC converter bushing using wide-band PD measurement instrumentation is discussed in Jacob *et al.* (2012).

The characteristics of PDs in a cavity for both new and aged oil impregnated press board-paper samples are studied in Ariastina and Blackburn (2001). Pompili *et al.* (2005) studies the variations in the number of pulses within the pulse burst, their sequential separation in time and amplitude variation as a function of the viscosity of transformer oil. Kumar *et al.* (2008) reviews the recent techniques used for PD analysis with its advantages and suitability over conventional method for proper on-line condition monitoring of large power transformers.

A PD results in localised and nearly instantaneous release of energy. This produces a number of effects such as electromagnetic, thermal, acoustic, optic, and chemical and structural changes in the material. Hence, the methods developed to detect PD within HV transformers can be grouped into five categories. They are chemical, optical, electromagnetic, electrical, and acoustic methods. These are discussed briefly in subsequent sub-sections.

#### **1.2.2.1 Chemical method**

The two primary chemical tests employed by power companies for the detection of PD are DGA and high performance liquid chromatography (Mohammadi *et al.* 2009). Chemical testing does not provide any information about the position of the PD or the extent of the insulation damage.

### 1.2.2.2 Optical method

In visual or optical detection method, visual observations can be carried out in a darkened room, after the eyes have become adapted to the level of darkness. Binoculars of large aperture can be used as an aid, if necessary. A photographic record can also be made, but fairly long exposure times are usually necessary. For special purposes, photo-multipliers or image intensifiers are used (IEC 60270 2000). A methodology to detect the location of single as well as multiple PD sources by optical method is presented in Biswas *et al.* (2012). It has been found that the intensity of optical signal corresponds with the amplitudes of PD and with the discharge energy. The optical detection is not widely used as it is invasive. It is difficult to implement optical method in HV transformers due to the opaque nature of mineral oil (Mohammadi *et al.* 2009).

### 1.2.2.3 Electromagnetic method

The PDs in oil radiate electromagnetic waves with frequencies up to the ultra high frequency (UHF) range (300 MHz – 3000 MHz) (Coenen and Tenbohlen 2012). The PD can be located in power transformers by measuring the UHF waves from a PD source (Sinaga *et al.* 2012). Zeng *et al.* (2015) have shown the use of semi-definite-relaxation method for UHF signal based PD localisation. These PD measurements are performed using a broadband antenna on an oil valve (Aschenbrenner and Kranz 2005). The source location of PDs by UHF is a very efficient technique for condition monitoring of power transformers due to its high sensitivity (Tang *et al.* 2006). In the UHF method, the difference in arrival times of electromagnetic waves to antennas in the transformer is estimated for the PD source localisation (Mirzaei *et al.* 2013). Mirzaei *et al.* (2015, 2013) describes a method of locating a PD source within a power transformer by measurement of UHF electromagnetic waves with receiving antennas in the transformer. A localisation method based on the particle swarm optimisation algorithm is used. Through the oil filling valve of the transformer, UHF probes can be inserted into the tank (and into the oil volume) of an operating transformer. In most transformer designs, the accessibility is normally limited to three sensors or less, since transformers rarely possess more than three oil valves for installation of UHF probes (Coenen and Tenbohlen 2012).



#### 1.2.2.4 Electric method

Electrical location methods are based on the analysis of the measured time resolved PD signals at the transformer terminals. The time resolved PD signals at the terminals represent the response of the transformers electrical circuit to the excitation by a PD current pulse in the nanosecond range. The shape of the PD current pulse, at the place of origin, is strongly dependent on the medium (oil, paper, gas bubble etc.). For any type of PD pulse (shape) and for any position of the PD defect in the insulating system of the transformer, there exists a specific response of the transformer electrical (RLC equivalent) circuit. The measured PD signals can be categorised into three components: capacitive component; travelling wave component; and the oscillating component. These signal components are strongly dependent on: (i) the design of the transformer; (ii) the PD defect location with respect to the terminals, where the time resolved signal is detected; and (iii) the form of the original PD current pulse (Fuhr *et al.* 1993). In Mondal *et al.* (2018), a ladder network is constructed from the terminal measurements. The simulated responses obtained from the networks for signals of known pulse width at all locations are used as reference data. Predicting the location of the PD source from the maximum correlation of the simulated reference data and test data is discussed in Mondal *et al.* (2018). Homaei *et al.* (2014) proposes a neuro-fuzzy technique that uses unsupervised pattern recognition to localise PD source in power transformers. The pulse shape, its relative phase location within AC cycle of the HV transformer, and the signal intensity gives information about the type of PD fault. It also helps in indicating the severity of the insulation damage. Multiple PD sources result in overlapped pattern. The classification of multiple PD sources, that occur simultaneously, using a logistic regression algorithm is discussed in Janani *et al.* (2017). Electrical detection method has many limitations. The primary limitation of electrical testing is its susceptibility to noise. Another problem with electrical detection is that the received pulse characteristics are highly dependent on the geometry of the HV transformer (Mohammadi *et al.* 2009).

#### 1.2.2.5 Acoustic method

Acoustic emission (AE) techniques are passive technique based on detecting the acoustic signals emitted from discharges (Lundgaard 1992a). A PD results in acoustic waves

(Lundgaard 1992*b*). The wave can be detected by a suitable sensor, the output of which can be analysed using a conventional data acquisition system. Su *et al.* (2008) proposes a waveguide atop the HV winding, in a cast-resin dry-type transformer, to improve the propagation of the PD acoustic signals occurring in winding to AE sensors. The shape of the detected signal depends on the source, the detection apparatus and the sensor. Meunier and Vaillancourt (1996) studies the propagation of acoustic signals in medium-size power transformer and a relationship was established between the apparent charge of electrical PD signals and the level of acoustic signals produced. Acoustic methods have many advantages compared to all the other methods used for PD detection. In the case of large apparatus like power transformers, the PD source localisation is as important as identifying it. Acoustic methods provide an indication of PD source location within an electrical apparatus. It can be applied in the field without disturbing transformer operation (Howells and Norton 1981). They are non-invasive and immune to electromagnetic noise. The sensitivity of this method does not vary with the test object capacitance (Lundgaard 1992*a*). The acoustic method is chosen for the present study because of its various advantages.

### **1.2.3 Acoustic emission technique**

During early eighties, Harrold (1979*a,b*, 1985, 1986) has dealt with the fundamentals of acoustics in his papers. The relationship between the acoustical parameters and corona discharge quantities were also studied. Application of acoustical techniques for detection and location of corona discharges in electrical apparatus such as rotating machines, transformers, capacitors, and specialised insulation systems have been discussed.

In early nineties, Lundgaard (1992*a,b*) has explained the practical application of the AE technique for the PD detection where the electrical methods are insensitive (as in the case of large capacitors). The major advantages of AE technique are its immunity to electromagnetic interference under field conditions and the ability to locate the PD sources within a large apparatus such as power transformers. The AE tests are sometimes not sensitive to intense discharges within the internal winding of a transformer (Olivieri *et al.* 2000). Therefore, the acoustic methods are often combined with other PD detection methods in order to increase the reliability of the final diagnosis of power

transformers (Li *et al.* 2016a; Rubio-serrano *et al.* 2012; Wang *et al.* 2006). Lundgaard (1992b) has explained the benefit of acoustic techniques and emphasises the application of acoustic technique for on-site testing.

### 1.2.3.1 Basics of acoustic emission

#### *Definitions*

Definitions of few basic standard terms used in ‘acoustic emission partial discharge (AEPD) detection’ according to IEEE Std C57.127 (2007) are as given below.

- ***Acoustic Emission***: The phenomena whereby transient elastic waves are generated by the rapid release of energy from localised sources within a material, or the transient waves so generated.
- ***Barkhausen effect and magnetostriction noise***: Noise associated with the deformation of magnetic domains in the core of a transformer.
- ***Direct acoustic (oil-borne) path***: Path of propagation from the PD acoustic signal source directly (straight line) to the sensor location on the tank wall, without obstruction such as winding, core, or major blocking/bracing.
- ***Structure-borne path***: Propagation of the PD acoustic signal through the transformer structure.

#### *Basic concepts*

Some of the basic concepts of ‘AEPD detection’ are discussed here.

- ***Acoustic wave motion***: Sound propagates through a medium by means of wave motion, i.e., the propagation of a local disturbance through the medium. For a liquid, the disturbance produces compression and rarefaction in the medium, i.e., local changes in pressure ( $P$ ) which produces local changes in density ( $\rho$ ) and displacement of molecules. Three basic equations are combined to form the general differential equation of acoustic wave motion, for an acoustic wave with a velocity ‘ $v$ ’, given in equation (1.1). These equations describe continuity, conservation of momentum, and elasticity of the medium (Lundgaard 1992a).

$$\nabla^2 P = \frac{1}{v^2} \frac{\partial^2 P}{\partial t^2} \quad (1.1)$$

- **Acoustic impedance and intensity:** The sound velocity in a liquid is determined by the elastic properties of the liquid. Various forces act on a small volume of liquid. The net sum of forces causes the particle to move with a velocity ( $v$ ). For a plane wave, the ratio between the sound pressure and the particle velocity is called the specific acoustic impedance (Lundgaard 1992b).
- **Transmission coefficient:** When an acoustic wave propagates from one medium to another which has a different density or elasticity, reflection and refraction will take place. This results in a reduction of the energy in the transmitted wave. The laws which govern these phenomena are the same as for electromagnetic radiation. The transmission coefficient ( $\alpha_{transmission}$ ) is determined by the difference in acoustic impedance for the two media (Lundgaard 1992a). In the case of normal incidence of a plane wave, for two media with the acoustic impedance  $z_1$  and  $z_2$ , the transmission coefficient is as given in equation (1.2).

$$\alpha_{transmission} = \frac{4z_1z_2}{(z_1 + z_2)^2} \quad (1.2)$$

The acoustic waves bend around corners and obstacles as a result of wave diffraction. The bending of waves as a result of diffraction becomes less marked as the wavelength decreases relative to the dimensions of the obstacle. In the presence of many obstacles, diffraction is often called scattering (Lundgaard 1992a).

### 1.2.3.2 Detection and analysis of acoustic signals

A permanently installed on-line acoustic monitoring system can provide an early indication of an incipient fault to a remote location. The acoustic monitoring system consists of sensors, pre-amplifier, filters, and data acquisition system. The typical block schematic of acoustic detection systems is as shown in Figure 1.3. The sensors are placed nearer to the locations where faults may be anticipated based on past experience or highest probability of problems occurrence. The use of a band-pass filter is optional. Its purpose is to negate the effects of signals that are not associated with PDs as much as possible. The data acquisition/processing systems are able to transmit collected data and/or warning alerts to locations outside the substation (IEEE Std C57.127 2007).

An AE burst is a group of AE oscillations constituting a transient signal. A typical

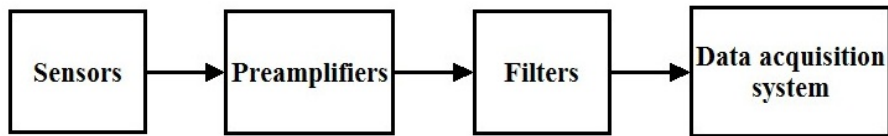


Figure 1.3 Typical block schematic of acoustic detection system.

AE burst is shown in Figure 1.4. The maximum magnitude of the AE signal is the amplitude of the signal. The rise time is the time from the first threshold crossing to the maximum amplitude. Duration is the time from the first threshold crossing to the last threshold crossing. The count is the number of AE oscillations that exceed the counter threshold level. AE oscillation rate or count rate is the number of AE oscillations that exceed the counter threshold level in a time interval, often 1 s, or a number of cycles, depending on the instrument being used (IEEE Std C57.127 2007). The AE signals obtained from the electrical apparatus are captured by the sensors and amplified to required levels by suitable pre-amplifiers. These signals are then transferred to the signal processing instrument, where it is further amplified and filtered. The filtered AE signal will be passed through a comparator set with a predetermined threshold. The signal processing unit has the option to set the threshold which would be set by the operator of the instrument.

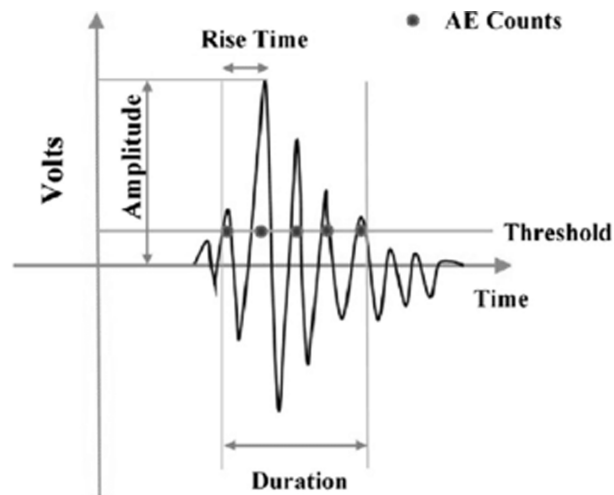


Figure 1.4 Typical AE burst and its parameters.

An attempt has been made to understand the available literature in areas of detection

and analysis of AE signals. The different sensors and the sensor arrangements along with the methods for detecting the sensor faults are available in the literature. The analysis of AE signals are carried out for: (i) identifying and locating two simultaneous PD sources; (ii) classification of common PD types using acoustic signals; and (iii) de-noising of acoustic signals. The pertinent literature published in these areas are as follows.

Zhu *et al.* (1988) have studied the AE method to detect the PD in insulation of power transformer by the simulation of six typical oil gaps. The frequency spectra of the AE due to PD in these gaps have been investigated. The AE due to magnetic noise and the frequency spectra associated with the magnetic noise have also been investigated and presented in their paper. Boczar (2001) has studied frequency spectra and associated bandwidths of the AE signals due to PD. The spectral analysis carried out in his work has enabled to identify a specific type of PD from the associated frequency spectra. Boczar and Zmarzly (2004) applies the wavelet analysis for processing the AE pulses generated by PD in oil insulation systems. The frequency structures of AE pulses generated by PD in six basic forms such as: a) those due to multi point-plane, b) surface type, c) multi-point type with press board insulation, d) gas bubble, e) point-plane spark gap, and f) indefinite potential particle have been studied and reported in their paper. The research carried out is aimed at creating fingerprint for each of these PD forms, which would make unique identification possible.

Boczar (2005) checks the identification possibilities of PD in the case of generation of AE pulses by two sources of discharges due to point-plane gaps, with the plane electrode at the ground potential. The two sources can be identified simultaneously using the time-frequency analysis. Wang *et al.* (2005) have studied the shift in the acoustic energy of the acoustic waves generated by PD in the transformer oil at different temperature. Acoustic waves generated by PD at two temperatures, namely, 25°C and 40°C were studied. Authors have analysed the data with FFT; their findings revealed that acoustic energy at 40°C is larger than that at 25°C. Nagamani *et al.* (2005) have carried out experimental studies to characterise AE signals by simulation of defects in power transformers like PD, arcing, and core vibration. Detection and location of

simulated defects have been verified with the AE system. The authors have performed FFT based analysis to discriminate noise from PD. Application of AE technique in the field has also been discussed.

Kundu *et al.* (2007) have analysed AE signals using discrete wavelet transform (DWT) by decomposing them into five different frequency bands such as D1 (250 kHz - 500 kHz), D2 (125 kHz - 250 kHz), D3 (62.50 kHz - 125 kHz), D4 (31.25 kHz - 62.5 kHz), and D5 (15.625 kHz - 31.25 kHz). The AEPD signals, for different sensor to source distance, were analysed through laboratory experiments. Chen *et al.* (2007) proposes a non-contact type of acoustic measurement system. The noise suppression is carried out by applying wavelet transform. Thus, provides the correct PD signal identification rate.

Lee *et al.* (2008) tests different commercial sensors to assess their characteristics and found that magnetic sensor has similar sensitivity with coupling capacitor, and UHF sensor has better signal to noise ratio. Sharkawy *et al.* (2008) uses a support vector machine classifier to classify particles in transformer mineral oil according to material and size. Wavelet multi-resolution analysis data of the acoustic signals together with higher order statistics of the particle inter-collision times and magnitudes comprise the input features to the classifier. Richeng *et al.* (2008) applied array signal processing technique on PD source localisation, to estimate the location parameter of multiple PD sources in transformer.

Mohammadi *et al.* (2009) studied the AE signals generated due to PD and analyses the signals in time, frequency, and time-frequency domains. Investigation indicated that frequency domain descriptors for classifying different PD patterns provided good results. Boczar *et al.* (2009) tries to recognise and divide the PDs generated in gases, solid, and liquid dielectrics using the AE method by applying single-direction artificial neural networks.

Venkatesh *et al.* (2011) studies three different defects namely corona discharge, discharge initiated due to floating particle, and discharge formation due to particle movement. The discharges initiated by these defects under standard lightning impulse were studied adopting AE technique.

Kundu *et al.* (2012) presents the identification and localisation of two simultaneous PD sources using AE technique. The AE signals are measured for laboratory simulated PD in an oil-press board insulation system for three different electrode systems. Energy distribution in different frequency bands of DWT decomposed signal along with box counting fractal dimension is used for the classification of two simultaneous PD sources.

Harbaji *et al.* (2015) have dealt with the classification of common PD types under different AE measurement conditions. The PD from a sharp point to ground plane, surface discharge, PD from a void in the insulation, and PD from semi parallel planes are considered. The collected AE signals are processed using pattern classification techniques to identify their corresponding PD types. Boya *et al.* (2015) have proposed the identification of multiple PD sources by applying blind signal separation techniques to recover the signals from each source when using AE technique.

Al-Masri *et al.* (2016a) presents an algorithm for the detection of a bias fault (error due to improper calibration or ageing of AEPD sensors) when detecting PD in the transformer insulation system using acoustic signals. Al-Masri *et al.* (2016b) uses a multiple-model extended Kalman filters, that compensate for increased measurement noise, to estimate the location of the PD. Biswas *et al.* (2016) uses the cross-wavelet transform based feature extraction with ensemble binary support vector machine based classifier for locating multiple PD sources within the tank. Sarkar *et al.* (2016) presents a fibre bragg grating based intensity-modulated fibre-optic PD sensor. The proposed sensor is designed to be placed inside the transformer tank. It can detect high-frequency acoustic wave emitted due to the occurrence of PDs. Hussein *et al.* (2016) investigate power spectral subtraction de-noising that uses FFT to restrain the random noise encountered in measured acoustic PD signals. The de-noising performance is compared with those of wavelet-based de-noising techniques in addition to the mathematical morphological filter. Xie *et al.* (2016) compares the cross, circular, and square array sensors commonly used in the acoustic PD detection. Sparse signal decomposition theory is applied to find three different directions of arrival of the signal from the PD source to the array sensor and it is found that the acoustic performance of the circular array is the



best.

Hekmati and Hekmati (2017) proposes an optimum arrangement of AE sensors for different PD origins within transformer tank. Kanakambaran *et al.* (2017) applies a cross recurrence plot analysis based technique on signals captured using fibre bragg grating sensors to improve the accuracy of detection and localisation of PDs. Castro *et al.* (2017) assess the performance of macro fibre composite sensors for measuring AE signals from PD in power transformers filled with mineral oil. These sensors are low-profile and flexible, that allows them to attach to uneven transformer wall surface. Hussein *et al.* (2017) classifies three different types of acoustic PD signals. These signals are due to a sharp point, surface-PD, and void-PD. The spectrum of the PD signals is obtained using FFT. The low-frequency components are truncated and selected as PD representative features. These features are then fed to the classifier.

Ma *et al.* (2018) introduces PD detection system based on phase-shifted fibre bragg gratings. The proposed sensor is installed inside the power transformer, which takes the advantage of the optical fibre status. The frequency response experiments indicate that the sensitivity of the proposed sensor is higher than that of the conventional ultrasonic sensor. Hussein *et al.* (2018) addresses the random noise suppression using power spectral subtraction de-noising. The study applies this technique to the acoustic PD signals contaminated with white noise and uses a scheme of noise power spectrum density estimation.

### **1.2.3.3 Acoustic emission technique for partial discharge source localisation**

The acoustic methods for the detection of discharges will play a most important role wherever the location of the discharge site is of prime concern Harrold (1979a, 1986). A computer-aided PD acoustic location system is described in Tang *et al.* (1996). The PD detection and localisation are carried out in the factory and in the field. There are two general categories of AEPD location system: (i) all-acoustic system and (ii) combined acoustic-electrical system.

- ***Types of AEPD location system***

- ***All-acoustic system***: The all-acoustic system consists of one or more ul-

trasonic transducers that are sensitive to the AE generated by a PD event. To detect and locate one or more PD sources, the externally mounted sensors are moved to different locations on the transformer tank wall. A more precise location of a PD source is determined by the relative arrival times of the acoustic signals at each of the sensors. The all-acoustic system uses the time-difference of arrival (TDOA) approach for PD source localisation. Since, no voltage or current measurements are required, the all-acoustic system is a suitable tool for PD source localisation in in-service transformers (operating transformers in the field) (IEEE Std C57.127 2007).

- **Combined acoustic-electrical system:** The acoustic system with an electrical PD trigger uses current or voltage measurement device that detects the PD signal electrically, along with the array of acoustic sensors. The electric signal is usually considered as detected instantaneously. The arrival time of the electric signal is taken as time zero for the PD event because of the above assumption. The propagation time between the PD source and the sensor location is the difference in arrival times of the electric signal and an acoustic signal at that sensor. The combined acoustic-electrical system uses the time of arrival (TOA) approach for PD source localisation. One advantage of the combined system is that the electrical measurement provides confirmation that the acoustic sensors are locating a PD event and not an acoustic noise source. The electrical signal is also a convenient trigger that can be used to start the data acquisition at the acoustic sensors (IEEE Std C57.127 2007).

The block diagram for an all-acoustic system and a combined acoustic-electrical system is given in Figure 1.5.

- **Physical model**

A physical model of an AEPD system is such that, a large number of AE sensors are placed on the transformer enclosure. These sensors are named  $S_1, S_2, S_3, \dots, S_n$ .  $(x_i, y_i, z_i)$  are the coordinates of the sensors and  $(x, y, z)$  are the coordinates of the PD source (Markalous *et al.* 2008).

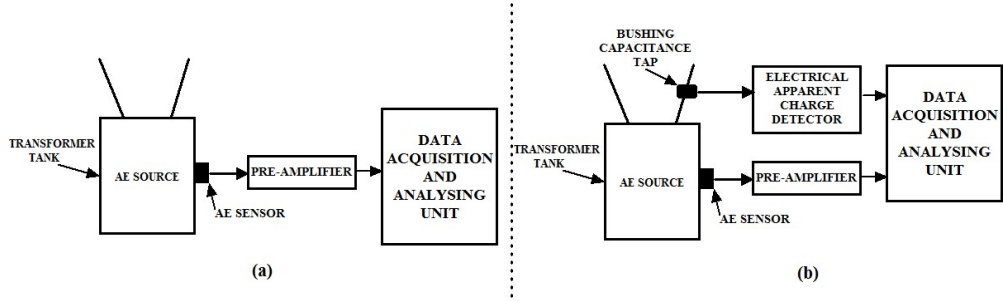


Figure 1.5 The block diagram for (a) all-acoustic system and (b) combined acoustic-electrical system.

- **Mathematical model**

A mathematical model can be developed for the AEPD location system. Non-linear sphere equations are formed by considering each sensor as the centre of the sphere and distance between the sensor and PD source as radius (Veloso *et al.* 2006). The radius of the sphere is given by the product of propagation speed of acoustic wave ( $v$ ) and acoustic arrival time of the respective sensor. The different time approaches for solving mathematical model are: (i) absolute-time approach; and (ii) time-difference approach. These are discussed below.

- **Absolute-time approach:** The instant at which the PD occurs is known in the case of combined acoustic-electrical system. This corresponds to an absolute-time measurement and it is illustrated in Figure 1.6. The associated sphere functions with the three unknown PD coordinates in space ( $x, y, z$ ), the measured signal arrival times  $T_i$ , the assumed sound velocity  $v$  and the cartesian sensor coordinates ( $x_i, y_i, z_i$ ) is given in equation (1.3) (Markalous *et al.* 2008). Since, there are three unknowns, a minimum of three sensors are required to locate the PD source.

$$\begin{aligned}
 (x - x_1)^2 + (y - y_1)^2 + (z - z_1)^2 &= (vT_1)^2, \\
 (x - x_2)^2 + (y - y_2)^2 + (z - z_2)^2 &= (vT_2)^2, \\
 (x - x_3)^2 + (y - y_3)^2 + (z - z_3)^2 &= (vT_3)^2.
 \end{aligned} \tag{1.3}$$

- **Time-difference Approach:** The exact instant at which the PD occurs is unknown in the case of all-acoustic PD measurements. The sensor nearest

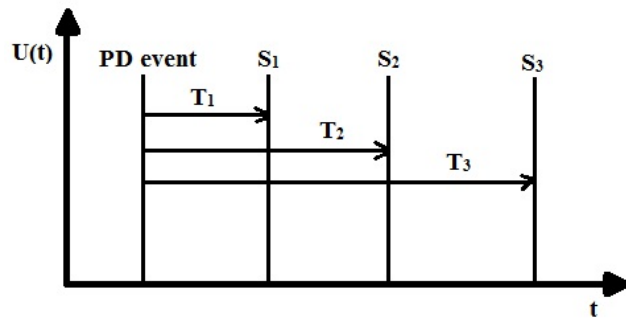


Figure 1.6 Schematic visualisation of absolute-time approach for a combined acoustic-electrical system.

to the PD source will receive the acoustic signal first. The acoustic sensor which is first hit by an acoustic wave triggers a recording process on all sensors, simultaneously. The time-delay for the signal reception of all other sensors with respect to the nearest sensor are designated as  $t_{12}$ ,  $t_{13}$ , ...,  $t_{1n}$  etc. The corresponding time-difference measurement is illustrated in Figure 1.7. Along with the three unknown PD coordinates in space ( $x$ ,  $y$ ,  $z$ ) there is another temporal unknown  $T_1$ , which is the arrival time of the PD signal to the nearest sensor (Markalous *et al.* 2008). Since there are four unknowns, a minimum of four sensors are required to locate the PD source. The associated sphere functions with the four unknowns are given in equation (1.4).

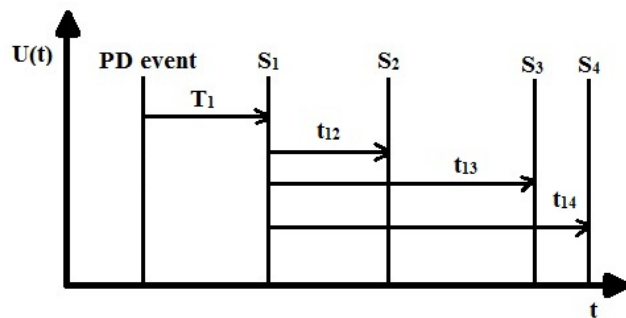


Figure 1.7 Schematic visualisation of time-difference approach for an all-acoustic system.

$$\begin{aligned}
(x - x_1)^2 + (y - y_1)^2 + (z - z_1)^2 &= (vT_1)^2, \\
(x - x_2)^2 + (y - y_2)^2 + (z - z_2)^2 &= (v(T_1 + t_{12}))^2, \\
(x - x_3)^2 + (y - y_3)^2 + (z - z_3)^2 &= (v(T_1 + t_{13}))^2, \\
(x - x_4)^2 + (y - y_4)^2 + (z - z_4)^2 &= (v(T_1 + t_{14}))^2. \quad (1.4)
\end{aligned}$$

Once the arrival time of the acoustic signal from the PD source to AE sensor is estimated, the other requirements for locating the source of PD in a power transformers are the knowledge of ‘velocity of sound in oil’ and an ‘algorithm to solve the mathematical model’ of the acoustic PD location system. The discussion related to the velocity and algorithms is given below.

- ***Velocity of sound in oil***

The sonic velocity in transformer oil is not constant but depend upon a complex relationship which include the temperature of the oil, its gas and moisture content as well as the frequency content of the propagating signal (Howells and Norton 1984).

- ***Effect of temperature:*** Temperature has a significant effect on the propagating velocity of the signal. At low temperature where the oil was approaching the physical consistency of that of grease, there appears to be a limiting maximum velocity. Obviously, the velocity drops off dramatically as the temperature increases.
- ***Effect of moisture content:*** The addition of moisture to the oil has the effect of reducing the sonic velocity. However, the effect is small when compared to the effect of temperature.
- ***Effect of gas content:*** Any absorbed gas in the oil causes a small but measurable decrease in the sonic velocity. It also appears that the type of gas which is absorbed has more effect on the velocity than just the quantity of gas.
- ***Effect of frequency content of the propagating signal:*** The speed of sound

in transformer oil is dependent on the frequency of the signal propagating in it. The higher the frequency, the faster will be the wave propagation.

In transformers, the oil occupies most of the insulating space. Therefore, the velocity of waves propagating in transformers could be considered as its velocity in the oil (Tang *et al.* 2006). According to IEEE Std C57.127 (2007), the acoustic wave velocity typically used for the PD source localisation in transformers is 1413 m/s at 20°C. In Howells and Norton (1984), the sonic velocity in oil is measured over the temperature range of -30°C to 130°C. Estimating the mean oil temperature and then using the corresponding sound velocity for PD localisation is a good guess (Markalous *et al.* 2008). Most of the studies have treated transformer as a homogeneous medium and substituted the velocity of sound in oil as the velocity of acoustic wave propagation from the source to sensor (Coenen and Tenbohlen 2012; Kraetge *et al.* 2013; Lu *et al.* 2000; Markalous and Feser 2004; Markalous *et al.* 2008).

The acoustic wave velocity (at various temperatures) used for PD source localisation in published literature in three different test conditions: (i) laboratory experiment without barrier; (ii) laboratory experiment with barrier; and (iii) on-site transformer are given in Table 1.2. All these literature have taken the acoustic wave velocity at various temperatures from the reference Howells and Norton (1984).

- **Algorithms**

In numerical computation, solving systems of non-linear equations is perhaps the most difficult task, and it is unavoidable in a spectrum of engineering applications (Li *et al.* 2016b). Many algorithms have been developed for the solution of system of non-linear equation. These algorithms can be classified into iterative and non-iterative methods. Typical features of some of the algorithms are discussed below.

- **Newton's method:** Newton's method is driven by derivative information and is derived from Taylor's series. In the solution of systems of equations, this method employs a linear model to solve the equations. The function is first

Table 1.2 The acoustic wave velocity (at various temperatures) used for PD source localisation in published literature

Test condition	References	Experimental set-up	Velocity	Temperature
Laboratory Experiment without barrier	(Markalous and Feser 2004)	A rod-plane PD source in a small test tank	1410 m/s	21.5°C
Laboratory Experiment with barrier	(Markalous and Feser 2004)	A PD is stimulated with an electrode on ground at the inner side of the high voltage winding in an oil immersed transformer housing.	1410 m/s	21.5°C
	(Lu <i>et al.</i> 2000)	An oil tank, in which a needle-to-back electrode is mounted (transformer insulating paper is inserted between the needle and the back).	1400 m/s	25°C
	(Markalous and Feser 2004)	An oil filled transformer tank containing a disc winding package at HV, surrounded by two press board cylinders, with a stimulated PD, at the inner side of the coil.	1417 m/s	21°C
Onsite PD measurement	(Markalous and Feser 2004)	200 MVA single-phase transformer	1387 m/s	26°C
	(Coenen and Tenbohlen 2012)	333 MVA, 400/220kV single phase auto-transformer	1400 m/s	Temperature not specified
	(Kraetge <i>et al.</i> 2013)	16 MVA transformer.	1400 m/s	Temperature not specified

evaluated using the initial guess supplied. If this estimate is satisfactory, the initial guess supplied is the solution for the system of non-linear equation. If this estimate is not satisfactory, refinement of the initial estimate is carried out through iterations till the results are satisfactory. A solution can be considered satisfactory when the difference among two successive solutions is less than a predefined tolerance (Cheney and Kincaid 2007). The performance and convergence characteristics of Newton's method are highly dependent on the initial guesses. So the primary goal is to effectively locate regions in which the roots are likely to exist. Once the neighbourhood of the root has been identified, this method provides a very efficient means of converging to the root. But there are many situations in which this information is not known (Punekar *et al.* 2012).

- **Genetic Algorithm:** The genetic algorithm (GA) is a search algorithm based on the mechanics of natural selection and natural genetics. It requires the natural parameter set of the optimisation problem to be coded as a finite length string over some finite alphabet. In many optimisation methods, we move from a single point in the decision space to the next using some transition rule. By contrast, GA works from a rich database of points, simultaneously climbing many peaks in parallel. Thus, the probability of finding a false peak is reduced over methods that go point to point (Reeves and Rowe 2002). The GA use random choice as a tool to guide the search towards the solution in the search space (Karr *et al.* 1998; Punekar *et al.* 2013; Veloso *et al.* 2006).
- **Pattern search:** In this method, it is assumed that a rectangular shaped transformer consists of a number of sub-modules. For each sub-module, using the acoustic propagation time to reference sensor and its distance from all other sensors, the undetermined pattern vector can be formed using the left hand side of equation (1.4). From the signal arrival time to reference sensor and the measured time-delays  $t_{12}$ ,  $t_{13}$ , and  $t_{14}$ , the standard pattern vector can be identified using the right hand side of equation (1.4). By comparing



the spatial distance between each sub-module's standard pattern vector and its undetermined pattern vector, the sub-module with the minimum spatial distance between the two pattern vectors may be the PD site (Lu *et al.* 2000). The disadvantage of this method is that it requires knowledge of transformer internal dimensions which is not always known (Kundu *et al.* 2009).

- **Particle swarm optimisation:** In particle swarm optimisation (PSO), the inner volume of the transformer is meshed with a small length  $dl$ . Each node in the transformer represented by  $(i, j, k)$  have coordinates  $x = i \times dl$ ,  $y = j \times dl$ , and  $z = k \times dl$ . Each multidimensional particle has two values of  $p_{id}(t)$  and  $v_{id}(t)$  which represent the position and the velocity of the  $d^{th}$  dimension of the  $i^{th}$  particle in  $t^{th}$  iteration. Each particle with two best values is updated in each stage of the movement of the swarm. The  $P_{best}(t)$  and  $g_{best}(t)$  are the  $i_{th}$  particle best solution and the global best value ever obtained by any particle in the population, respectively. Each particle updates its new velocity and position with the two values of  $P_{best}(t)$  and  $g_{best}(t)$ . The stopping criteria of the iteration process can be the maximum number of repetitions, or the maximum changes in the best fitness less than the defined tolerance. This algorithm can also be used for the simultaneous location of two PD sources. A PSO route-searching algorithm is employed for searching the position of the PD source in Wang *et al.* (2017). The particles of the PSO algorithm at the conventional searching process quickly converge and as a result, the possibility of falling into the local minimum point is also high (Hooshmand *et al.* 2013).
- **Non-iterative method:** In non-iterative method, any two of the spheres intersect in a plane and the source can be located on this intersecting plane. Two such planes intersect in a line and the PD source can be located on this line. The line intersects any one of the spheres in two points, resulting in a quadratic equation. One of the solutions of this quadratic equation is the PD source location (Kundu *et al.* 2009). The non-iterative method does not have any convergence problem. The solution of the non-iterative method

is dependent on the sensor position, and the relative distance between the sensor and the PD source. The selection of actual PD source location from the solutions of the quadratic equation is also difficult.

– ***Global positioning system algorithm:***

The global positioning system (GPS) algorithm is another method used for the PD source localisation (Kurz *et al.* 2005; Markalous *et al.* 2005). In this method, the selection of the actual PD source location from multiple solutions is difficult (Liu 2016).

With the understanding of AE technique for PD source localisation, based on the literature survey, the motivation for the present research is given in the following section.

### **1.3 Motivation**

Transformers are a major component in power system and the cost of transformer failure is high regarding both direct costs and downtime. The PDs are often a predecessor of serious fault in transformers. In large power apparatus like transformers, locating the source of PD is as important as identifying it. The PD source localisation helps in risk assessment and in planning of maintenance activities, making it cost and time efficient. According to literature, the measurement methods to detect and locate PD have been under development since the 1930's (Bartnikas 2002; Stone 1991, 2005). Being non-invasive, AEPD source location technique can be used for on-line PD source location detection (Eleftherion 1995; Lundgaard 1992*a,b*). Although numerous algorithms have been developed to solve the mathematical model of an AEPD location system, the existing algorithms have many limitations and hence, improvements are needed. The other factor affecting the accuracy of location detection is the error in time measurement (from the PD source to various sensors). The necessity for improving the existing algorithms and the importance in studying the effect of error in time measurement (on the accuracy of PD source localisation) are the motivations for the present research.

## 1.4 Objectives

Based on the literature review related to AE based PD detection techniques in condition monitoring of transformers, following aspects have been identified as the objectives of the present research work.

1. Development of an algorithm or improvements in existing algorithms for AEPD source localisation using an all-acoustic system.
2. Development of a new non-iterative algorithm for AEPD source localisation using a combined acoustic-electrical system.
3. Development of mathematical methods to identify erroneous time measurements.
4. Substantiating the above findings through numerical experiments, laboratory experiments on models in the HV laboratory, and/or by applying it to data from published literature, wherever possible.

## 1.5 Organisation of the thesis

### Chapter 1: Introduction

Chapter 1 includes an introduction to the various condition assessment techniques used for power transformers; the different methods used for partial discharge detection in transformers; and AE technique applied to PD source localisation in transformers. A pertinent literature review is also given culminating into motivation for the present research work. The objectives of the present research work are listed. A glimpse of the research investigation and organisation of the thesis are also given.

### Chapter 2: Algorithms for PD source localisation: All-acoustic system

In Chapter 2, the implementation of Newton's method and non-iterative method for the AEPD source localisation in an all-acoustic system are analysed. The conditions for which these algorithms fail to locate the PD source positions are identified. A hybrid method combining GA and Newton's method is proposed. The sensor positioning guidelines are also suggested so that the hybrid method overcomes the limitations of the Newton's method. An extension is proposed for the existing non-iterative methods, so

that it works for cases with zero time-difference. The numerical and laboratory experiments carried out for the performance verification of the proposed improvements are also explained in this chapter.

### **Chapter 3: Algorithms for PD source localisation: Combined acoustic-electrical system**

In Chapter 3, a non-iterative method is devised for PD source localisation using the combined acoustic-electrical system. The guidelines for the sensor placement for the reliable implementation of the proposed method are also suggested. In addition, the effect of the PD source position on the performance of the proposed method is analysed. The proposed method is also applied to the experimental data published in the literature. The performance of the proposed non-iterative method is compared with that of Newton's method and hybrid method (iterative methods).

### **Chapter 4: Effect of error in time measurement on PD source localisation**

In Chapter 4, the effect of error in time measurement on the accuracy of the PD source localisation is analysed. Two mathematical methods for the identification of erroneous time-delay measurements for an all-acoustic system are proposed: (i) using discriminant; and (ii) using Jacobian-determinant. The method for mathematically identifying the invalid absolute-time measurements using discriminant for a combined acoustic-electrical system is also proposed in this chapter. The performance verification of the proposed methods, by the application of proposed method to published data, for both AEPD location systems are also given in this chapter.

### **Chapter 5: Conclusions and scope for further study**

Chapter 5 summarises the research work reported in the thesis along with the scope for future research work.

The overview of the research work carried out and reported in the thesis is presented in the form of a block schematic in Figure 1.8. This gives a quick overall organisation of the thesis and the inter-connectivity of the chapters.

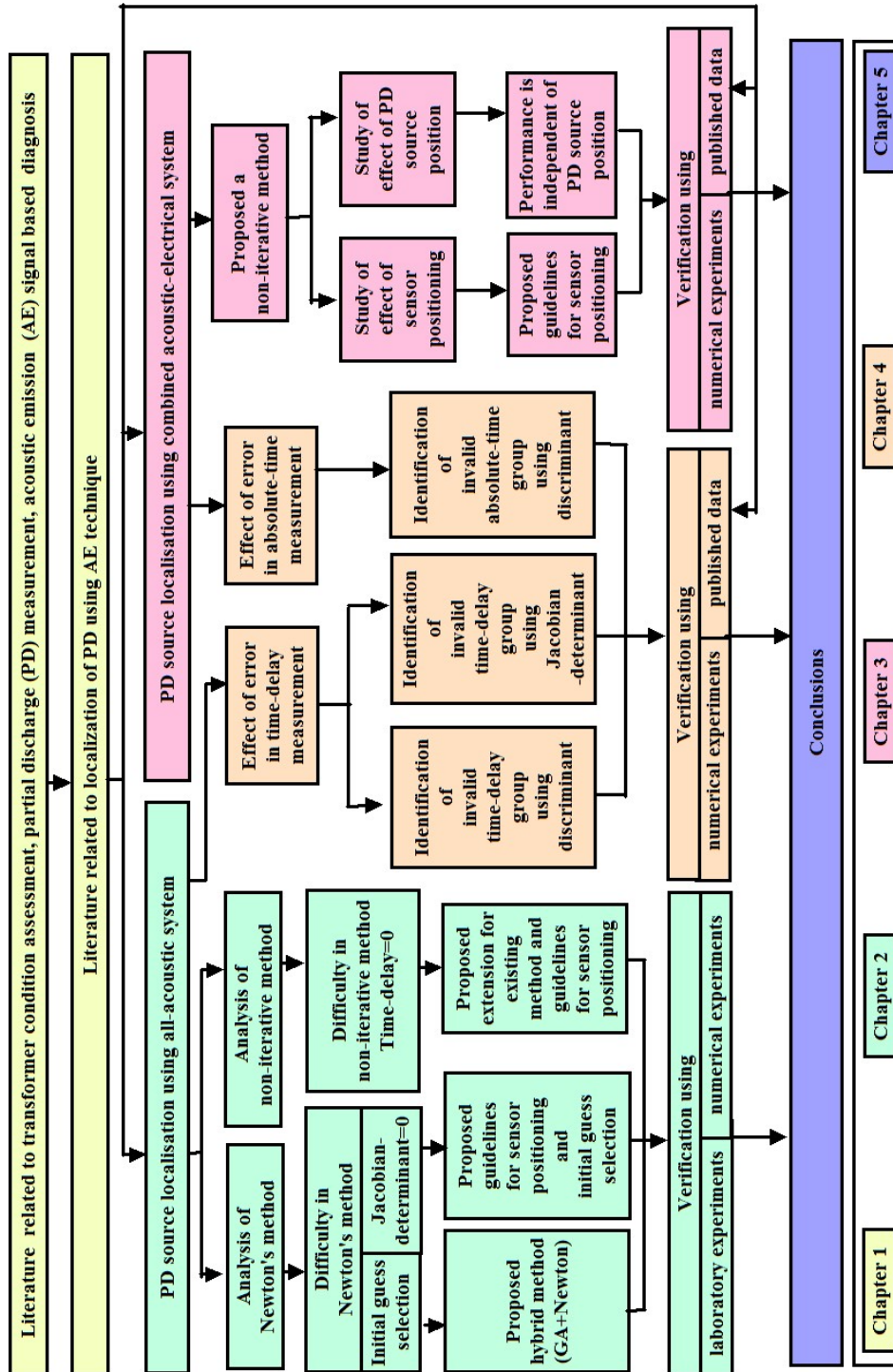


Figure 1.8 Overview of the research work.



## Chapter 2

# Algorithms for PD source localisation: All-acoustic system

### 2.1 Introduction

The PD measurement plays a key role in the condition assessment of power transformers (Lundgaard 1992a). Locating the source of the PD is as important as detecting it. The PD source localisation assists in predictive maintenance (Stone 1991). There will be significant reduction in the time consumption for the repair of the transformer, if the source of the discharge is located accurately. The PD source localisation in transformers can be carried out on-line using an all-acoustic system. An all-acoustic system uses an array of AE sensors for the detection and the localisation of the PD source (IEEE Std C57.127 2007).

In the instrumentation system for the PD source localisation using the AE technique, a localisation algorithm (that assists in finding the position of the PD within the power transformer) will be incorporated in the locating stage (Búa-Núñez *et al.* 2014). The efficacy of this algorithm plays a key role in the rapid and the precise localisation of the PD source.

The commonly used algorithms for solving the mathematical model of an AEPD system are Newton's method and least square iterative algorithm (Huang *et al.* 2001; Punekar *et al.* 2012). The convergence of these algorithms is dependent on the quality of the initial guess. Moreover, the computational time required for the iterative algorithms is more compared to non-iterative algorithms.

The GA is also used for the PD source localisation (Liu 2016; Puneekar *et al.* 2013; Veloso *et al.* 2006). The GA can rapidly locate the regions where the solutions are likely to exist, but it cannot guarantee the convergence to an exact solution (Karr *et al.* 1998). The pattern recognition method also has been used for the PD source localisation (Lu *et al.* 2000). In this method, the transformer tank is divided into several sub-modules. The accuracy will be greater with a larger number of sub-modules, but the amount of data that is to be handled will be enormous. Difficulty also arises when the internal dimensions of the transformer tank are unknown (Kundu *et al.* 2009; Liu 2016). The GPS algorithm is another method used for the PD source localisation (Kurz *et al.* 2005; Markalous *et al.* 2005). In this method, the selection of the actual PD source location from multiple solutions is difficult (Liu 2016). Park *et al.* (2012) presents an algorithm to find the position of the PD occurrence using the TDOA measured by five AE sensors.

The non-iterative method for AEPD source localisation is given in Kundu *et al.* (2009). In Kundu *et al.* (2009), this method is proved to be superior to other existing methods, such as the least square algorithm, pattern recognition method, and an existing iterative algorithm. However, the major disadvantage of this non-iterative method is that its performance is dependent on the relative distances between the PD source and the sensors.

From the above discussion, it is clear that the existing algorithms have some limitations in a precise localisation of the PD source. The Newton's method and non-iterative method for the AEPD source localisation are implemented in this chapter. The conditions for which these methods fail to locate the PD source positions are identified. The improvements are proposed for these existing methods, so that a precise localisation of the PD source is possible.

This chapter is organised as follows: Section 2.2 elaborates the mathematical model of an all-acoustic system for the PD source localisation; Section 2.3 explains the implementation of Newton's method for PD source localisation; Section 2.4 explains the implementation of the existing non-iterative method; Section 2.5 gives the numerical experiments carried out for the performance verification of these methods; Section 2.6 explains the laboratory experiments conducted to verify the efficacy of these PD source



localisation algorithms; This is followed by conclusions in Section 2.7.

## 2.2 Mathematical model of an all-acoustic system

The AE techniques are based on detecting the signals emitted from the discharge by using multiple AE sensors located on the transformer's tank wall. The sensors are named  $S_1, S_2, \dots, S_n$ , where 'n' is the total number of sensors used. The sensor nearest to the PD source first receives the acoustic signals (Markalous *et al.* 2008). This sensor is named  $S_1$ . The time-delay in signal reception of the other sensors with respect to the sensor  $S_1$  is calculated. The sensors are named  $S_2, S_3, S_4$  etc., in the increasing order of their time-delays. To solve for the PD coordinates, the AEPD system is modelled mathematically. The non-linear sphere equations are formed by considering each sensor as the centre of the sphere and the distance between the sensor and the PD source as radius. The product of the velocity ( $v$ ) of sound in transformer oil and the acoustic signal arrival time ( $T_n$ ) to the sensor gives the radius of the  $n^{th}$  sphere. The spheres intersect with each other at the PD source location (Veloso *et al.* 2006). The sensors  $S_1, S_2, \dots, S_n$  have their coordinates given by  $(x_1, y_1, z_1), (x_2, y_2, z_2), \dots$  and  $(x_n, y_n, z_n)$ , respectively. Difference in time  $t_{12}$  is the time-delay in acoustic signal arrival at the sensor  $S_2$  with respect to the sensor  $S_1$ . Difference in time  $t_{13}$  is the time-delay in signal arrival at the sensor  $S_3$  with respect to the sensor  $S_1$ , and so on. The 'n' non-linear sphere equations are given in equation (2.1).

$$\begin{aligned}
 (x - x_1)^2 + (y - y_1)^2 + (z - z_1)^2 &= (vT_1)^2, \\
 (x - x_2)^2 + (y - y_2)^2 + (z - z_2)^2 &= (v(T_1 + t_{12}))^2, \\
 (x - x_3)^2 + (y - y_3)^2 + (z - z_3)^2 &= (v(T_1 + t_{13}))^2, \\
 &\dots\dots \\
 (x - x_n)^2 + (y - y_n)^2 + (z - z_n)^2 &= (v(T_1 + t_{1n}))^2.
 \end{aligned} \tag{2.1}$$

In the system of the non-linear sphere equations, for an all-acoustic system, given in equation (2.1), the coordinates of the PD source ( $x, y, z$ ) and the acoustic signal arrival time to the nearest sensor ( $T_1$ ) are the unknown quantities. Since there are four unknowns a minimum of four AE sensors are required to locate the PD source. In

numerical computation, solving the system of non-linear equations is perhaps the most difficult task, and it is unavoidable in a spectrum of engineering applications (Li *et al.* 2016b). Many algorithms have been developed for the solution of the system of non-linear equations. An existing iterative method (Newton's method) and non-iterative method for the PD source localisation are analysed in the following sections.

## 2.3 Newton's method for PD source localisation

The most commonly used and the oldest method for solving the system of non-linear equations is Newton's method (Karr *et al.* 1998). In solving the system of equations, this method employs a linear model to solve the equations. The functions are first evaluated using the initial guesses supplied. If this estimate is satisfactory, the initial guesses supplied are the solutions for the system of non-linear equations. If this estimate is not satisfactory, refinement of the initial estimate is carried out through iterations till the results are satisfactory. A solution is considered to be satisfactory when the difference among two successive solutions is less than a predefined tolerance (Cheney and Kincaid 2007).

### 2.3.1 Implementation of Newton's method

In Newton's method, the four functions  $F_1$ ,  $F_2$ ,  $F_3$ , and  $F_4$  are formed using four non-linear sphere equations as given in equation (2.2) to equation (2.5). The vector  $[F]$  denotes the vector of four functions  $[F_1 F_2 F_3 F_4]$ .

$$F_1 = (x - x_1)^2 + (y - y_1)^2 + (z - z_1)^2 - (vT_1)^2 \quad (2.2)$$

$$F_2 = (x - x_2)^2 + (y - y_2)^2 + (z - z_2)^2 - (v(T_1 + t_{12}))^2 \quad (2.3)$$

$$F_3 = (x - x_3)^2 + (y - y_3)^2 + (z - z_3)^2 - (v(T_1 + t_{13}))^2 \quad (2.4)$$

$$F_4 = (x - x_4)^2 + (y - y_4)^2 + (z - z_4)^2 - (v(T_1 + t_{14}))^2 \quad (2.5)$$

The vector  $[X]$  denotes the vector of unknown variables  $[x y z T_1]$ . The initial guess  $[x^0 y^0 z^0 T_1^0]$  for the unknown quantities form a vector, denoted by  $[IG^0]$ . The Jacobian matrix ( $[J]$ ) is the matrix of partial derivatives as given in equation (2.6).

$$[J] = \frac{\partial F}{\partial X} \quad (2.6)$$

The set of four functions ( $[F_1; F_2; F_3; F_4]$ ) are evaluated to form the vector  $[F^0]$  by substituting initial guess  $[IG^0]$  for the unknown quantities. The Jacobian matrix  $[J]$  is also evaluated to form the matrix  $[J^0]$  by substituting  $[IG^0]$  for the unknown quantities.

The correction factor  $H$  can be found by using equation (2.7).

$$H = [J^0]^{-1} \times [F^0] \quad (2.7)$$

The corrections are then added to the solution vector as in equation (2.8), and the process is iterated to convergence (Cheney and Kincaid 2007).

$$[IG^1] = [IG^0] + H \quad (2.8)$$

The stopping criteria chosen for Newton's method are: (i) the maximum number of iterations is 100; and (ii) difference between two solutions in successive iteration is smaller than  $1 \times 10^{-6}$  (tolerance). The solution thus obtained is the estimated PD source location. The generalised flowchart for PD source localisation in power transformers using the Newton's method is given in Figure 2.1.

### 2.3.2 Challenges faced when implementing Newton's method

When Newton's method is used for the PD source localisation, the vector  $[F^0]$  and the matrix  $[J^0]$  are formed by substituting  $[IG^0]$  for the unknown quantities. One of the major challenge while implementing Newton's method is the difficulty in choosing an efficient initial guess.

The inverse of the Jacobian matrix is evaluated to find the correction factor (see equation (2.7)). The inverse of a matrix cannot be found if the matrix is singular. The Jacobian matrix becoming singular is another major challenge while implementing Newton's method.

Therefore, the possibility of Newton's method failing to locate the PD source are:

- The algorithm not converging to the solution due to a bad initial guess;
- The Jacobian matrix becoming singular.

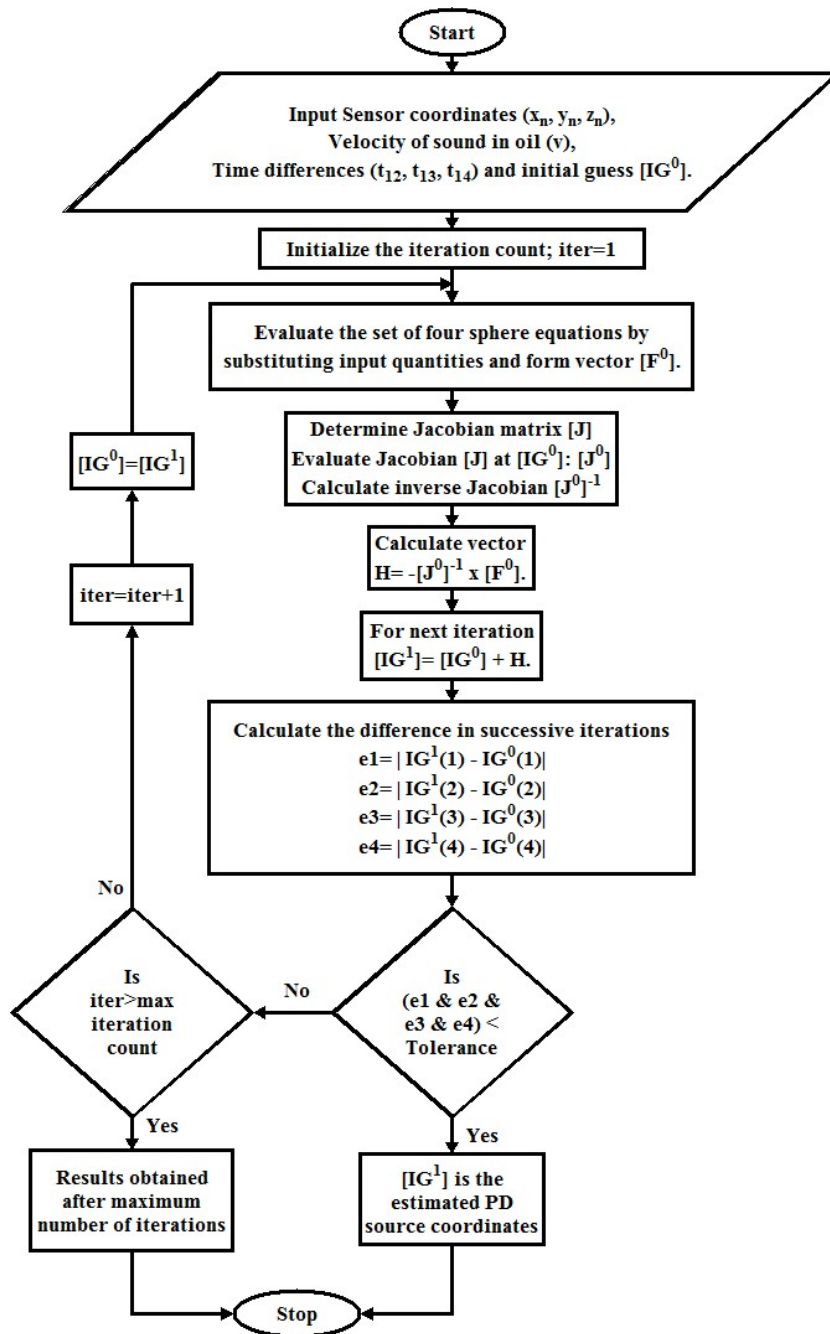


Figure 2.1 Generalised flowchart for PD source localisation in power transformers using the Newton's method.

### 2.3.3 Proposed improvements of Newton's method for PD source localisation

The major challenges while implementing Newton's method, for AEPD source local-

isation, are the difficulty in choosing an efficient initial guess and the Jacobian matrix becoming singular. The following sub-sections address these challenges and discuss the possibility of overcoming them using hybrid method (Section 2.3.3.1) and AE sensor positioning (Section 2.3.3.2).

### 2.3.3.1 Hybrid method

The characteristics and convergence of Newton's method is highly dependent on the quality of the initial guess. The GA can rapidly locate regions where the solutions are likely to exist, though it cannot guarantee the convergence to an exact solution. Newton's method, which is an iterative method, can solve non-linear equations with a greater accuracy, if proper initial guess is used (Karr *et al.* 1998). It is highly unlikely to expect an exact detection of the PD source location by using any of these algorithms alone. Combining GA and Newton's method is a good inkling to solve the problem of the PD source localisation. The hybrid method combines the advantages of both GA and Newton's method. The GA can be used to locate an appropriate initial guess, which are then supplied to Newton's method for solving the system of non-linear equations. The computational overhead of additional GA operation is negligible when compared to the computation involved in finding the inverse of the Jacobian matrix (Karr *et al.* 1998).

The GA is a search algorithm based on the mechanics of natural selection and natural genetics. In many optimisation methods, we move from a single point in the decision space to the next using some transition rule. By contrast, the GA works from a rich database of points, simultaneously climbing many peaks in parallel. Thus, the probability of finding a false peak is reduced over methods that go point to point (Reeves and Rowe 2002).

The GA implementation for the present work starts with forming an objective function based on the mathematical model of AEPD system (equation (2.1)) with four AE sensors. A random initial population of unknown quantities ( $[x, y, z, T_1]$ ) is created with a population size of 120 (Veloso *et al.* 2006). Each individual in the population are applied to the objective function to obtain a fitness function value (that should be minimised ideally to zero to arrive at an optimal solution). From the initial population,

new generations are created with a crossover fraction of 0.8 and elite count of 6. The stopping criteria chosen for the GA are: (i) maximum number of generation is 400; (ii) tolerance on fitness function value is  $1 \times 10^{-6}$ ; and (iii) stall generation limit is 50. The upper and lower bounds for  $x$ ,  $y$  and  $z$ -coordinates of the PD source are chosen such that they are within the bounds of the transformer tank. The lower bound for the acoustic signal arrival time ( $T_1$ ) is chosen as ‘zero’ and the upper bound is the ‘time required for the PD signal to travel maximum dimension of the tank’. The GA is implemented using MATLAB optimisation toolbox (Mathworks 2011). The GA trials are repeated 10 times, or until the best fitness function value is less than 0.1. The variables ( $[x, y, z, T_1]$ ) corresponding to the best fitness function value, obtained using the GA, are supplied as initial guess for Newton’s method. The solution thus obtained using Newton’s method (hybrid; GA-Newton method) is the estimated PD source location.

### **2.3.3.2 AE Sensor positioning for Newton’s method**

The position of the sensors on the transformer’s tank wall is the key factor, which results in a singular Jacobian matrix. The inverse of the Jacobian matrix is computed for all iterations of Newton’s method. The determinant of Jacobian matrix becomes zero if the rows (or columns) of the matrix are linearly dependent. If the Jacobian matrix is singular, then the algorithm fails to proceed with further iterations. The Jacobian matrix can become singular because of initial guess, PD source position (relative distances between the sensors and PD source), and the AE sensor position. As the location of PD source in a transformer is highly random, it is not possible to avoid singular Jacobian matrix by adjusting the PD source position. Therefore, a careful positioning of the sensors on the transformer’s tank wall and a careful initial guess selection can help in avoiding a singular Jacobian matrix.

The conditions for which the Jacobian determinant becomes zero (implies the Jacobian matrix is singular) are demonstrated using numerical examples. A transformer tank of size  $1 \text{ m} \times 1 \text{ m} \times 1 \text{ m}$  is considered for the demonstration. Four AE sensors are placed on the transformer’s tank wall. A  $[4 \times 3]$  sensor matrix can be formed by using the  $x$ ,  $y$ , and  $z$ -coordinates of the four sensors. The linear independence of the rows (or columns) of a non-square matrix can be checked by computing the null space

of the matrix. The null space, denoted by  $N(A)$  of a matrix  $A$  consists of all vectors  $x$  such that  $[A][x] = 0$ , The rows (or columns) of  $A$  are independent exactly when  $N(A)$  contains only a zero vector (Strang 1980).

Five different set of coordinate values are considered for the four sensors (as numerical examples):

- Set-1: All x-coordinates of the sensors are same;
- Set-2: All y-coordinates of the sensors are same;
- Set-3: All z-coordinates of the sensors are same;
- Set-4: All z-coordinates of the sensors are equal to zero; and
- Set-5: The null space of the sensor matrix contains a non-zero vector.

The numerical examples for the coordinates of the sensor for these five set of sensor arrangements are given in Table 2.1.

For the first three set of sensor arrangements (Set-1 to Set-3) there are infinitely many locations inside the transformer tank, which are equidistant from all the four sensors. If these locations happen to be the PD source position, then the Jacobian matrix becomes singular for any initial guess of Newton's method. These PD source positions are also given in Table 2.1.

In case of the last two set of sensor arrangements (Set-4 and Set-5), for any PD source location inside the transformer tank, the Jacobian matrix becomes singular if the initial guess considered for implementing Newton's method is a zero vector.

In addition, for any sensor arrangement, when all the sensors are equidistant from the PD source, the Jacobian matrix becomes singular if we use 'zero' as initial guess for the acoustic signal arrival time ( $T_1$ ) to the nearest sensor. The various generalized conditions for which the Jacobian matrix becomes singular and the suggested remedy via sensor re-positioning evolved from the numerical analysis are given in Table 2.2.

Therefore, from Table 2.2, the proposed guidelines for the AE sensor arrangement are as follows:

Table 2.1 The numerical examples of sensor arrangements (Set-1 to Set-5) with the corresponding PD source locations and the initial guesses that results in a singular Jacobian matrix

Set Number	Set 1			Set 2			Set 3			Set 4			Set 5		
Coordinate name	x	y	z	x	y	z	x	y	z	x	y	z	x	y	z
Sensor coordinates (m)	0.500	0.300	0.000	0.150	0.500	0.000	0.000	0.900	0.400	0.000	0.345	0.435	0.300	0.200	0.000
	0.500	0.750	0.000	0.800	0.500	0.000	1.000	0.900	0.400	0.735	0.525	0.000	0.300	0.600	0.000
	0.500	0.300	1.000	0.150	0.500	1.000	0.000	0.200	0.400	1.000	0.745	0.725	0.900	0.200	0.000
	0.500	0.750	1.000	0.800	0.500	1.000	1.000	0.200	0.400	0.325	0.435	1.000	0.900	0.600	0.000
PD coordinates (m)	*	0.525	0.500	0.475	*	0.500	0.500	0.550	*	*	*	*	*	*	*
Initial guess	Any initial guess			Any initial guess			Any initial guess			Zero vector			Zero vector		

\* Any coordinate value inside the transformer tank can be considered.



1. Sensors should be placed such that all the  $x$ , all the  $y$  or all the  $z$ -coordinates of the sensors are not zero or equal.
2. The null space of the sensor matrix (formed by the sensor coordinates) should contain only a zero vector, i.e. the rows and columns of the sensor matrix should be linearly independent.

In conclusion, these proposed guidelines for AE sensor positioning and avoiding a ‘zero’ initial guess for the acoustic signal arrival time ( $T_1$ ) helps in preventing the Jacobian matrix from becoming singular (for any PD position inside the tank).

## 2.4 Non-iterative method for PD source localisation

The existing non-iterative method uses the concept of the intersection of spheres. Two spheres intersect in a plane, and the source can be located on this intersecting plane. Two such planes intersect in a line and the PD source can be located on this line. The line intersects any one of the spheres in two points resulting in a quadratic equation. One of the solutions of this quadratic equation is the PD source location (Kundu *et al.* 2009).

In this method, a set of constants ( $k_1 - k_{20}$ ) are calculated using the known values of the sensor coordinates ( $x_n, y_n, z_n$ ), the velocity of sound in oil ( $v$ ), and the measured time-delays ( $t_{12}, t_{13}, t_{14}$ ) (Kundu *et al.* 2009). These constants are further used in calculating the four unknown quantities, namely, the PD source coordinates ( $x, y, z$ ) and the acoustic wave propagation time ( $T_1$ ) from source to the nearest sensor (Kundu *et al.* 2009). An analogous set of constants are derived in the present work, and the derivation is given in the subsequent sub-section.

### 2.4.1 Implementation of non-iterative method

The PD source is located by solving the system of non-linear sphere equations given in equation (2.9) to equation (2.12)

$$(x - x_1)^2 + (y - y_1)^2 + (z - z_1)^2 = (vT_1)^2 \quad (2.9)$$

$$(x - x_2)^2 + (y - y_2)^2 + (z - z_2)^2 = (v(T_1 + t_{12}))^2 \quad (2.10)$$

Table 2.2 The generalised conditions for which the Jacobian matrix becomes singular and the suggested remedy via sensor re-positioning

Condition number	Initial guess	Sensor positioning	PD position (time-delays)	Suggested remedy via sensor re-positioning
1	Any	All x, all y, or all z-coordinates are same	All sensors are equidistant from PD source	Sensors should be placed such that all x, all y, or all z-coordinates of the sensors are not equal
2	Zero vector	All x, all y, or all z-coordinates are zero	Any	Sensors should be placed such that all x, all y, or all z-coordinates of the sensors are not zero
3	Zero vector	The null space of the sensor matrix contains a non-zero vector	Any	The null space of the sensor matrix formed by the sensor coordinates should contain only a zero vector, i.e. the rows and columns of the sensor matrix should be linearly independent
4	$T_1=0$	Any	All sensors are equidistant from PD source	Cannot be avoided by sensor positioning

$$(x - x_3)^2 + (y - y_3)^2 + (z - z_3)^2 = (v(T_1 + t_{13}))^2 \quad (2.11)$$

$$(x - x_4)^2 + (y - y_4)^2 + (z - z_4)^2 = (v(T_1 + t_{14}))^2 \quad (2.12)$$

Any two of the spheres intersect in a plane and the source can be located on this intersecting plane. The equation of the plane formed by the intersection of two spheres can be obtained by taking the difference of the corresponding sphere equations. By taking the difference of equation (2.9) and equation (2.10), equation (2.9) and equation (2.11), and equation (2.9) and equation (2.12), three planes are obtained. These planes are given by equation (2.13) to equation (2.15).

$$2(x_1 - x_2)x + 2(y_1 - y_2)y + 2(z_1 - z_2)z - 2v^2t_{12}T_1 = x_1^2 - x_2^2 + y_1^2 - y_2^2 + z_1^2 - z_2^2 + v^2t_{12}^2 \quad (2.13)$$

$$2(x_1 - x_3)x + 2(y_1 - y_3)y + 2(z_1 - z_3)z - 2v^2t_{13}T_1 = x_1^2 - x_3^2 + y_1^2 - y_3^2 + z_1^2 - z_3^2 + v^2t_{13}^2 \quad (2.14)$$

$$2(x_1 - x_4)x + 2(y_1 - y_4)y + 2(z_1 - z_4)z - 2v^2t_{14}T_1 = x_1^2 - x_4^2 + y_1^2 - y_4^2 + z_1^2 - z_4^2 + v^2t_{14}^2 \quad (2.15)$$

From the plane equation (2.13) to equation (2.15), the unknown variable  $T_1$  has to be eliminated. The equation for  $T_1$  is obtained in terms of  $x$ ,  $y$ , and  $z$  from equation (2.13) and is given in equation (2.16). By substituting equation (2.16) in equation (2.14) and equation (2.15), we get two plane equations given in equation (2.17) and equation (2.18).

$$T_1 = \frac{2(x_1 - x_2)x + 2(y_1 - y_2)y + 2(z_1 - z_2)z - x_1^2 + x_2^2 - y_1^2 + y_2^2 - z_1^2 + z_2^2 - v^2t_{12}^2}{2v^2t_{12}} \quad (2.16)$$

$$2x\sigma_1 + 2y\sigma_3 + 2z\sigma_5 = \sigma_8 \quad (2.17)$$

$$2x\sigma_2 + 2y\sigma_4 + 2z\sigma_6 = \sigma_9 \quad (2.18)$$

where the constants  $\sigma_1$  to  $\sigma_9$  are given in equation (2.19) to equation (2.27), respectively.

$$\sigma_1 = \frac{(x_1 - x_2)}{2t_{12}v^2} - \frac{(x_1 - x_3)}{2t_{13}v^2} \quad (2.19)$$

$$\sigma_2 = \frac{(x_1 - x_2)}{2t_{12}v^2} - \frac{(x_1 - x_4)}{2t_{14}v^2} \quad (2.20)$$

$$\sigma_3 = \frac{(y_1 - y_2)}{2t_{12}v^2} - \frac{(y_1 - y_3)}{2t_{13}v^2} \quad (2.21)$$

$$\sigma_4 = \frac{(y_1 - y_2)}{2t_{12}v^2} - \frac{(y_1 - y_4)}{2t_{14}v^2} \quad (2.22)$$

$$\sigma_5 = \frac{(z_1 - z_2)}{2t_{12}v^2} - \frac{(z_1 - z_3)}{2t_{13}v^2} \quad (2.23)$$

$$\sigma_6 = \frac{(z_1 - z_2)}{2t_{12}v^2} - \frac{(z_1 - z_4)}{2t_{14}v^2} \quad (2.24)$$

$$\sigma_7 = \frac{t_{12}^2v^2 + x_1^2 - x_2^2 + y_1^2 - y_2^2 + z_1^2 - z_2^2}{2t_{12}v^2} \quad (2.25)$$

$$\sigma_8 = \sigma_7 - \frac{t_{13}^2v^2 + x_1^2 - x_3^2 + y_1^2 - y_3^2 + z_1^2 - z_3^2}{2t_{13}v^2} \quad (2.26)$$

$$\sigma_9 = \sigma_7 - \frac{t_{14}^2v^2 + x_1^2 - x_4^2 + y_1^2 - y_4^2 + z_1^2 - z_4^2}{2t_{14}v^2} \quad (2.27)$$

Two planes intersect in a line and the PD source can be located on this line. The equation of the line formed by the intersection of two planes given in equation (2.17) and equation (2.18) are obtained as follows. Let  $P$  be a vector parallel to the required line, then

$$P = \begin{vmatrix} \hat{i} & \hat{j} & \hat{k} \\ 2\sigma_1 & 2\sigma_3 & 2\sigma_5 \\ 2\sigma_2 & 2\sigma_4 & 2\sigma_6 \end{vmatrix}$$

where  $\hat{i}$ ,  $\hat{j}$ , and  $\hat{k}$  are the unit vectors in x, y, and z directions, respectively.

$$P = \hat{i}4(\sigma_3\sigma_6 - \sigma_4\sigma_5) - \hat{j}4(\sigma_1\sigma_6 - \sigma_2\sigma_5) + \hat{k}4(\sigma_1\sigma_4 - \sigma_2\sigma_3) \quad (2.28)$$

$$P = \hat{i}4\sigma_{11} - \hat{j}4\sigma_{10} + \hat{k}4\sigma_{12} \quad (2.29)$$

where the constants  $\sigma_{10}$  to  $\sigma_{12}$  are given in equation (2.30) to equation (2.32), re-

spectively.

$$\sigma_{10} = \sigma_1 \sigma_6 - \sigma_2 \sigma_5 \quad (2.30)$$

$$\sigma_{11} = \sigma_3 \sigma_6 - \sigma_4 \sigma_5 \quad (2.31)$$

$$\sigma_{12} = \sigma_1 \sigma_4 - \sigma_2 \sigma_3 \quad (2.32)$$

Therefore,

$$x_0 = 4\sigma_{11} \quad (2.33)$$

$$y_0 = -4\sigma_{10} \quad (2.34)$$

$$z_0 = 4\sigma_{12} \quad (2.35)$$

The point  $(x_1, y_1, z_1)$  on the line can be located at  $z = 0$  plane. Thus, substitute  $z = 0$  in the planes given in equation (2.17) and equation (2.18) to get  $(x_1, y_1, z_1)$  given in equation (2.36) to equation (2.38), respectively.

$$x_1 = \frac{\sigma_{14}}{\sigma_{15}} \quad (2.36)$$

$$y_1 = -\frac{\sigma_{13}}{\sigma_{15}} \quad (2.37)$$

$$z_1 = 0 \quad (2.38)$$

where the constants  $\sigma_{13}$  to  $\sigma_{15}$  are given in equation (2.39) to equation (2.41), respectively.

$$\sigma_{13} = \sigma_2 \sigma_8 - \sigma_1 \sigma_9 \quad (2.39)$$

$$\sigma_{14} = \sigma_4 \sigma_8 - \sigma_3 \sigma_9 \quad (2.40)$$

$$\sigma_{15} = 2(\sigma_1 \sigma_4 - \sigma_2 \sigma_3) \quad (2.41)$$

The equation of the line formed by the intersection of two planes given in equation (2.17) and equation (2.18) is given in equation (2.42)

$$\frac{x - \frac{\sigma_{14}}{\sigma_{15}}}{\frac{\sigma_{11}}{\sigma_{12}}} = \frac{y + \frac{\sigma_{13}}{\sigma_{15}}}{-\frac{\sigma_{10}}{\sigma_{12}}} = z = A \quad (2.42)$$

From equation (2.42), any point on the line  $(x, y, z)$  can be obtained and is given in equation (2.43) to equation (2.45).

$$x = \frac{\sigma_{11}}{\sigma_{12}}A + \frac{\sigma_{14}}{\sigma_{15}} \quad (2.43)$$

$$y = -\frac{\sigma_{10}}{\sigma_{12}}A - \frac{\sigma_{13}}{\sigma_{15}} \quad (2.44)$$

$$z = A \quad (2.45)$$

The value of  $T_1$  is obtained in terms of  $A$  by substituting equation (2.43) to equation (2.45) in equation (2.16).

$$T_1 = \frac{2A\sigma_{16} - \sigma_{17}}{2v^2t_{12}} \quad (2.46)$$

where the constants  $\sigma_{16}$  and  $\sigma_{17}$  are given in equation (2.47) and equation (2.48), respectively.

$$\sigma_{16} = z_1 - z_2 - \frac{\sigma_{10}(y_1 - y_2) - \sigma_{11}(x_1 - x_2)}{\sigma_{12}} \quad (2.47)$$

$$\begin{aligned} \sigma_{17} = & t_{12}^2v^2 + x_1^2 - x_2^2 + y_1^2 - y_2^2 + z_1^2 - z_2^2 \\ & + \frac{2\sigma_{13}(y_1 - y_2) - 2\sigma_{14}(x_1 - x_2)}{\sigma_{15}} \end{aligned} \quad (2.48)$$

The line intersects any one of the spheres in two points, resulting in a quadratic equation. To find the quadratic equation formed by the intersection of line given in equation (2.42) and sphere given in equation (2.9), equation (2.43) to equation (2.46) are substituted in equation (2.9). The resulting quadratic equation in variable  $A$  is given in equation (2.49).

$$\sigma_{20}A^2 + \sigma_{21}A + \sigma_{22} = 0 \quad (2.49)$$

where the constants  $\sigma_{18}$  to  $\sigma_{22}$  are given in equation (2.50) to equation (2.54), respectively.

$$\sigma_{18} = y_1 + \frac{\sigma_{13}}{\sigma_{15}} \quad (2.50)$$

$$\sigma_{19} = x_1 - \frac{\sigma_{14}}{\sigma_{15}} \quad (2.51)$$

$$\sigma_{20} = \left(\frac{\sigma_{10}}{\sigma_{12}}\right)^2 + \left(\frac{\sigma_{11}}{\sigma_{12}}\right)^2 - \left(\frac{\sigma_{16}}{t_{12}v}\right)^2 + 1 \quad (2.52)$$

$$\sigma_{21} = -2z_1 + \frac{2\sigma_{10}\sigma_{18}}{\sigma_{12}} - \frac{2\sigma_{11}\sigma_{19}}{\sigma_{12}} + \frac{\sigma_{16}\sigma_{17}}{t_{12}^2v^2} \quad (2.53)$$

$$\sigma_{22} = \sigma_{18}^2 + \sigma_{19}^2 + z_1^2 - \frac{\sigma_{17}^2}{4t_{12}^2 v^2} \quad (2.54)$$

The unknown quantities  $(x, y, z, T_1)$  are estimated by substituting the value of  $A$  in equation (2.43) to equation (2.46). The generalised flowchart for PD source localisation in power transformers using the existing non-iterative method is given in Figure 2.2. The challenges faced when using the existing non-iterative method for the PD source localisation are discussed in the following sub-section.

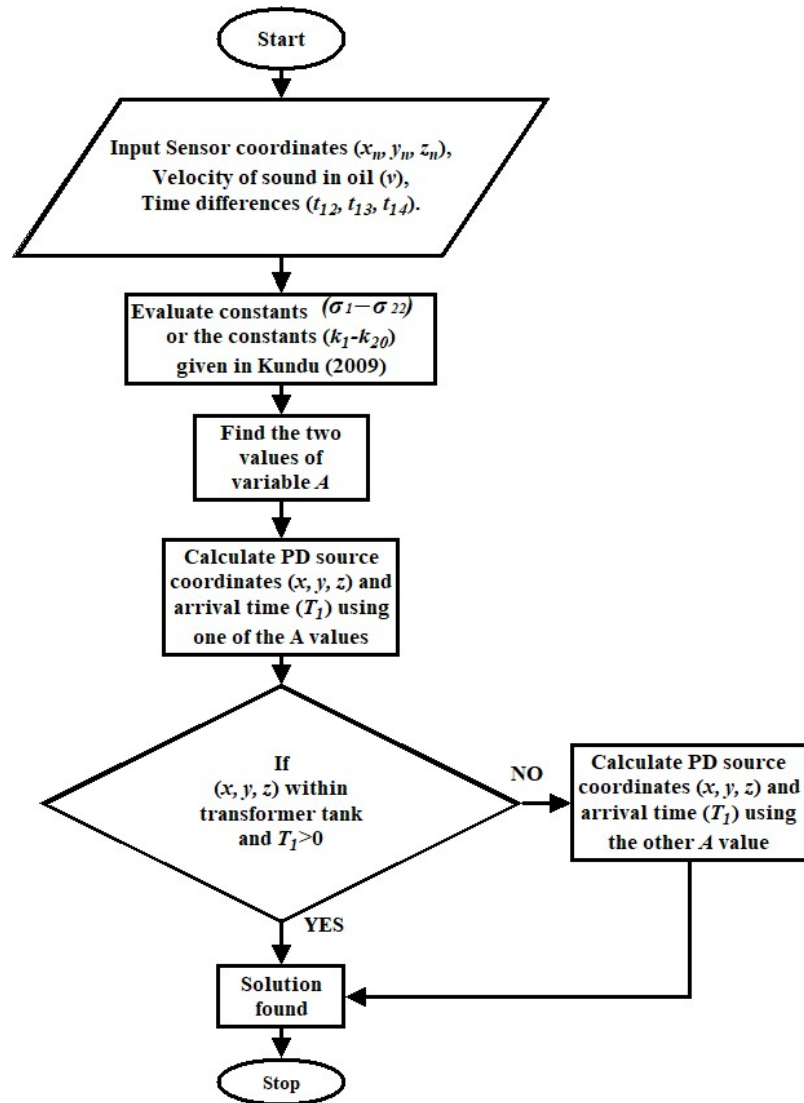


Figure 2.2 Generalised flowchart for PD source localisation in power transformers using the existing non-iterative method.

## 2.4.2 Challenges faced when implementing non-iterative method

In this method, a set of constants ( $\sigma_1 - \sigma_{22}$ ) are calculated using the known values of the sensor coordinates ( $x_n, y_n, z_n$ ), the velocity of sound in oil ( $v$ ), and the measured time-delays ( $t_{12}, t_{13}, t_{14}$ ). These constants are further used in calculating the four unknown quantities, namely, the PD source coordinates ( $x, y, z$ ) and the acoustic wave propagation time ( $T_1$ ) from source to the nearest sensor. This method fails to locate the PD source whenever numerical values of some of the constants ( $\sigma_1 - \sigma_{22}$ ) cannot be determined. The constants become undetermined (NaN) when zero appears in the denominator of these constants. These constants may become undetermined because of the time-delays (relative distances between the PD source and the sensors), the sensor positioning, or both. The conditions for which the non-iterative method fails to locate the PD source are analysed and summarised in Table 2.3. The existing non-iterative method given in Kundu *et al.* (2009) also fails to locate the PD source for these same conditions.

## 2.4.3 Proposed improvement of non-iterative method for PD source localisation

The conditions 1 to 12 given in Table 2.3 are overcome by proposing an extension to the existing non-iterative method and by the AE sensor positioning. These are discussed subsequently.

### 2.4.3.1 Extension of the existing non-iterative method

The non-iterative method can be implemented reliably only when the method can locate the PD source irrespective of its position within the tank. The existing non-iterative method can locate the PD source if and only if there is one sensor nearest to the PD source. Conditions 10, 11, and 12 given in Table 2.3 occur when there are two or more sensors nearest to the PD source. These situations result into one or more time-delays becoming zero. As the PD position inside the transformer tank is highly random, these conditions cannot be avoided. Thus, while using the time-difference approach based



Table 2.3 Conditions for which the existing non-iterative method fails to locate the PD source

Condition number	Sensor positioning	Time-delays	Associated constants that turn out to be undetermined
1	$x_1 = x_2 = x_3 = x_4$	For any time-delays	$\sigma_{16}$ to $\sigma_{21}$
2	$y_1 = y_2 = y_3 = y_4$		
3	$x_1 = x_2 = x_3$ and $y_1 = y_2 = y_3$		
4	$x_1 = x_2 = x_4$ and $y_1 = y_2 = y_4$		
5	$x_1 - x_2 = y_1 - y_2$ and $x_1 - x_3 = y_1 - y_3$ and $x_1 - x_4 = y_1 - y_4$		
6	$y_2 = y_3 = y_4$	$t_{12} = t_{13} = t_{14}$	$\sigma_{16}$ to $\sigma_{21}$
7	$x_2 = x_3 = x_4$	$t_{12} = t_{13} = t_{14}$	
8	$x_2 = x_3$ and $y_2 = y_3$	$t_{12} = t_{13}$	
9	$x_2 = x_4$ and $y_2 = y_4$	$t_{12} = t_{14}$	
10	For any sensor positioning	$t_{12} = t_{13} = t_{14} = 0$	$\sigma_1$ to $\sigma_9$ and $\sigma_{20}$ to $\sigma_{22}$
11		$t_{12} = t_{13} = 0$	
12		$t_{12} = 0$	

non-iterative method, it is important to consider the three special cases in which one or more time-delays become zero (see Table 2.3). These cases are:

- Case 1 (Condition 10): All the four sensors are equidistant from the PD source location ( $t_{12} = t_{13} = t_{14} = 0$ ).
- Case 2 (Condition 11): Three sensors are equidistant from the PD source location and nearer to the PD source location than the other sensor ( $t_{12} = t_{13} = 0$ ).

- Case 3 (Condition 12): Two sensors are equidistant from the PD source location and nearer to the PD source location than the other two sensors ( $t_{12} = 0$ ).

If the four sensors can be placed on the surface of a sphere, then the centre of the sphere is equidistant from all the four sensors. If the PD source position happens to be at this equidistant point, then it results in Case 1.

If the three sensors (among the four) are not collinear, then between each pair of sensors there will be an equidistant plane. These planes intersect in a line such that every point on this line is equidistant from the three sensors. If the PD source position happens to be on this line, when these three sensors (among the four) are the nearest sensors to the PD source, then it results in Case 2.

Between any two sensors (among the four), there will be a plane such that every point in the plane is equidistant from two sensors. If the PD source position is in this plane, when these two sensors are the nearest sensors to the PD source, then it results in Case 3.

The non-iterative method can be implemented reliably only when we consider these three special cases with the existing method. The constants and equations for finding the unknown quantities ( $x, y, z, T_1$ ) for all three special cases are derived. They are given in the subsequent sub-sections. The generalised flowchart for AEPD source localisation in transformers using the proposed non-iterative method (existing non-iterative method with proposed extension) is given in Figure 2.3. In the flow chart, the highlighted portion shows the proposed extension of the existing non-iterative method.

#### 2.4.3.2 Case 1: $t_{12} = t_{13} = t_{14} = 0$

$$\alpha_1 = (x_2^2 - x_1^2) + (y_2^2 - y_1^2) + (z_2^2 - z_1^2) \quad (2.55)$$

$$\alpha_2 = (x_3^2 - x_1^2) + (y_3^2 - y_1^2) + (z_3^2 - z_1^2) \quad (2.56)$$

$$\alpha_3 = (x_4^2 - x_1^2) + (y_4^2 - y_1^2) + (z_4^2 - z_1^2) \quad (2.57)$$

$$\alpha_4 = x_2 - x_1 \quad (2.58)$$

$$\alpha_5 = y_2 - y_1 \quad (2.59)$$

$$\alpha_6 = z_2 - z_1 \quad (2.60)$$

$$\alpha_7 = x_3 - x_1 \quad (2.61)$$

$$\alpha_8 = y_3 - y_1 \quad (2.62)$$

$$\alpha_9 = z_3 - z_1 \quad (2.63)$$

$$\alpha_{10} = x_4 - x_1 \quad (2.64)$$

$$\alpha_{11} = y_4 - y_1 \quad (2.65)$$

$$\alpha_{12} = z_4 - z_1 \quad (2.66)$$

$$\alpha_{13} = \frac{2\alpha_4\alpha_8 - 2\alpha_5\alpha_7}{\alpha_4} \quad (2.67)$$

$$\alpha_{14} = \frac{2\alpha_4\alpha_9 - 2\alpha_6\alpha_7}{\alpha_4} \quad (2.68)$$

$$\alpha_{15} = \frac{\alpha_1\alpha_7 - \alpha_2\alpha_4}{\alpha_4} \quad (2.69)$$

$$\alpha_{16} = \frac{2\alpha_5\alpha_{10}\alpha_{14} - 2\alpha_6\alpha_{10}\alpha_{13} - 2\alpha_4\alpha_{11}\alpha_{14} + 2\alpha_4\alpha_{12}\alpha_{13}}{\alpha_4\alpha_{13}} \quad (2.70)$$

$$\alpha_{17} = \frac{\alpha_3\alpha_4\alpha_{13} - \alpha_1\alpha_{10}\alpha_{13} - 2\alpha_5\alpha_{10}\alpha_{15} + 2\alpha_4\alpha_{11}\alpha_{15}}{\alpha_4\alpha_{13}} \quad (2.71)$$

$$x = \frac{\alpha_1\alpha_{13}\alpha_{16} + 2\alpha_5\alpha_{14}\alpha_{17} + 2\alpha_5\alpha_{15}\alpha_{16} - 2\alpha_6\alpha_{13}\alpha_{17}}{2\alpha_4\alpha_{13}\alpha_{16}} \quad (2.72)$$

$$y = \frac{-\alpha_{14}\alpha_{17} - \alpha_{15}\alpha_{16}}{\alpha_{13}\alpha_{16}} \quad (2.73)$$

$$z = \frac{\alpha_{17}}{\alpha_{16}} \quad (2.74)$$

$$T_1 = \sqrt{\frac{(x - x_1)^2 + (y - y_1)^2 + (z - z_1)^2}{v^2}} \quad (2.75)$$

### 2.4.3.3 Case 2: $t_{12} = t_{13} = 0$

$$\beta_1 = (x_2^2 - x_1^2) + (y_2^2 - y_1^2) + (z_2^2 - z_1^2) \quad (2.76)$$

$$\beta_2 = (x_3^2 - x_1^2) + (y_3^2 - y_1^2) + (z_3^2 - z_1^2) \quad (2.77)$$

$$\beta_3 = (x_4^2 - x_1^2) + (y_4^2 - y_1^2) + (z_4^2 - z_1^2) - v^2 t_{14}^2 \quad (2.78)$$

$$\beta_4 = x_2 - x_1 \quad (2.79)$$

$$\beta_5 = y_2 - y_1 \quad (2.80)$$

$$\beta_6 = z_2 - z_1 \quad (2.81)$$

$$\beta_7 = x_3 - x_1 \quad (2.82)$$

$$\beta_8 = y_3 - y_1 \quad (2.83)$$

$$\beta_9 = z_3 - z_1 \quad (2.84)$$

$$\beta_{10} = \frac{\beta_1 \beta_8 - \beta_2 \beta_5}{2(\beta_5 \beta_7 - \beta_4 \beta_8)} \quad (2.85)$$

$$\beta_{11} = \frac{\beta_6 \beta_8 - \beta_5 \beta_9}{\beta_5 \beta_7 - \beta_4 \beta_8} \quad (2.86)$$

$$\beta_{12} = \frac{\beta_1 \beta_7 - \beta_2 \beta_4}{2(\beta_5 \beta_7 - \beta_4 \beta_8)} \quad (2.87)$$

$$\beta_{13} = \frac{\beta_6 \beta_7 - \beta_4 \beta_9}{\beta_5 \beta_7 - \beta_4 \beta_8} \quad (2.88)$$

$$\beta_{14} = \frac{\beta_3 + 2\beta_{10}(x_4 - x_1) - 2\beta_{12}(y_4 - y_1)}{2v^2 t_{14}} \quad (2.89)$$

$$\beta_{15} = \frac{\beta_{11}(x_4 - x_1) - \beta_{13}(y_4 - y_1) + (z_4 - z_1)}{v^2 t_{14}} \quad (2.90)$$

$$\beta_{16} = \beta_{11}^2 + \beta_{13}^2 + 1 - v^2 \beta_{15}^2 \quad (2.91)$$

$$\begin{aligned} \beta_{17} = & 2v^2 \beta_{14} \beta_{15} - 2\beta_{11}(\beta_{10} + x_1) - \\ & 2\beta_{13}(\beta_{12} - y_1) - 2z_1 \end{aligned} \quad (2.92)$$

$$\beta_{18} = (\beta_{10} + x_1)^2 + (\beta_{12} - y_1)^2 + z_1^2 - v^2 \beta_{14}^2 \quad (2.93)$$

$$A = \frac{-\beta_{17} \pm \sqrt{\beta_{17}^2 - 4\beta_{16}\beta_{18}}}{2\beta_{16}} \quad (2.94)$$

$$x = \beta_{11}A - \beta_{10} \quad (2.95)$$

$$y = \beta_{12} - A\beta_{13} \quad (2.96)$$

$$z = A \quad (2.97)$$

$$T_1 = \beta_{14} - A\beta_{15} \quad (2.98)$$

#### 2.4.3.4 Case 3: $t_{12} = 0$

$$\gamma_1 = (x_2^2 - x_1^2) + (y_2^2 - y_1^2) + (z_2^2 - z_1^2) \quad (2.99)$$

$$\gamma_2 = (x_3^2 - x_1^2) + (y_3^2 - y_1^2) + (z_3^2 - z_1^2) - v^2 t_{13}^2 \quad (2.100)$$

$$\gamma_3 = (x_4^2 - x_1^2) + (y_4^2 - y_1^2) + (z_4^2 - z_1^2) - v^2 t_{14}^2 \quad (2.101)$$

$$\gamma_4 = x_2 - x_1 \quad (2.102)$$

$$\gamma_5 = y_2 - y_1 \quad (2.103)$$

$$\gamma_6 = z_2 - z_1 \quad (2.104)$$

$$\gamma_7 = \frac{x_3 - x_1}{2v^2 t_{13}} - \frac{x_4 - x_1}{2v^2 t_{14}} \quad (2.105)$$

$$\gamma_8 = \frac{y_3 - y_1}{2v^2 t_{13}} - \frac{y_4 - y_1}{2v^2 t_{14}} \quad (2.106)$$

$$\gamma_9 = \frac{z_3 - z_1}{2v^2 t_{13}} - \frac{z_4 - z_1}{2v^2 t_{14}} \quad (2.107)$$

$$\gamma_{10} = \frac{\gamma_2}{2v^2 t_{13}} - \frac{\gamma_3}{2v^2 t_{14}} \quad (2.108)$$

$$\gamma_{11} = \frac{\gamma_1 \gamma_8 - \gamma_5 \gamma_{10}}{2(\gamma_5 \gamma_7 - \gamma_4 \gamma_8)} \quad (2.109)$$

$$\gamma_{12} = \frac{\gamma_6 \gamma_8 - \gamma_5 \gamma_9}{\gamma_5 \gamma_7 - \gamma_4 \gamma_8} \quad (2.110)$$

$$\gamma_{13} = \frac{\gamma_1 \gamma_7 - \gamma_4 \gamma_{10}}{2(\gamma_5 \gamma_7 - \gamma_4 \gamma_8)} \quad (2.111)$$

$$\gamma_{14} = \frac{\gamma_6 \gamma_7 - \gamma_4 \gamma_9}{\gamma_5 \gamma_7 - \gamma_4 \gamma_8} \quad (2.112)$$

$$\gamma_{15} = \frac{\gamma_2 + 2\gamma_{11}(x_3 - x_1) - 2\gamma_{13}(y_3 - y_1)}{2v^2 t_{13}} \quad (2.113)$$

$$\gamma_{16} = \frac{\gamma_{12}(x_3 - x_1) - \gamma_{14}(y_3 - y_1) + (z_3 - z_1)}{v^2 t_{13}} \quad (2.114)$$

$$\gamma_{17} = \gamma_{12}^2 + \gamma_{14}^2 + 1 - v^2 \gamma_{16}^2 \quad (2.115)$$

$$\begin{aligned} \gamma_{18} = & 2v^2 \gamma_{15} \gamma_{16} - 2\gamma_{12}(\gamma_{11} + x_1) \\ & - 2\gamma_{14}(\gamma_{13} - y_1) - 2z_1 \end{aligned} \quad (2.116)$$

$$\gamma_{19} = (\gamma_{11} + x_1)^2 + (\gamma_{13} - y_1)^2 + z_1^2 - v^2 \gamma_{15}^2 \quad (2.117)$$

$$A = \frac{-\gamma_{18} \pm \sqrt{\gamma_{18}^2 - 4\gamma_{17}\gamma_{19}}}{2\gamma_{17}} \quad (2.118)$$

$$x = \gamma_{12}A - \gamma_{11} \quad (2.119)$$

$$y = \gamma_{13} - A\gamma_{14} \quad (2.120)$$

$$z = A \quad (2.121)$$

$$T_1 = \gamma_{15} - A\gamma_{16} \quad (2.122)$$

#### 2.4.3.5 AE sensor positioning for the non-iterative method

The sensor placement plays an important role in the successful localisation of the PD source. From the analysis given in Table 2.3, conditions 1 to 4 and conditions 6 to 9 can be avoided by choosing distinct  $x$ -coordinate values and distinct  $y$ -coordinate values for the four sensors. Condition 5 (implies sensors placed in a straight line) can be avoided by not placing all four sensors in a straight line on the transformer tank wall. A similar

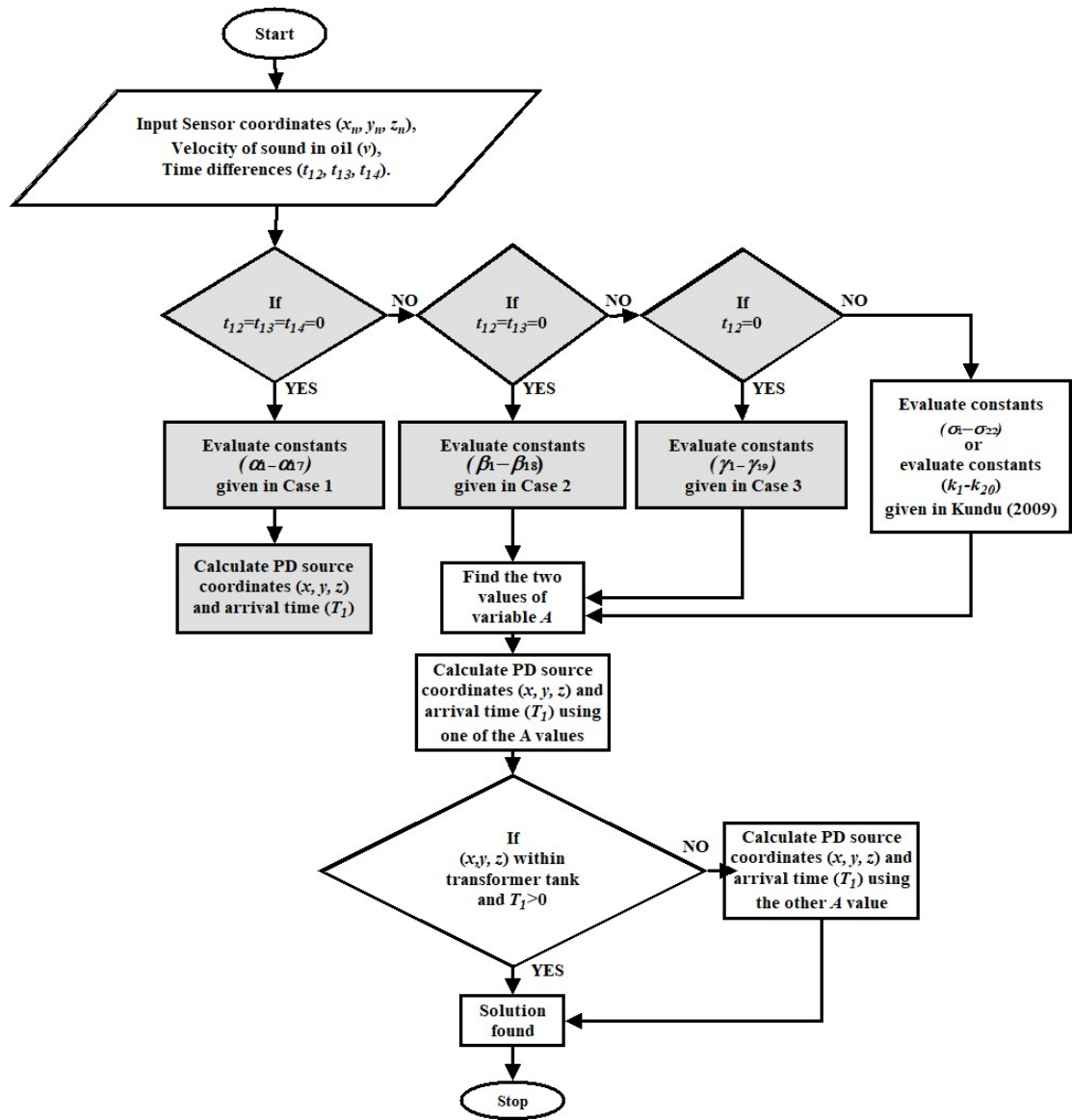


Figure 2.3 Generalised flowchart for PD source localisation in power transformers using the proposed non-iterative method (the highlighted portion shows the proposed extension of the existing non-iterative method).

analysis is conducted for the proposed extension of the non-iterative method. From the analysis, in Case 1 of the proposed method, when all the  $z$ -coordinate values of the sensors are same, the constant  $\alpha_{16}$  becomes zero. The constant  $\alpha_{16}$  appears in the denominator of equation (2.72) to equation (2.74); hence, the algorithm fails to locate the PD source. To avoid such a situation, the sensors should have distinct  $z$ -coordinate values.

Therefore, the proposed guidelines for the sensor arrangement are as follows

1. The sensors should be placed with distinct  $x$ -coordinate values,  $y$ -coordinate values, and  $z$ -coordinate values.
2. All the four sensors should not be placed in a straight line.

## **2.5 Performance verification of algorithms: numerical experiments**

The efficacy of the various methods such as Newton's method, hybrid method, existing non-iterative method, and proposed non-iterative method are tested using numerical experiments. Computer codes are developed for the implementation of these methods for the PD source localisation.

### **2.5.1 Data for numerical experiments**

A transformer tank of size  $1\text{ m} \times 1\text{ m} \times 1\text{ m}$  is considered for the analysis. Four AE sensors are placed on the transformer's tank wall conforming to the proposed guidelines for the sensor positioning given in Section 2.3.3.2 (for Newton's method) and Section 2.4.3.5 (for proposed non-iterative method). The coordinate of such a set of four sensors that are used for the numerical experiment are given in Table 2.4. One sample point (PD source location) corresponding to each case (Cases 1 to 3 explained in Section 2.4.3.1) and one random PD source position are considered for the numerical experiments. These four PD source positions (PD-1 to PD-4) along with the sensor sequence based on acoustic signal arrival time and the corresponding time-delays are given in Table 2.5.

### **2.5.2 Procedure for numerical experiments**

The PD source is located using Newton's method, hybrid method, existing non-iterative method, and proposed non-iterative method. The localisation results of all these methods are compared in terms of accuracy and computational time. For iterative methods like Newton's method and hybrid method, the PD source estimation is repeated 100



Table 2.4 Coordinates of the sensors used for the numerical experiment (conforming to the guidelines given in sub-sections 2.3.3.2 and 2.4.3.5)

Serial number of the sensor	Sensor coordinates (m)		
	$x_n$	$y_n$	$z_n$
1	0.00	0.85	0.20
2	0.60	0.65	0.00
3	1.00	0.45	0.40
4	0.80	0.25	1.00

Table 2.5 Coordinates of the PD source used for the numerical experiment, sensor sequence based on signal arrival time, and the corresponding time-delays

Serial number	PD position	PD source coordinates (m)			Time-delays ( $\mu s$ )			Sensor sequence based on signal arrival time			
		$x$	$y$	$z$	$t_{12}$	$t_{13}$	$t_{14}$	S1	S2	S3	S4
1	PD-1	0.40	0.55	0.60	0	0	0	1	2	3	4
2	PD-2	0.55	0.95	0.65	0	0	73.6	1	2	3	4
3	PD-3	0.85	0.60	0.75	0	246	405	4	3	2	1
4	PD-4	0.25	0.65	0.45	116	263	332	1	2	3	4

times using 100 different initial guesses. The initial guess for Newton's method is generated using the MATLAB random number generator. The initial guess for hybrid method is estimated using the GA. The average of these 100 PD source locations calculated, excluding the diverged trials, is considered as the estimated PD source location for iterative methods. The trials are said to be diverged when the solution is having a negative value for any of the PD source coordinates ( $x$ ,  $y$ ,  $z$ ) or for the acoustic signal arrival time to the nearest sensor ( $T_1$ ).

### 2.5.3 Results and Discussion

A comparison of the PD source localisation results of Newton's method and hybrid method based on 100 trials for each PD source position (PD-1 to PD-4) are given in Table 2.6. The various trials that diverged or with high distance error (greater than 10%), along with the corresponding initial guess, when using Newton's method for the localisation of PD source positions PD-1, PD-2, PD-3, and PD-4 are given in Tables 2.7, 2.8, 2.9, and 2.10, respectively.

The estimated PD source coordinates (in a tank with maximum tank dimension

given in equation (2.123)), the distance percentage error (as given in equation (2.124)), and the computational time when using the different algorithms for the four PD source positions are given in Table 2.11.

$$\text{Maximum tank dimension} = \sqrt{l^2 + b^2 + h^2} \quad (2.123)$$

where  $l$ ,  $b$ , and  $h$  are the length, breadth, and height of the transformer tank.

$$\text{Distance percentage error} = \frac{\text{Distance between actual and located PD source}}{\text{Maximum tank dimension}} \times 100 \quad (2.124)$$

Table 2.6 The comparison of PD source localisation result of Newton's method and hybrid method based on 100 trials for each PD source position

Method	PD sample	Maximum error (%)	Number of trials diverged	Number of trials with error greater than 10%
Newton's method	PD-1	0.0000	4	0
	PD-2	26.180	3	3
	PD-3	243.68	5	4
	PD-4	7.5600	5	0
Hybrid method	PD-1	0.0000	0	0
	PD-2	0.0600	0	0
	PD-3	7.9400	0	0
	PD-4	0.1400	0	0

The distance percentage error calculated for the estimated PD source position PD-3, for 100 trials, for Newton's method and hybrid method is shown in Figure 2.4. The trials with more than 1% error is shown in the figure. The error is marked as NaN for the divergent trials. The divergent trials occurred for Newton's method and the maximum error in the case of convergent trials in Newton's method is 243.68%. Whereas, in hybrid method, there are no divergent trials and all the trials have error less than 10%.

From Table 2.6, when localising the PD source using Newton's method, the distance error for one of the trials goes as high as 243.68% for PD-3. The maximum error in PD source localisation is less for the hybrid method, when compared to Newton's method, for all the four PD source locations. Moreover, some of the trials diverged when using

Table 2.7 The PD source localisation results of the diverged trials or the trials with high distance error (greater than 10%) when using Newton's method for localising PD-1

Serial number	Initial guess			Solution			Distance error (%)		
	PD source coordinates (m)			PD source coordinates (m)					
	$x$	$y$	$z$	$x$	$y$	$z$			
1	0.8950	0.0246	0.1341	0.4000	0.5500	0.6000	0.0933	-0.45	NaN
2	0.9884	0.4421	0.9726	0.4000	0.5500	0.6000	0.0549	-0.46	NaN
3	0.0024	0.0581	0.9582	0.4000	0.5500	0.6000	0.1300	-0.68	NaN
4	0.9536	0.2309	0.0054	0.4000	0.5500	0.6000	0.4100	-1.59	NaN

Table 2.8 The PD source localisation results of the diverged trials or the trials with high distance error (greater than 10%) when using Newton's method for localising PD-2

Serial number	Initial guess				Solution				Distance error (%)
	PD source coordinates (m)			Acoustic signal arrival time, $T_1$ (ms)	PD source coordinates (m)			Acoustic signal arrival time, $T_1$ (ms)	
	$x$	$y$	$z$		$x$	$y$	$z$		
1	0.6719	0.7912	0.3172	0.0218	0.2500	0.1500	0.5500	-0.581	NaN
2	0.9767	0.4942	0.1942	0.1000	0.0792	-0.3055	0.4931	-1.202	NaN
3	0.0483	0.1164	0.1853	0.0399	-0.3744	-1.5150	0.3419	-2.849	NaN
4	0.8808	0.2633	0.1290	0.3500	0.6401	1.1903	0.6800	0.835	14.92
5	0.4511	0.0333	0.1454	0.3000	0.7081	1.3717	0.7027	1.082	26.18
6	0.0262	0.1343	0.5978	0.0337	0.6463	1.2067	0.6821	0.857	15.94

Table 2.9 The PD source localisation results of the diverged trials or the trials with high distance error (greater than 10%) when using Newton's method for localising PD-3

Serial number	Initial guess			Solution			Distance error (%)	
	PD source coordinates (m)			PD source coordinates (m)				Acoustic signal arrival time, $T_1$ (ms)
	x	y	z	x	y	z		
1	0.2790	0.9609	0.6015	0.0430	1.0430	2.0430	-0.3900	NaN
2	0.9903	0.0172	0.8829	0.0454	-0.1424	0.2720	-0.3800	NaN
3	0.8812	0.3037	0.9343	0.4360	0.2180	0.5041	-0.0571	NaN
4	0.7992	0.5012	0.5969	0.3861	0.1720	0.4744	-0.0988	NaN
5	0.1324	0.9914	0.9423	-0.0480	-0.2286	0.2165	-4.6000	NaN
6	0.9643	0.5599	0.7531	3.6929	3.2231	2.4388	2.6710	243.68
7	0.9065	0.9214	0.9942	1.5686	1.2630	1.1769	0.8910	61.59
8	0.8927	0.4764	0.9095	0.5398	0.3138	0.5657	0.0298	26.59
9	0.5986	0.5166	0.9748	0.6256	0.3930	0.6167	0.1020	19.23

Table 2.10 The PD source localisation results of the diverged trials or the trials with high distance error (greater than 10%) when using Newton's method for localising PD-4

Serial number	Initial guess			Solution			Distance error (%)
	PD source coordinates (m)			PD source coordinates (m)			
	x	y	z	x	y	z	
1	0.9833	0.8232	0.9179	0.3953	0.4864	0.5436	NaN
2	0.9811	0.9833	0.4852	0.5573	0.3041	0.6478	NaN
3	0.9133	0.9739	0.6818	0.3682	0.5170	0.5261	NaN
4	0.9232	0.2026	0.1102	0.5573	0.3041	0.6478	NaN
5	0.7892	0.9453	0.7553	0.3666	0.5187	0.5251	NaN

Table 2.11 Estimated PD source coordinates, acoustic signal arrival time, distance percentage error, and computational time: comparison of different methods for the four PD source positions

Methods	PD sample	PD source coordinates (m)			Acoustic signal arrival time, $T_1$ (ms)	Distance error (%)	Computational time (s)
		$x$	$y$	$z$			
Newton's method	PD-1	0.4000	0.5500	0.6000	0.7937	0.00	0.7327
	PD-2	0.5559	0.9657	0.6520	0.5292	0.97	0.8519
	PD-3	0.8722	0.6205	0.7632	0.3083	1.90	1.2416
	PD-4	0.2503	0.6497	0.4502	0.2866	0.03	2.0293
Hybrid method	PD-1	0.4000	0.5500	0.6000	0.4519	0.00	10.554
	PD-2	0.5499	0.9498	0.6500	0.0005	0.01	13.110
	PD-3	0.8309	0.5824	0.7387	0.2737	1.64	8.7277
	PD-4	0.2501	0.6499	0.4500	0.0003	0.01	10.021
Existing non-iterative method	PD-1	*	*	*	*	*	*
	PD-2	*	*	*	*	*	*
	PD-3	*	*	*	*	*	*
Proposed non-iterative method**	PD-4	0.2500	0.6500	0.4500	0.2875	0.00	0.0202
	PD-1	0.4000	0.5500	0.6000	0.4532	0.00	0.0527
	PD-2	0.5500	0.9500	0.6500	0.5079	0.00	0.0258
	PD-3	0.8500	0.6000	0.7500	0.2896	0.00	0.0281
	PD-4	0.2500	0.6500	0.4500	0.2875	0.00	0.0202

\* The method failed to locate the PD source position.

\*\* The proposed non-iterative method has better accuracy and less computational time. These results are highlighted in the table.

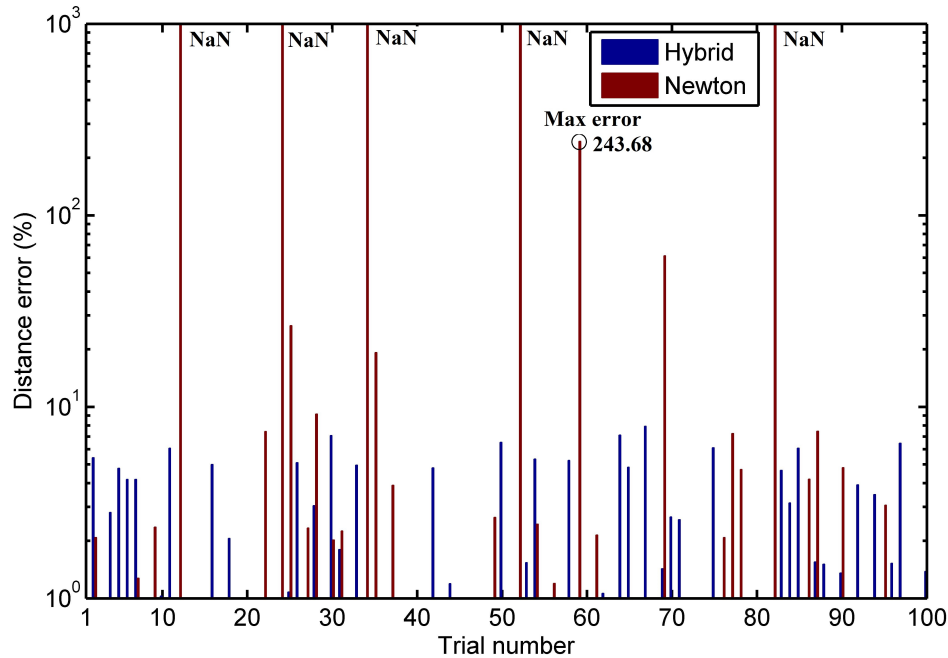


Figure 2.4 The distance error calculated for the estimated PD source position PD-3, for 100 trials, for Newton method and hybrid method. NaN are the errors of divergent trials, which occurred only in the case of Newton's method.

Newton's method for the PD source localisation. Whereas, in hybrid method, for all the 100 trials for each PD source positions (PD-1 to PD-4), the maximum error was less than 10% and none of the trials diverged. From Figure 2.4, it is seen that, there are divergent trials in the case of Newton's method. Whereas, in the case of hybrid method the error is coming less than 10% for all the trials. Therefore, the high error and divergence when using Newton's method with random initial guess can be avoided by using hybrid method.

When the four algorithms for the PD source localisation are compared in Table 2.11, it is seen that Newton's method resulted in comparatively higher error in PD source localisation and hybrid method has the highest computational time. The existing non-iterative method cannot locate the PD source position when one or more of the time-delays are zero. The proposed non-iterative method accurately located the PD source position with the lowest computational time (in the order of tens of ms).

Hybrid method has higher accuracy in PD source localisation when compared to



Newton's method. However, the computational time requirement is high. The comparative study shows that the proposed non-iterative method is the best algorithm for AEPD source localisation in terms of accuracy and computational time. This is shown in Table 2.11 by highlighting the PD source localisation results of the proposed non-iterative method.

## **2.6 Verification of the algorithms: laboratory experiments**

The laboratory experiments are conducted for verifying the efficacy of the proposed improvements of both Newton's method and non-iterative method. When the time-delays are measured experimentally, the error in localisation can be due to both the inaccuracy in time measurement and the inefficacy of the algorithm. In order to prove the suitability of these algorithms to be used for practical application, the PD source is located with the experimentally measured time-delays. The experiments are conducted in the diagnostic laboratory of Central Power Research Institute (CPRI), Bangalore, India.

### **2.6.1 Experimental Set-up**

The entire laboratory experimental setup can be grouped into three major components: (i) the experimental tank and the point electrode; (ii) the HV source and the measuring instruments; and (iii) the AE workstation. These are explained below.

#### **2.6.1.1 The experimental tank and the point electrode**

The size of the experimental tank is 1.015 m x 1.007 m x 1.007 m ( $l \times b \times h$ ) and the wall thickness is 5 mm. The tank made up of mild steel is filled with transformer oil. The tip diameter of the point electrode is 30  $\mu\text{m}$ . The bottom of the tank is considered as the plane electrode. The point-to-plane electrode gap is 0.420 m. The bottom left rear corner of the tank is considered as the origin (0, 0, 0) in three dimensional space. The coordinates of the tip of the point electrode at which PD occurs is (0.505, 0.420,

0.670) m. The schematic of the experimental tank with the electrode arrangement to simulate the PD defect is shown in Figure 2.5.

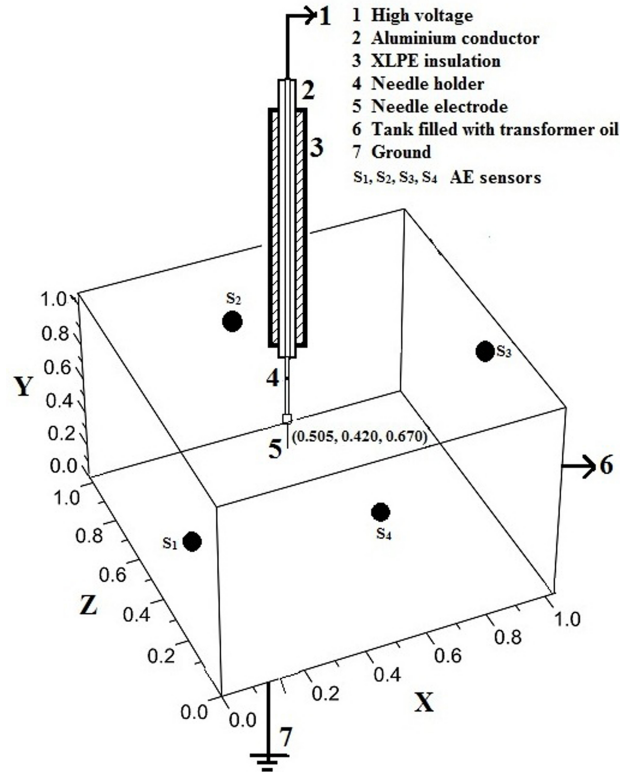


Figure 2.5 The oil test tank with the point-to-plane electrode arrangement to simulate the PD (all dimensions are in m).

### 2.6.1.2 The HV source and the measuring instruments

The high voltage source and the measuring instruments are used to source the simulated defect and to measure the related parameters, respectively. The HV source with a voltage rating of 75 kV (rms) and current rating of 1.1 A (rms) is used for the experiments. It is a variable 0 - 75 kV HV source. The output voltage is measured, using a 1000:1 HV capacitor divider, with a resolution of 0.1 kV. The diameter of the needle electrode (simulating PD) is measured using a digital vernier calliper (make: Mitutoyo Corporation, Japan; measuring range: 0 - 300 mm; resolution: 0.001 mm; accuracy:  $\pm 0.01$  mm). The tip profile of the needle electrode is measured using a profile projector with digital measurement and recording (make: Sipcon, India; measuring range: 0 -

100 mm; resolution: 0.0001 mm; accuracy:  $\pm 0.001$  mm).

### 2.6.1.3 The AE workstation

The AE workstation is a DSP based data acquisition system. The system consists of sixteen channels made from four numbers of 4-channel DSP boards. AE signal data is acquired from sixteen piezo-electric sensors of type DT15I. These signals are captured and stored in the associated programmable computer. The sensors have a frequency range of 100 kHz - 1 MHz and resonant frequency of 150 kHz with integrated pre-amplifier of 40 dB gain. The data acquisition system has a sampling rate of 1 Mega samples per second. To discriminate between the AEPD signals and the surrounding noise, the threshold is set to 30 dB in the AE workstation. The acoustic signals that crosses the set threshold is considered the AEPD signal and the corresponding signal arrival time to the AE sensor is noted for the time-delay measurement. The AE workstation is fully equipped with the relevant software for the detection and analysis of the captured AE signals. The various components of the AE workstation used in the present study are shown in Figure 2.6.

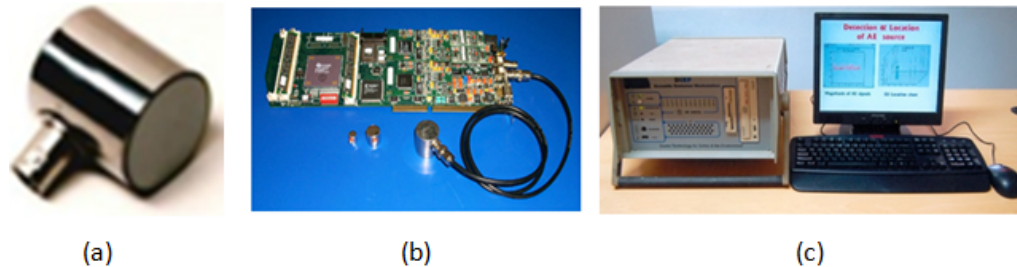


Figure 2.6 Components of AE workstation at CPRI; (a) AE sensor with integrated pre-amplifier (b) AE-DSP board (c) 16-channel AE workstation (source: M/s. Physical acoustics corporation, USA).

## 2.6.2 Experimental Procedure

The variable HV source is connected to an electrode system to generate the PD. The voltage is gradually increased from 0 V and the PDs are generated in the oil medium when the voltage is raised to 16.5 kV (rms). The four AE sensors are mounted on the outer surface of the tank using a magnetic holder. Silicone grease is used as the

acoustic couplant between the tank wall and the AE sensor. The PD source localisation experiments are conducted with two different sensor arrangements explained as follows:

1. Random sensor positioning ( $SA_1$ )

The sensor arrangement  $SA_1$  is a random positioning of the AE sensors, conforming to the proposed guidelines given in Section 2.3.3.2 (for Newton's method) and Section 2.4.3.5 (for proposed non-iterative method). The coordinates of the four sensors are given in Table 2.12. The AE signals due to PD are captured by the AE sensors. The order in which the AE sensors detected the acoustic signal is in the sequence of serial number 3, 4, 2, and 1 (as given in Table 2.12) for the chosen sensor arrangement  $SA_1$ . Therefore the sensors are sequenced ( $S1, S2, S3, S4$ ) based on the signal arrival time as (3, 4, 2, 1). The sensor  $S1$  (sensors with serial number 3 in Table 2.12) which is nearest to the PD source is chosen as the reference sensor.

2. Sensor positioning calculated theoretically ( $SA_2$ )

In sensor arrangement  $SA_2$ , the coordinates of the four sensors are calculated theoretically such that two sensors are equidistant from the PD source and nearest to the PD source than the other two sensors (Case 3; described in Section 2.4.3.1). The coordinates of the four sensors are given in Table 2.13. The sensor with serial number 2 (in Table 2.13) is adjusted near around the theoretically calculated coordinate values until the two sensors (sensors with serial numbers 2 and 3 in Table 2.13) are equidistant and the data acquisition system detects a zero time-delay between the acoustic signal reception of these two sensors. Thus, the efficacy of the different algorithms in localising the PD source when the time-delay is zero is confirmed by creating a similar scenario in the laboratory experimental set-up. The AE signals due to PD are captured by the AE sensors. The order in which the AE sensors detected the acoustic signal is in the sequence of serial number 2, 3, 4, and 1 (as given in Table 2.13) for the chosen sensor arrangement  $SA_2$ . Therefore the sensors are sequenced ( $S1, S2, S3, S4$ ) based on the signal arrival time as (2, 3, 4, 1). The sensor  $S1$  (sensors with serial numbers 2 in Table 2.13) which is nearest to the PD source is chosen as the reference sensor.

Table 2.12 Coordinates of the sensors used for the experimental studies and the sensor sequence based on signal arrival time for the sensor arrangement  $SA_1$

Serial number of the sensor	Sensor coordinates (m)			Sensor sequence based on signal arrival time
	$x_n$	$y_n$	$z_n$	
1	0.750	0.550	0.000	$S_4$
2	0.000	0.650	0.700	$S_3$
3	0.350	0.450	1.007	$S_1$
4	1.015	0.400	0.600	$S_2$

Table 2.13 Coordinates of the sensors used for the experimental studies and the sensor sequence based on signal arrival time for the sensor arrangement  $SA_2$

Serial number of the sensor	Sensor coordinates (m)			Sensor sequence based on signal arrival time
	$x_n$	$y_n$	$z_n$	
1	0.550	0.650	0.000	$S_4$
2	0.000	0.400	0.507	$S_1$
3	0.350	0.800	1.007	$S_2$
4	1.015	0.750	0.700	$S_3$

### 2.6.3 Results and Discussion

The AE signals from the PD source are detected by the four sensors on the transformer's tank wall. The screen-shot of the event display captured from the AE workstation for the sensor arrangement  $SA_1$  is given in Figure 2.7. The AEPD signals detected by the four sensors and the time-delay in signal reception of the sensors  $S_2$  (channel 4),  $S_3$  (channel 2), and  $S_4$  (channel 1) with respect to the sensor  $S_1$  (channel 3) for the sensor arrangement  $SA_1$  is depicted in Figure 2.7. The screen-shot of the event display captured from the AE workstation for the sensor arrangement  $SA_2$  is given in Figure 2.8. The AEPD signals detected by the four sensors and the time-delay in signal reception of the sensors  $S_2$  (channel 3),  $S_3$  (channel 4), and  $S_4$  (channel 1) with respect to the sensor  $S_1$  (channel 2) for the sensor arrangement  $SA_2$  is depicted in Figure 2.8. The time-delays measured by the data acquisition system for the two different sensor arrangements are given in Table 2.14. The time-delay ( $t_{12}$ ) between the signal reception of  $S_1$  and  $S_2$  is zero for sensor arrangement  $SA_2$ .

Table 2.14 Measured time-delays for the two sensor arrangements  $SA_1$  and  $SA_2$

Sensor arrangement	Time-delays ( $\mu s$ )		
	$t_{12}$	$t_{13}$	$t_{14}$
$SA_1$	101	128	247
$SA_2$	0	54	125

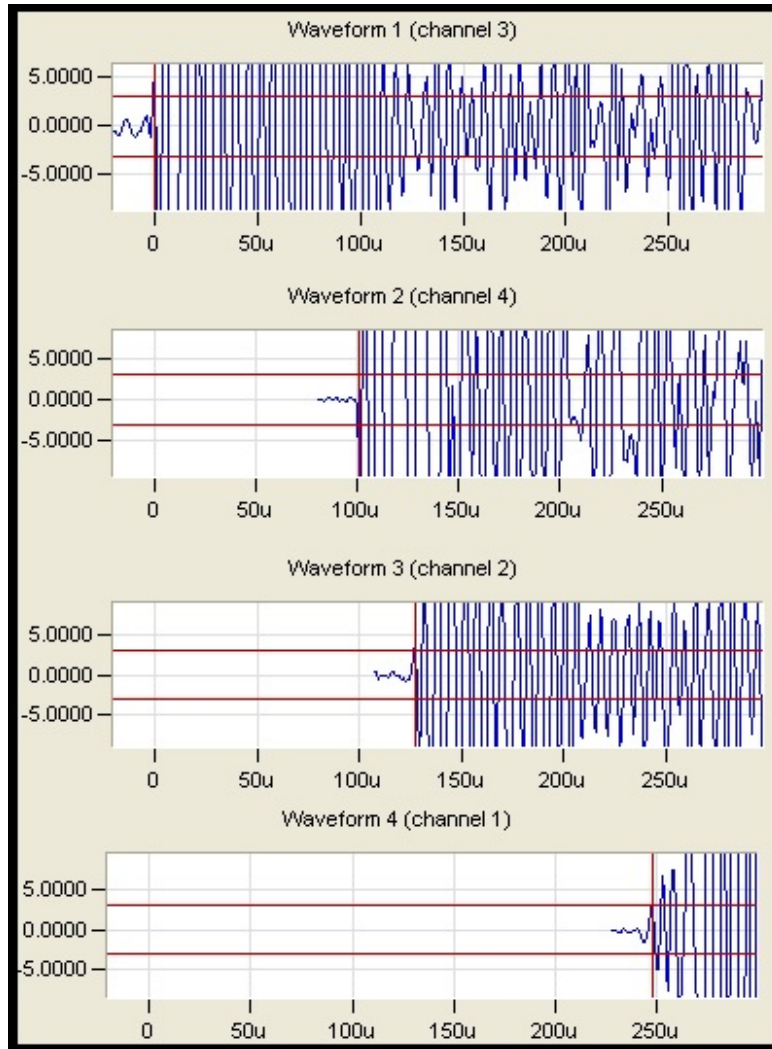


Figure 2.7 The screen-shot of the event display captured from the AE workstation for the sensor arrangement  $SA_1$ . The AEPD signals detected by the four sensors and the time-delay in signal reception of the sensors  $S_2$  (channel 4),  $S_3$  (channel 2), and  $S_4$  (channel 1) with respect to the sensor  $S_1$  (channel 3) are seen.

The PD source is located using Newton's method, hybrid method, existing non-iterative method, and proposed non-iterative method. The localisation results of all

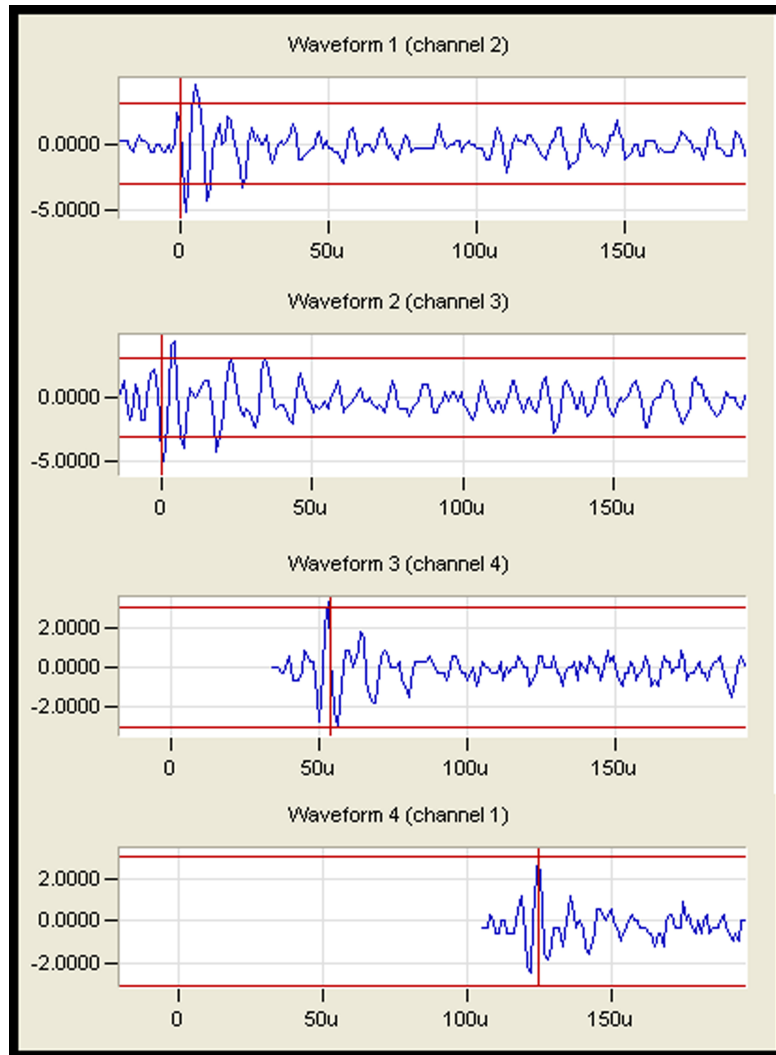


Figure 2.8 The screen-shot of the event display captured from the AE workstation for the sensor arrangement  $SA_2$ . The AEPD signals detected by the four sensors and the time-delay in signal reception of the sensors  $S_2$  (channel 3),  $S_3$  (channel 4), and  $S_4$  (channel 1) with respect to the sensor  $S_1$  (channel 2) are seen. The time-delay ( $t_{12}$ ) between the signal reception of  $S_1$  and  $S_2$  is zero.

these methods are compared in terms of distance error and computational time. For iterative methods like Newton's method and hybrid method, which requires an initial guess, the PD source estimation is repeated 100 times using 100 different initial guesses. The initial guess for Newton's method is generated using the MATLAB random number generator. The initial guess for hybrid method is estimated using the GA. The average of these 100 PD source locations calculated, excluding the diverged trials, is considered

as the estimated PD source location for iterative methods. The trials are said to be diverged when the solution is having a negative value for any of the PD source coordinates  $(x, y, z)$  or the acoustic signal arrival time to the nearest sensor  $(T_1)$ .

A comparison of the PD source localisation results of Newton's method and hybrid method based on 100 trials is given in Table 2.15. The trials that diverged or with high distance error (greater than 10%) when using Newton's method with sensor arrangements  $SA_1$  and  $SA_2$  are given in Tables 2.16 and 2.17, respectively.

Table 2.15 The comparison of PD source localisation result of Newton's method and hybrid method based on 100 trials for each sensor arrangement

Method	Sensor arrangement	Maximum error (%)	Number of trials diverged	Number of trials with error greater than 10%
Newton's method	$SA_1$	23.0	2	5
	$SA_2$	5.70	7	0
Hybrid method	$SA_1$	0.45	0	0
	$SA_2$	0.17	0	0

The estimated PD source coordinates (in a tank with maximum tank dimension given in equation (2.123)), the distance percentage error (as given in equation (2.124)), and the computational time when using the different algorithms for both the sensor arrangement ( $SA_1$  and  $SA_2$ ) are given in Table 2.18.

From Table 2.15, when localising the PD source using Newton's method, the distance error for one of the trials goes as high as 23% for PD-3. Moreover, some of the trials diverged when using Newton's method for the PD source localisation. Whereas, in hybrid method, for all the 100 trials for each sensor arrangement ( $SA_1$  and  $SA_2$ ), the maximum error was less than 10% and none of the trials diverged. Therefore, the high error and divergence when using Newton's method with random initial guess can be avoided by using hybrid method.

When the four algorithms for PD localisation are compared in Table 2.18, Newton's method resulted in comparatively higher error in PD localisation. The existing non-iterative method cannot locate the PD source position when one or more of the time-delays are zero. The hybrid method and the proposed non-iterative method has the same accuracy. However, the computational time for proposed non-iterative method is few



Table 2.16 The PD source localisation results of the diverged trials or the trials with high distance error (greater than 10%) when using Newton's method for PD source localisation with sensor arrangement SA<sub>1</sub>

Serial number	Initial guess				Solution				Distance error (%)
	PD source coordinates (m)			Acoustic signal arrival time, $T_1$ (ms)	PD source coordinates (m)			Acoustic signal arrival time, $T_1$ (ms)	
	x	y	z		x	y	z		
1	0.5046	0.0140	0.8456	1.07	0.4250	-0.0057	0.7561	0.60	NaN
2	0.2008	0.0428	0.0577	0.20	1.5861	6.3289	-0.6010	-4.40	NaN
3	0.5406	0.0450	0.8633	1.02	0.4325	0.0354	0.7473	0.56	23.0
4	0.7810	0.5086	0.9418	1.18	0.4333	0.0399	0.7464	0.56	22.8
5	0.5138	0.4868	0.9375	1.09	0.4372	0.0606	0.7419	0.54	21.5
6	0.8164	0.2513	0.9086	0.99	0.4484	0.1219	0.7288	0.50	17.9
7	0.6557	0.9373	0.9579	0.21	0.5407	0.6258	0.6208	0.09	12.4

Table 2.17 The PD source localisation results of the diverged trials or the trials with high distance error (greater than 10%) when using Newton's method for PD source localisation with sensor arrangement SA<sub>2</sub>

Serial number	Initial guess			Solution			Distance error (%)
	PD source coordinates (m)			PD source coordinates (m)			
	<i>x</i>	<i>y</i>	<i>z</i>	<i>x</i>	<i>y</i>	<i>z</i>	
1	0.4816	0.0702	0.3147	0.5495	0.6699	0.4389	NaN
2	0.0835	0.9904	0.1225	0.5495	0.6699	0.4389	NaN
3	0.9674	0.0624	0.6935	0.5495	0.6699	0.4389	NaN
4	0.7289	0.1804	0.8159	0.5495	0.6699	0.4389	NaN
5	0.6417	0.0329	0.7162	0.5495	0.6699	0.4389	NaN
6	0.9639	0.4957	0.0345	0.5495	0.6699	0.4389	NaN
7	0.2020	0.0797	0.8283	0.5495	0.6699	0.4389	NaN

Table 2.18 Estimated PD source coordinates, acoustic signal arrival time, distance percentage error, and computational time: comparison of the different methods for each sensor arrangement

Methods	Sensor arrangement	PD source coordinates (m)			Acoustic signal arrival time, $T_1$ (ms)	Distance error (%)	Computational time (s)
		$x$	$y$	$z$			
Newton's method	SA <sub>1</sub>	0.4992	0.3995	0.6693	0.28	1.25	1.83
	SA <sub>2</sub>	0.5052	0.4224	0.6680	0.37	0.21	1.12
Hybrid method	SA <sub>1</sub>	0.5020	0.4144	0.6661	0.26	0.45	12.6
	SA <sub>2</sub>	0.5051	0.4223	0.6681	0.38	0.16	23.0
Existing non-iterative method	SA <sub>1</sub>	0.5019	0.4139	0.6662	0.27	0.45	0.16
	SA <sub>2</sub>	*	*	*	*	*	*
Proposed non-iterative method**	SA <sub>1</sub>	0.5019	0.4139	0.6662	0.27	0.45	0.16
	SA <sub>2</sub>	0.5051	0.4223	0.6681	0.38	0.16	0.06

\* The method failed to locate the PD source position.

\*\* The proposed non-iterative method has better accuracy and less computational time. These results are highlighted in the table.

order less than that of hybrid method. Even though there is improvement in terms of accuracy for hybrid method when compared to Newton's method, it is at the cost of increased computational time. When compared in terms of accuracy and computational time, the proposed non-iterative method is found to be the best method for AEPD source localisation. This is shown in Table 2.18 by highlighting the PD source localisation results of the proposed non-iterative method. Thus, the efficacy of the proposed non-iterative method is proved using both numerical and laboratory experiments.

## 2.7 Summary

The implementation of Newton's method and non-iterative method for the AEPD source localisation is analysed in this chapter. The conditions for which these methods fail to locate the PD source positions are identified. The improvements are proposed for implementing these methods for a precise PD source localisation.

The major challenges while implementing Newton's method for the PD source localisation are the difficulty in choosing an efficient initial guess and the Jacobian matrix becoming singular.

The difficulty in identifying an efficient initial guess is solved by proposing a hybrid method. In the hybrid method an efficient initial guess is identified for Newton's method using the GA. The efficacy of the proposed hybrid method is verified using numerical and laboratory experiments. When hybrid method is used, the trials will not diverge and also the distance percentage error in PD source localisation is always less than 10%. This proves the superiority of proposed hybrid method in PD source localisation over Newton's method.

The occurrence of a singular Jacobian matrix when using Newton's method for AEPD source localisation can be prevented by proper acoustic sensor positioning on the tank wall and a careful initial guess selection. The proposed guidelines to avoid singular Jacobian matrix are: (i) the sensors should be placed such that all the  $x$ , all the  $y$  or all the  $z$ -coordinates of the sensors are not zero or equal; (ii) the null space of the sensor matrix (formed by the sensor coordinates) should contain only a zero vector; and (iii) the initial guess for acoustic signal arrival time ( $T_1$ ) should not be chosen as zero.

Thus, by proposing a hybrid method (which identifies a good initial guess for Newton's method via GA), and by proposing guidelines for acoustic sensor positioning and initial guess selection, the challenges in implementing Newton's method for AEPD source localisation are resolved.

When analysing the existing non-iterative method for the PD source localisation, the three special cases for which the existing non-iterative method fail to locate the AEPD source are identified. A non-iterative method for AEPD source localisation in power transformers, which works for any time-delays (including zero) is proposed and its efficacy is demonstrated via numerical and laboratory experiments. The proposed extension of the existing non-iterative method helps in making the non-iterative method for PD source localisation more reliable. A guideline for the sensor positioning that helps in the reliable execution of the proposed time-difference approach based non-iterative method is also suggested.

The comparative study of iterative and non-iterative methods for AEPD source localisation proves that the proposed non-iterative method works superior to other methods in terms of accuracy and computational time for AEPD source localisation.



## Chapter 3

# Algorithms for PD source localisation: Combined acoustic-electrical system

### 3.1 Introduction

The combined acoustic-electrical system is used in the factory or plant environment for the PD source localisation in power transformers. The simplest approach for the PD source localisation is by measuring the electrical signal simultaneously with the acoustic signal. The combined acoustic-electrical system pairs a current or voltage measurement device, that can detect the PD electrically, with the array of acoustic sensors. In the combined acoustic-electrical system, instead of the time-delay, the absolute time of acoustic signal arrival at each sensor is used for the PD source localisation (IEEE Std C57.127 2007). The combined acoustic-optical system (Wang *et al.* 2006), and the system with a simultaneous measurement of optical and UHF signal (Li *et al.* 2016a) also use absolute time for the PD source localisation.

The major advantage of the combined acoustic-electrical PD-locator-system is that it avoids false PD alarms, caused by using either the electrical or acoustic method independently. The false alarm from the electrical signals can be due to the corona in the air (Lundgaard 1992b). The noises of the oil pumps and the magnetostriction in the core can generate emissions with a frequency range similar to that of the acoustic PD itself (Grossmann and Feser 2005; Kweon *et al.* 2005). The false alarms from the acoustic signals can also be caused by rain (Lundgaard 1992b). The major disadvantage of using an acoustic system along with an electric PD measurement in the field

is that it may be difficult to obtain a clean electric PD measurement due to the electrical noise (Chan *et al.* 2014; Stone 1991). In the off-line test or in the laboratory environment, these noises can be eliminated by shielding or by properly bonding the metal components. Therefore, the combined acoustic-electrical PD-locator-system is more suitable in the factory or plant environment than in the field (IEEE Std C57.127 2007). Blackburn *et al.* (1991) have presented the findings of simultaneous application of electric/acoustic method for the detection and location of PDs in power transformers. Typical case study of  $(330/\sqrt{3})$  kV, 35 MVA transformer has been reported.

In the combined acoustic-electrical PD-locator-system, the PD source is located by solving the mathematical model of an AEPD system, which is a system of non-linear sphere equations. From Chapter 2, it is seen that, the non-iterative method is the best algorithm for solving a system of non-linear equations. However, a non-iterative algorithm to solve the mathematical model of a combined acoustic-electrical system is not available in the published literature.

In this chapter, a non-iterative method is devised for PD source localisation using the combined acoustic-electrical system, which can overcome some lacunae identified in the existing algorithms (as seen from Chapter 2). The guidelines for the sensor placement for the reliable implementation of the proposed method are also suggested. In addition, the effect of the PD source position on the performance of the proposed method is analysed. The proposed method is also applied to the experimental data published in Al-Masri *et al.* (2016a). The performance of the proposed non-iterative method is compared with that of Newton's method and hybrid method (iterative methods).

This chapter is organised as follows: Section 3.2 elaborates the mathematical model of a combined acoustic-electrical system for the PD source localisation; Section 3.3 presents the proposed non-iterative method for the PD source localisation; Section 3.4 gives the performance verification of the proposed method by using numerical experiments; Section 3.5 discusses the application of proposed method to the published data; This is followed by summary of the chapter in Section 3.6.



## 3.2 Mathematical model of a combined acoustic-electrical system

The combined acoustic-electrical system pairs a current or voltage measurement device, that can detect the PD electrically, with the array of acoustic sensors. The electrical signal triggers the signal measurement. Multiple AE sensors are located on the transformer's tank wall. These sensors detect the acoustic signal emitted by the PD source. Here, the electrical signal is considered to be detected instantaneously. Thus, the absolute signal arrival time at each sensor is measured as the time-difference between the electrical PD detection, and the acoustic signal detection by the acoustic sensor.

The sensors are named  $S_1, S_2, \dots, S_n$ , where  $n$  is the total number of sensors used, and the corresponding absolute signal arrival time at each sensor is  $T_1, T_2, \dots, T_n$ . To solve for the PD coordinates, the AEPD system is modelled mathematically. The system of non-linear sphere equations, given in equation (3.1), are formed by considering each sensor as the centre of the sphere and the distance between the sensor and the PD source as radius. The product of the velocity ( $v$ ) of sound in transformer oil and the acoustic signal arrival time ( $T_n$ ) to the sensor gives the radius of the sphere. The spheres intersect with each other at the PD source location (Veloso *et al.* 2006). The sensors  $S_1, S_2 \dots S_n$  have their coordinates given by  $(x_1, y_1, z_1), (x_2, y_2, z_2), \dots$  and  $(x_n, y_n, z_n)$ , respectively.

$$\begin{aligned}
 (x - x_1)^2 + (y - y_1)^2 + (z - z_1)^2 &= (vT_1)^2, \\
 (x - x_2)^2 + (y - y_2)^2 + (z - z_2)^2 &= (vT_2)^2, \\
 (x - x_3)^2 + (y - y_3)^2 + (z - z_3)^2 &= (vT_3)^2, \\
 &\dots\dots \\
 (x - x_n)^2 + (y - y_n)^2 + (z - z_n)^2 &= (vT_n)^2.
 \end{aligned} \tag{3.1}$$

In the system of the non-linear sphere equations given in equation (3.1), the coordinates of the PD source  $(x, y, z)$  are the unknown quantities. Since there are three unknowns, a minimum of three AE sensors are required to locate the PD source, unlike the four sensors needed for the all-acoustic system (time-difference approach). In

numerical computation, solving the system of non-linear equations is perhaps the most difficult task, and it is unavoidable in a spectrum of engineering applications (Li *et al.* 2016b). In the literature, the mathematical model of the absolute-time approach based systems are solved using iterative or search algorithms (Al-Masri *et al.* 2016a,b). In the following section, a non-iterative algorithm is developed for the combined acoustic-electrical system.

### 3.3 Proposed non-iterative PD source localisation method

The PD source coordinates are located by solving the mathematical model of the combined acoustic-electrical system. In the system of non-linear equations, equation (3.2) to equation (3.4), the unknown quantities are the coordinates of the PD source ( $x, y, z$ ). Since there are three unknowns, a minimum of three sensors are required to locate the PD source.

$$(x - x_1)^2 + (y - y_1)^2 + (z - z_1)^2 = (vT_1)^2 \quad (3.2)$$

$$(x - x_2)^2 + (y - y_2)^2 + (z - z_2)^2 = (vT_2)^2 \quad (3.3)$$

$$(x - x_3)^2 + (y - y_3)^2 + (z - z_3)^2 = (vT_3)^2 \quad (3.4)$$

where  $(x_n, y_n, z_n)$ ,  $n = 1$  to  $3$ , are the coordinates of the three sensors,  $T_n$ ,  $n = 1$  to  $3$ , is the absolute time of propagation of the acoustic signal from the source to the three sensors, and  $v$  is the velocity of acoustic signal in transformer oil.

All the spheres intersect with each other at the PD source location. The points of intersection of two spheres lie on a plane in which the PD source can be located. The equations of the two intersecting planes that are formed by the intersection of the spheres (equation (3.2) & equation (3.3), and equation (3.2) & equation (3.4)) are given in equation (3.5) and equation (3.6), respectively:

$$k_1x + k_2y + k_3z = k_4, \quad (3.5)$$

$$k_5x + k_6y + k_7z = k_8, \quad (3.6)$$

where the constants in these equations are given in equation (3.7) to equation (3.14):

$$k_1 = 2(x_2 - x_1), \quad (3.7)$$

$$k_2 = 2(y_2 - y_1), \quad (3.8)$$

$$k_3 = 2(z_2 - z_1), \quad (3.9)$$

$$k_4 = (x_2^2 - x_1^2) + (y_2^2 - y_1^2) + (z_2^2 - z_1^2) + v^2(T_1^2 - T_2^2), \quad (3.10)$$

$$k_5 = 2(x_3 - x_1), \quad (3.11)$$

$$k_6 = 2(y_3 - y_1), \quad (3.12)$$

$$k_7 = 2(z_3 - z_1), \quad (3.13)$$

$$k_8 = (x_3^2 - x_1^2) + (y_3^2 - y_1^2) + (z_3^2 - z_1^2) + v^2(T_1^2 - T_3^2). \quad (3.14)$$

The points of intersection of the two planes lie on a line on which the PD source can be located. The line formed by the intersecting planes, equation (3.5) and equation (3.6), is given in equation (3.15):

$$\frac{x - k_9}{k_{10}} = \frac{y - k_{11}}{k_{12}} = \frac{z}{k_{13}} = A, \quad (3.15)$$

where the constants in this equation are given in equation (3.16) to equation (3.20):

$$k_9 = \frac{k_1 k_4 k_6 - k_2 k_4 k_5 - k_1 k_2 k_8 + k_2 k_4 k_5}{k_1 (k_1 k_6 - k_2 k_5)}, \quad (3.16)$$

$$k_{10} = k_2 k_7 - k_3 k_6, \quad (3.17)$$

$$k_{11} = \frac{k_1 k_8 - k_4 k_5}{k_1 k_6 - k_2 k_5}, \quad (3.18)$$

$$k_{12} = k_3 k_5 - k_1 k_7, \quad (3.19)$$

$$k_{13} = k_1 k_6 - k_2 k_5. \quad (3.20)$$

The variable  $A$  in equation (3.15) needs to be determined. The coordinates of any point on the line  $(x, y, z)$  are obtained from equation (3.15) and are given in equation (3.21) to equation (3.23):

$$x = k_9 + k_{10}A, \quad (3.21)$$

$$y = k_{11} + k_{12}A, \quad (3.22)$$

$$z = k_{13}A. \quad (3.23)$$

The PD source can be located on the line (equation (3.15)) as well as on the spheres (equation (3.2) to equation (3.4)). The line intersects any one of the spheres in two points, resulting in a quadratic equation. The quadratic equation (3.24) is formed by

substituting the coordinates given in equation (3.21) to equation (3.23) in the sphere equation (3.2):

$$k_{14}A^2 + k_{15}A + k_{16} = 0, \quad (3.24)$$

where the constants in this equation are given in equation (3.25) to equation (3.27):

$$k_{14} = k_{10}^2 + k_{12}^2 + k_{13}^2, \quad (3.25)$$

$$k_{15} = 2k_9k_{10} + 2k_{11}k_{12} - 2k_{10}x_1 - 2k_{12}y_1 - 2k_{13}z_1, \quad (3.26)$$

$$k_{16} = x_1^2 + y_1^2 + z_1^2 - 2k_9x_1 - 2k_{11}y_1 - v^2T_1^2 + k_9^2 + k_{11}^2. \quad (3.27)$$

The solutions of the quadratic equation (3.24) give the values of the variable  $A$ . By substituting the values of variable  $A$  in equation (3.21) to equation (3.23), two sets of solution can be obtained for the coordinates of the PD source ( $x$ ,  $y$ ,  $z$ ). Among these solutions one is the actual location that is accepted, and the other is rejected. The rejection of a solution can be due to any of the PD source coordinates being negative or outside the transformer tank dimensions. The generalised flowchart for the PD source localisation in transformers using the newly devised non-iterative method in a combined acoustic-electrical system is given in Figure 3.1. This method is applicable to any mixed acoustic system where the time of origin of the PD is known (absolute time approaches).

The efficacy of the proposed method is studied using the numerical experiments and the application of the proposed method to the published data from the literature (Al-Masri *et al.* 2016a). The guidelines for a suitable sensor positioning is also suggested, which will result in the reliable implementation of the proposed method. It will also help in overcoming the ambiguity in choosing the actual solution (PD source location) among the two available solutions.

### 3.4 Performance verification of the proposed method

The two important facets to be examined for any PD source localisation method are the effect of the sensor positioning and the effect of the PD source position on its performance. The occurrence of the PD at a location is random. Hence, a good PD source localisation method should locate the PD source irrespective of its position within the tank. For this, two analyses are carried out: (i) the first numerical experiment based analysis is made to examine the effect of the sensor positioning on the performance of

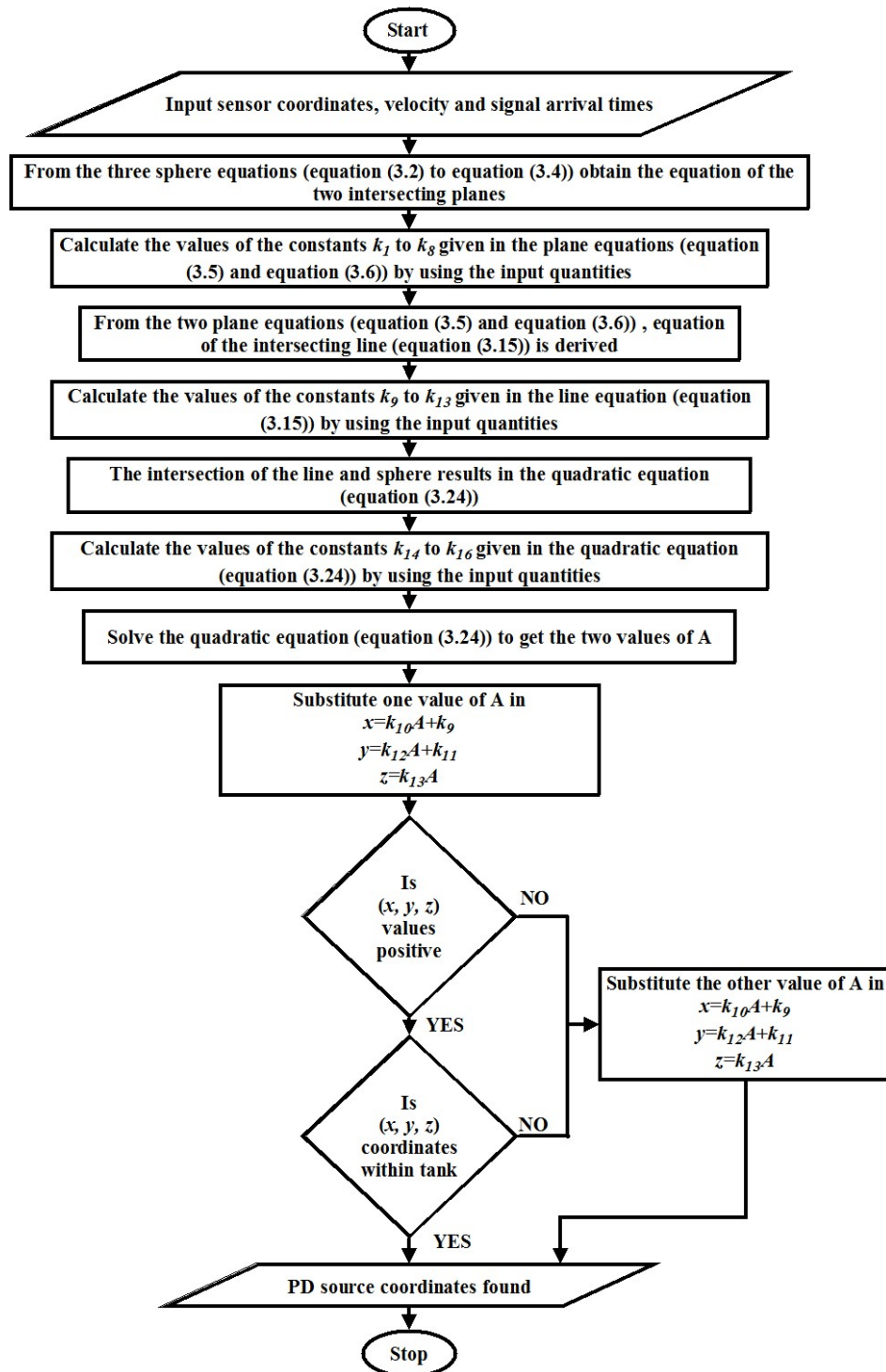


Figure 3.1 Generalised flowchart for PD source localisation in power transformers using the newly devised non-iterative method for the combined acoustic-electrical system.

the proposed method; and (ii) the second numerical experiment based analysis is carried out to find the effect of the PD source position (the relative distances between the PD source and the sensors) on the performance of the method. For the verification of the proposed method, relevant computer codes are developed.

### **3.4.1 Effect of the sensor positioning**

An effective localisation of the PD source is highly dependent on the initial placement of the AE sensors on the transformer's tank wall. For a three-phase transformer, when the phase in which the PD source present is unknown, a layout of an initial placement of the sensors for PD source localisation is suggested in IEEE Std C57.127 (2007). These sensors are placed on one plane of the transformer's tank wall. This arrangement is given for a factory or plant environment (IEEE Std C57.127 2007). To study the effect of sensor positioning on the proposed method, numerical experiments are carried out considering a similar sensor arrangement as suggested in IEEE Std C57.127 (2007).

The numerical experiment reveals that such a sensor arrangement can cause the failure of the proposed algorithm in certain conditions. Hence, some guidelines are required for the reliable implementation of the proposed algorithm. These guidelines are evolved by analyzing the results obtained from the numerical experiments.

#### **3.4.1.1 Details of numerical experiments**

A transformer tank of size 3 m x 3 m x 3 m is considered for the numerical experiment. Nine AE sensors are placed on the transformer's tank wall conforming to the layout suggested in IEEE Std C57.127 (2007) on the  $z = 0$  plane. The sensor coordinates considered for the numerical experiment are given in Table 3.1. The layout of the sensor arrangement with nine sensors for the numerical experiment is given in Figure 3.2.

A minimum of three sensors are required for PD source localisation. Since there are nine sensors, 84 ( ${}^9C_3$ ) combinations of the sensors are possible. Three randomly chosen PD sources are located by considering these combinations of sensors separately. The coordinates of the three chosen PD source positions are (2.8, 0.9, 1.7) m, (1.3, 1.4, 0.7) m and (0.5, 2.6, 2.8) m. The devised method is applied to locate these PD sources.

Among the 84 combinations of the sensors, 35 combinations of the sensors failed to locate the PD source. The same combination of sensors failed to locate the PD sources in all three cases for this arrangement of sensors. The reason for failure of the method in these cases is analysed. From equation (3.16) and equation (3.18) we can see that the denominators of these equations become zero whenever  $k_1 = 0$  or  $(k_1k_6 - k_2k_5) = 0$ . In such cases the constants  $k_9$  and  $k_{11}$  cannot be determined and the algorithm fails to locate the PD source. The conditions for which the algorithm fails to locate the PD source and the corresponding number of combinations failed are given in Table 3.2.

From the numerical experiment (with the devised method), when all the sensors are placed in the  $z = 0$  plane, among the two sets of solutions, only one set of solutions will have positive values for the  $x$ ,  $y$ , and  $z$  coordinates of the PD source and that will be the actual PD source location. The other solution will have a negative value for the  $z$ -coordinate of the PD source and that solution can be rejected. Thus, the problem of selecting the actual PD source location from the two available solutions can be solved by placing all the sensors in the  $z = 0$  plane. Conversely, the plane on which the sensors are placed is to be considered as  $z = 0$  plane.

From the analysis of the devised method, two more conditions can cause the failure of the method, which do not occur in the numerical experiments with the present layout (Figure 3.2). These conditions are (i)  $x_1 = x_2$  &  $y_1 = y_2$  and (ii)  $x_1 = x_3$  &  $y_1 = y_3$ . These conditions occur only when all the sensors are not placed on the same plane and hence do not show up in the present numerical experiments.

Considering all six conditions for which the devised method fails to locate the PD source, the new guidelines for the sensor placement are:

1. all the three sensors in a combination should have distinct  $x$ -coordinate values and distinct  $y$ -coordinate values
2. all the three sensors should be kept on one plane and that plane should be considered as  $z = 0$  plane, and
3. all the three sensors should not be kept in a straight line.

Such sensor arrangement helps in the reliable implementation of the devised algo-

rithm, and it will never fail to locate a PD source. The sensor coordinates for the nine sensors conforming to these evolved guidelines are given in Table 3.3. When the sensors are placed according to the new proposed guidelines, all 84 combinations of the sensors accurately locate all three PD sources (that are chosen randomly for the numerical experiment).

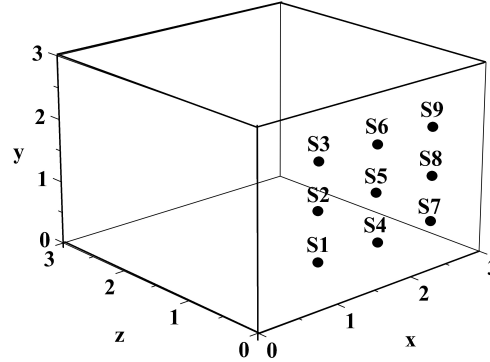


Figure 3.2 The sensor layout (similar to layout suggested in IEEE Std C57.127 (2007)) used for the numerical experiment.

Table 3.1 Coordinates of the sensor conferring to the layout given in IEEE Std C57.127 (2007) on the  $z = 0$  plane

Sensor number (S <sub>n</sub> )	Sensor coordinates		
	$x_n$ (m)	$y_n$ (m)	$z_n$ (m)
S1	0.75	0.75	0.00
S2	0.75	1.50	0.00
S3	0.75	2.25	0.00
S4	1.50	0.75	0.00
S5	1.50	1.50	0.00
S6	1.50	2.25	0.00
S7	2.25	0.75	0.00
S8	2.25	1.50	0.00
S9	2.25	2.25	0.00

### 3.4.2 Effect of the PD source position

The occurrence of the PD at a location is random. An effective method should accomplish the PD source localisation irrespective of its position. The second numerical



Table 3.2 The conditions for which the proposed non-iterative method fails to locate the PD source for the layout given in Figure 3.2

Condition number	Sensor positioning	Number of combinations failed	Suggested remedy via sensor re-positioning
1	$x_1 = x_2 = x_3$	3	The $x$ -coordinates of all the three sensors should not be same
2	$y_1 = y_2 = y_3$	3	The $y$ -coordinates of all the three sensors should not be same
3	$x_1 = x_2$	27	This condition can be avoided by proper sensor numbering. The sensors should be numbered in such a way that the first two sensors (out of three) should not have the same $x$ -coordinate value
4	$(x_2 - x_1)(y_3 - y_1) = (x_3 - x_1)(y_2 - y_1)$	2	The sensors should not be placed in a straight line

Table 3.3 Coordinates of the sensors used for numerical experiment conforming to proposed guidelines for sensor positioning

Sensor number (S <sub>n</sub> )	Sensor coordinates		
	$x_n$ (m)	$y_n$ (m)	$z_n$ (m)
S1	0.40	0.24	0.00
S2	0.60	1.76	0.00
S3	0.50	2.75	0.00
S4	1.24	0.25	0.00
S5	1.25	1.74	0.00
S6	1.26	2.76	0.00
S7	2.40	0.26	0.00
S8	2.50	1.75	0.00
S9	2.60	2.74	0.00

experiment based analysis is conducted to determine the effect of the PD source position on the performance of the devised method. The numerical experiment shows that the proposed method is reliable and can locate any PD source irrespective of its positions with the sensor arrangement guidelines suggested in subsection 3.4.1.

### 3.4.2.1 Details of numerical experiments

The transformer tank of size 3 m x 3 m x 3 m is divided into sub-modules of size 0.1 m x 0.1 m x 0.1 m. Each vertex of the sub-module is considered a PD source position. In this way, 24,389 PD source positions are considered within the tank. These PD source positions are located using the non-iterative method proposed for the combined acoustic-electrical system. The nine sensors given in Table 3.3 are used for the numerical experiments.

The proposed method for the combined acoustic-electrical system requires only three sensors to locate the PD source. Since there are nine sensors, 84 ( ${}^9C_3$ ) combinations of the sensors are possible. The 24,389 PD source positions are located separately using all 84 combinations of the sensors. The non-iterative method proposed for the combined acoustic-electrical system located all 24,389 PD source positions successfully.

In Chapter 2, it is seen that, the existing non-iterative method for an all-acoustic system fails to locate the PD source whenever there is more than one sensor nearest to the PD source. An extension was proposed for the existing non-iterative method in Chapter 2, so that it works for cases with zero time-delay. A zero time-delay implies that these sensors are equidistant from the PD source. In such cases, the absolute signal arrival time from the PD source to these sensors becomes equal. Table 3.4 shows five sample PD source positions that has equal absolute signal arrival time (implies time-delay is zero) from the PD source to any two sensors in the sensor combination. These PD sources are successfully located using the non-iterative method proposed for the combined acoustic-electrical system. The combination of the sensors that is used in this case is the first three sensors given in Table 3.3. The absolute times calculated for implementing the PD source localisation in the combined acoustic-electrical system are also given in Table 3.4. From Table 3.4, the absolute times  $T_1$  and  $T_2$  are equal for these PD source positions. This shows that the non-iterative method used in the combined acoustic-electrical system can locate the PD source even when there is more than one sensor nearest to the PD source and equidistant from the PD source.

From the above discussion, the performance of the non-iterative method proposed for the combined acoustic-electrical system is independent of the PD source position inside the transformer tank.

Table 3.4 Five sample PD source positions (PD-1 to PD-5), with equal absolute signal arrival time from the PD source to any two sensors in the sensor combination, that can be located using the proposed method

PD sample		PD-1	PD-2	PD-3	PD-4	PD-5
PD location (m)	$x$	0.5	0.5	0.5	0.5	0.5
	$y$	1	1	1	1	1
	$z$	0.3	0.7	1.4	1.6	2.5
Absolute signal arrival time ( $\mu s$ )	$T_1$	582.6	734.7	1130	1256	1851
	$T_2$	582.6	734.7	1130	1256	1851
	$T_3$	1257	1334	1586	1678	2160

### 3.5 Application of proposed method to the published data

The efficacy of the proposed method is verified by applying it to the experimental data published in Al-Masri *et al.* (2016a). From the published literature, the locations of the sensors, the location of the source of the PD, and the absolute signal arrival times (from the source to the sensors) that are reported have been used to verify the proposed method. The related data that are reported in Al-Masri *et al.* (2016a) are as follows. In the experiment, a transformer tank of size 1 m x 1 m x 0.5 m (l x b x h) is used. The experimental data is reported only for the *xy* plane (plane where  $z = \text{constant}$ ). A constant  $z$ -plane ( $z = 0.25$ ) is considered for the numerical experiment. Four acoustic sensors are used with the sensor coordinates S1(0.5, 0.0) m, S2(0.0, 0.5) m, S3(0.5, 1.0) m, and S4(1.0, 0.5) m. Five groups of absolute signal arrival times (AT-1 to AT-5) from a PD source position of (0.50, 0.25) m to the three sensors (S1, S2, and S3) are reported in Al-Masri *et al.* (2016a). These data taken from Al-Masri *et al.* (2016a) are given in Table 3.5.

Table 3.5 Absolute arrival time reported (Al-Masri *et al.* 2016a), and calculated for a known PD location (Al-Masri *et al.* 2016a) with the velocity of acoustic signal taken from IEEE Std C57.127 (2007)

	Group Name	$T_1$ ( $\mu\text{s}$ )	$T_2$ ( $\mu\text{s}$ )	$T_3$ ( $\mu\text{s}$ )
Experimental absolute time data reported in Al-Masri <i>et al.</i> (2016a)	AT-1	177	432	557
	AT-2	177	431	555
	AT-3	177	428	557
	AT-4	177	430	563
	AT-5	177	428	559
Theoretically calculated absolute time for the experimental set-up reported in Al-Masri <i>et al.</i> (2016a)	AT-6	176.93	395.62	530.79

As the location of the PD source is known, by taking the velocity of acoustic signal in oil as 1,413 m/s (IEEE Std C57.127 2007), the theoretical value of the acoustic signal propagation time from the PD source to each sensor can be calculated. This is given as group AT-6 in Table 3.5.

The PD source localisation is conducted using the proposed method (non-iterative method), Newton's method, and hybrid method. The initial guess for Newton's method are generated using MATLAB random number generator and the initial guess for hybrid method is identified using GA. The initial guess used for Newton's method and hybrid method for each group of absolute signal arrival times (AT-1 to AT-6) are given in Table 3.6.

The estimated PD source coordinates (in a tank with maximum tank dimension given in equation (2.123)), the distance percentage error (as given in equation (2.124)), and the computational time when using the different algorithms for each group of absolute signal arrival times (AT-1 to AT-6) are given in Table 3.7.

From Table 3.7, for the theoretically calculated signal arrival time (AT-6), with no error in time measurement, the PD source localisation is accurate with Newton's method, hybrid method, and proposed non-iterative method. When using Newton's method for PD source localisation, with the experimentally measured absolute signal arrival time AT-5, the method diverged. The iterative method may converge or diverge depending on the quality of the initial guess. The hybrid method and the non-iterative method gave same accuracy in PD source localisation. The proposed non-iterative method will never have a convergence problem and does not require an initial guess.

From Table 3.7, the time taken by Newton's method for estimating the PD source location is of the order of seconds and for the hybrid method it is of the order of tens of seconds. Whereas, for the proposed method, the time taken is of the order of  $10^{-3}$  to  $10^{-4}$  seconds. The time taken by the proposed method to locate the PD source is substantially less compared to Newton's method and hybrid method. Therefore, the proposed non-iterative method has superior performance, in terms of accuracy and com-

putational time, when compared to iterative methods. These results are highlighted in Table 3.7.

Table 3.6 The initial guess used for Newton's method and hybrid method for each group of absolute signal arrival times (AT-1 to AT-6)

Method	Group name	Initial guess for PD source coordinates (m)		
		$x_0$	$y_0$	$z_0$
Newton's method	AT-1	0.241691	0.403912	0.048227
	AT-2	0.131973	0.942051	0.478067
	AT-3	0.575209	0.059780	0.117390
	AT-4	0.353159	0.821194	0.007702
	AT-5	0.043024	0.168990	0.324558
	AT-6	0.731722	0.647746	0.225462
Hybrid method	AT-1	0.499999	0.250001	0.251034
	AT-2	0.531619	0.221560	0.138367
	AT-3	0.532119	0.223779	0.356968
	AT-4	0.524742	0.221561	0.363393
	AT-5	0.521463	0.214849	0.376205
	AT-6	0.522518	0.219331	0.368059

Table 3.7 The PD source localization results of Newton’s method, hybrid method, and proposed non-iterative method

Method	Group name	PD source coordinates (m)			Distance error (%)	Computational time (s)
		<i>x</i>	<i>y</i>	<i>z</i>		
Newton’s method	AT-1	0.5316	0.2216	1.0686	0.55	0.41
	AT-2	0.5321	0.2238	0.1430	0.08	1.38
	AT-3	0.5247	0.2216	0.1366	0.08	1.98
	AT-4	0.5215	0.2149	1.1014	0.57	0.36
	AT-5	0.5225	0.2193	-4.6780	NaN	0.16
	AT-6	0.5000	0.2500	0.2500	0.00	3.95
Hybrid method	AT-1	0.5316	0.2216	0.1384	0.08	19.0
	AT-2	0.5321	0.2238	0.3570	0.08	15.2
	AT-3	0.5247	0.2216	0.3634	0.08	15.0
	AT-4	0.5215	0.2149	0.3762	0.09	19.7
	AT-5	0.5225	0.2193	0.3681	0.08	15.1
	AT-6	0.5000	0.2500	0.2500	0.00	17.7
Proposed non-iterative method*	AT-1	0.5316	0.2216	0.1384	0.08	$5.15 \times 10^{-4}$
	AT-2	0.5321	0.2238	0.1430	0.08	$5.23 \times 10^{-4}$
	AT-3	0.5247	0.2216	0.1366	0.08	$5.01 \times 10^{-4}$
	AT-4	0.5215	0.2149	0.1238	0.09	$5.04 \times 10^{-4}$
	AT-5	0.5225	0.2193	0.1319	0.08	$5.59 \times 10^{-4}$
	AT-6	0.5000	0.2500	0.2500	0.00	$1.35 \times 10^{-3}$

\* The proposed non-iterative method has comparatively less computational time. These results are highlighted in the table.

### 3.6 Summary

A non-iterative method for the PD source localisation in a power transformer using a combined acoustic-electrical system is devised and tested.

For the reliable implementation of the proposed non-iterative method, the following guidelines are suggested: The sensors should be placed such that all three sensors should have distinct *x*-coordinate values and distinct *y*-coordinate values. Placing all the three sensors in the  $z = 0$  plane helps in easily identifying the actual PD source location from the two available solutions (by rejecting one of the solutions that has a negative

$z$ -coordinate value). All three sensors should not be placed in a straight line.

The proposed non-iterative method is independent of the relative distances between the sensors and the PD source. The computational time required for the non-iterative method is significantly less compared to Newton's method and hybrid method. The devised method being non-iterative does not have any convergence problem and does not require any initial guesses.



# Chapter 4

## Effect of error in time measurement on PD source localisation

### 4.1 Introduction

The geometrical localisation of the PD source is carried out using either the TDOA approach or the TOA approach. An all-acoustic system uses the TDOA approach and a combined acoustic-electrical system uses the TOA approach. In TDOA approach, multiple AE sensors are placed on the transformer's tank wall. Signals are first received by the sensor nearest to the PD source, and a recording process is triggered on all sensors simultaneously. The time-delay in signal reception of other sensors with respect to the nearest sensor is measured. In TOA approach, there is simultaneous detection of both the electrical and the acoustic signals. The electrical signal triggers the signal measurement. The multiple AE sensors located on the transformer's tank wall detect the acoustic signals emitted by the PD source. The electrical signal is considered to be detected instantaneously. Thus, the absolute signal arrival time at each AE sensor is measured as the time-difference between the electrical PD detection and the acoustic signal detection by the acoustic sensor (IEEE Std C57.127 2007).

The acoustic signal from the PD source can reach the AE sensor either through direct-path or structure-borne-path. The acoustic waves propagating from the source directly to the sensor in a straight line through the oil are the direct-path waves. The structure-borne-path waves are the acoustic waves that hit the nearby transformer tank wall and reach the sensor (propagating through the tank wall) (IEEE Std C57.127 2007).

The system of non-linear sphere equations given in equation (2.1) and equation (3.1) are formed by assuming that the acoustic sensors detect the direct-path waves. The radius of the sphere is the product of time (absolute-time of propagation of the acoustic signal from the source to the sensor) and velocity (velocity of acoustic signal in transformer oil). If all the sensors detect the direct-path wave, then the spheres intersect with each other at the PD location. Hence, the system of sphere equations will have a real solution. Therefore, it is very important that direct acoustic path based PD source localisation should be conducted. The peaks of the direct path and indirect path AE signals can be ascertain by applying filtering techniques. This significantly reduce the error in the PD source location, as the time difference estimated are more accurate (Dhole *et al.* 2008). A simplified model for wave propagation is suggested in Lundgaard *et al.* (1989). The product of wall thickness and resonant frequency of the acoustic sensor should be about 0.3 mm-Hz. This allows calculation of distance based on propagation in oil alone (Lundgaard *et al.* 1989).

The acoustic wave velocity in metal is greater than in oil. Therefore, the time taken by the structure-borne-path wave to reach the sensor will be lesser compared to the direct-path wave. If any sensor first detects the structure-borne-path wave, then the radius of the sphere formed with the corresponding sensor as center will have a smaller radius and it will not pass through the PD location. Hence, the system of sphere equations will not have a real solution. Therefore, in such cases the PD source will be located in the complex-number-field.

Even when the sensors detect the direct-path-wave, the problem can still arise due to error in signal arrival time measurements. Estimating the signal arrival time accurately, from the PD source to various sensors, is difficult due to the noise and the initial oscillation of the acquired AE burst signals (Kundu *et al.* 2009). Ghosh *et al.* (2017) presents a novel approach for the estimation of TDOA which is based on the source-filter model of acoustic theory. The TDOA is estimated by extraction of the excitation source signal from the acoustic signals. The de-noising of signals that are obtained from the AE sensors is essential, as extensive noise coupled with measured signals can cause ambiguities in the PD source localisation (Búa-Núñez *et al.* 2014; Chan *et al.* 2015;

Hooshmand *et al.* 2013). The measurement of signals in the UHF range is advantageous for a noise-immune analysis, as it is carried out in an electromagnetically clean enclosure of an HV apparatus (Mirzaei *et al.* 2015). However, the UHF detection technique uses oil filtration valves for the sensor insertio. Hence, it is invasive. The other major issue with UHF detection technique is the calibration capability of this measuring method (Akbari *et al.* 2016; Sinaga *et al.* 2012). In the case of a PD detection when using AE signals, the considerably slow propagation velocity of the acoustic waves inside the transformer allow for a better signal arrival time measurement (Kraetge *et al.* 2013). False indications of a PD can be minimised with the AE noise reduction. The acoustic wave attenuation and the transit time are extremely sensitive to the conditions of the medium in which they propagate (Harrold 1985). The acoustic velocity in transformer oil is not constant, but it depends on a complex relationship including the temperature of the oil, its gas content, the moisture content, and also the frequency content of the propagating signal (Howells and Norton 1984). The bias errors can be caused due to sensor fault, sensor ageing, or the proximity of the PD to a certain sensor when in comparison with the other sensors. If any sensor acquires a large bias error in the estimation of the acoustic signal arrival time, a convergence problem is to be expected in the algorithms that were used for the PD source localisation (Al-Masri *et al.* 2016a).

Irrespective of the algorithm used for the PD source localisation, if the measured signal arrival time from the PD source to various sensors are inaccurate, there will be a significant error in the detected PD source location. The effect of error in time measurement on the accuracy of the PD source localisation is analysed in this chapter.

This chapter is organised as follows: Section 4.2 elaborates the effect of error in time-delay measurement on all-acoustic system; Section 4.3 gives the analysis of the effect of error in absolute-time measurement on combined acoustic-electrical system; This is followed by summary of the chapter in Section 4.4.

## **4.2 Effect of error in time-delay measurement on all-acoustic system**

An all-acoustic system uses TDOA approach for the PD source localisation. The mathematical model of an all-acoustic system is explained in Section 2.2 and the system of time difference equations is given in equation (2.1).

In PD source localisation (using a fixed set of coordinates for four sensors and a specific velocity of acoustic signal), the normal practice is to acquire many groups of signals and measure the corresponding time-delays (Tang and Xie 2011). The time-delays  $t_{12}$ ,  $t_{13}$ , and  $t_{14}$  form one group. Each such group of time-delays give a location of the PD source. Irrespective of the algorithm used for PD source localisation, if measured time-delays are inaccurate, the estimated PD source location will have significant error.

### **4.2.1 Numerical experiments to study the effect of error in time-delay measurement**

Numerical experiments are carried out to study the effect of error in time-delay measurement on accuracy of the PD source localisation. The appropriate computer codes are developed for carrying out these numerical experiments.

#### **4.2.1.1 Data for numerical experiments**

The data used in Section 2.5 for the performance analysis of the algorithms for an all-acoustic system is used for studying the effect of time-delay measurement error. A transformer tank of size  $1\text{ m} \times 1\text{ m} \times 1\text{ m}$  is considered for the analysis. The coordinate of four sensors that are used for the numerical experiment are given in Table 4.1 (same as Table 2.4). One sample point (PD source location) corresponding to each case (Cases 1 to 3 explained in Section 2.4.3.1) and one random PD source position are considered

for the numerical experiments. These four PD source positions (PD-1 to PD-4) along with the sensor sequence based on acoustic signal arrival time and the corresponding time-delays are given in Table 4.2 (same as Table 2.5). The velocity of acoustic signal in transformer oil is taken as 1413 m/s (IEEE Std C57.127 2007).

Table 4.1 Coordinates of the sensors used for the numerical experiment

Serial number of the sensor	Sensor coordinates (m)		
	$x_n$	$y_n$	$z_n$
1	0.00	0.85	0.20
2	0.60	0.65	0.00
3	1.00	0.45	0.40
4	0.80	0.25	1.00

Table 4.2 Coordinates of the PD source used for the numerical experiment, sensor sequence based on signal arrival time, and the corresponding time-delays

Serial number	PD position	PD source coordinates (m)			Time-delays ( $\mu s$ )			Sensor sequence based on signal arrival time			
		$x$	$y$	$z$	$t_{12}$	$t_{13}$	$t_{14}$	S1	S2	S3	S4
1	PD-1	0.40	0.55	0.60	0	0	0	1	2	3	4
2	PD-2	0.55	0.95	0.65	0	0	73.6	1	2	3	4
3	PD-3	0.85	0.60	0.75	0	246	405	4	3	2	1
4	PD-4	0.25	0.65	0.45	116	263	332	1	2	3	4

#### 4.2.1.2 Procedure for numerical experiments

- Step-1: Choose one of the PD source positions
- Step-2: Find the sensor nearest to the PD source position.
- Step-3: Calculate the theoretical time-delays ( $t_{12}$ ,  $t_{13}$ , and  $t_{14}$ ) in the signal reception of the other sensors with respect to the nearest sensor.
- Step-4: Calculate the time ( $t_{ref}$ ) taken by the signal to travel the maximum tank dimension. The  $t_{ref}$  is given in equation (4.1). The  $t_{ref}$  is further used as the reference time in adding the time-delay errors to one of the time-delays, namely

$t_{14}$ . The error is systematically increased in  $t_{14}$  by adding 2% to 10% (in steps of 2%) of  $t_{ref}$ .

$$t_{ref} = \frac{\sqrt{l^2 + b^2 + h^2}}{\text{velocity of acoustic signal in oil}} \quad (4.1)$$

where  $l$ ,  $b$ , and  $h$  are the length, breadth, and height of the transformer tank.

- Step-5: Six time-delay-groups (TD-1 to TD-6) are formed for the PD source position. In these six groups, the first time-delay-group has the theoretically calculated time-delay. The error is systematically increased in  $t_{14}$  by adding 2% to 10% (in steps of 2%) of  $t_{ref}$ . Other groups are formed by replacing  $t_{14}$  in the first group with the erroneous time-delays.
- Step-6: The PD source is located by using the proposed non-iterative method for an all-acoustic system with all the time-delay-groups.
- Step-7: The distance percentage error is calculated (using equation (2.124)) for the located PD source position, in a tank with maximum tank dimension given in equation (2.123).
- Step-8: Repeat Step-2 to Step-7 for each PD source positions.
- Step-9: The results are analysed for understanding the effects of error in time-delay on the accuracy of PD source localisation.

The six group of time-delays formed for PD source positions PD-1, PD-2, PD-3, and PD-4 are given in Table 4.3, Table 4.4, Table 4.5, and Table 4.6, respectively.

#### 4.2.1.3 Results of numerical experiments

The PD source localisation results for the four PD source positions PD-1, PD-2, PD-3, and PD-4, with the six time-delay-groups, are given in Table 4.7, Table 4.8, Table

Table 4.3 The six time-delay-groups (TD-1 to TD-6) for the PD source position PD-1

Time-delay-group	Time-delays ( $\mu\text{s}$ )		
	$t_{12}$	$t_{13}$	$t_{14}$
TD-1	0	0	$t_{14} = 0$
TD-2	0	0	$t_{14} + (2\% \text{ of } t_{ref}) = 24.5$
TD-3	0	0	$t_{14} + (4\% \text{ of } t_{ref}) = 49.0$
TD-4	0	0	$t_{14} + (6\% \text{ of } t_{ref}) = 73.5$
TD-5	0	0	$t_{14} + (8\% \text{ of } t_{ref}) = 98.1$
TD-6	0	0	$t_{14} + (10\% \text{ of } t_{ref}) = 120$

Table 4.4 The six time-delay-groups (TD-1 to TD-6) for the PD source position PD-2

Time-delay-group	Time-delays ( $\mu\text{s}$ )		
	$t_{12}$	$t_{13}$	$t_{14}$
TD-1	0	0	$t_{14} = 73.6$
TD-2	0	0	$t_{14} + (2\% \text{ of } t_{ref}) = 98.1$
TD-3	0	0	$t_{14} + (4\% \text{ of } t_{ref}) = 120$
TD-4	0	0	$t_{14} + (6\% \text{ of } t_{ref}) = 150$
TD-5	0	0	$t_{14} + (8\% \text{ of } t_{ref}) = 170$
TD-6	0	0	$t_{14} + (10\% \text{ of } t_{ref}) = 200$

Table 4.5 The six time-delay-groups (TD-1 to TD-6) for the PD source position PD-3

Time-delay-group	Time-delays ( $\mu\text{s}$ )		
	$t_{12}$	$t_{13}$	$t_{14}$
TD-1	0	270	$t_{14} = 450$
TD-2	0	270	$t_{14} + (2\% \text{ of } t_{ref}) = 470$
TD-3	0	270	$t_{14} + (4\% \text{ of } t_{ref}) = 500$
TD-4	0	270	$t_{14} + (6\% \text{ of } t_{ref}) = 520$
TD-5	0	270	$t_{14} + (8\% \text{ of } t_{ref}) = 550$
TD-6	0	270	$t_{14} + (10\% \text{ of } t_{ref}) = 570$

Table 4.6 The six time-delay-groups (TD-1 to TD-6) for the PD source position PD-4

Time-delay-group	Time-delays ( $\mu s$ )		
	$t_{12}$	$t_{13}$	$t_{14}$
TD-1	120	260	$t_{14} = 330$
TD-2	120	260	$t_{14} + (2\% \text{ of } t_{ref}) = 360$
TD-3	120	260	$t_{14} + (4\% \text{ of } t_{ref}) = 380$
TD-4	120	260	$t_{14} + (6\% \text{ of } t_{ref}) = 410$
TD-5	120	260	$t_{14} + (8\% \text{ of } t_{ref}) = 430$
TD-6	120	260	$t_{14} + (10\% \text{ of } t_{ref}) = 450$

4.9, and Table 4.10, respectively. From Table 4.7 and Table 4.9, as the error in time-delay increases, the PD source is located outside the transformer tank dimension. Any algorithm used for the PD source localisation can locate these PD source positions (as they are in the real-number-field). Whenever a time-delay-group locate the PD source outside the transformer tank dimension (implies false localisation of the PD source), it can be spotted and discarded.

From Table 4.8 and Table 4.10, as the error in time-delay increases the PD source is located in the complex-number-field. These results are highlighted in Table 4.8 and Table 4.10. The error in time-delay measurement is sometimes so significant that there is no solution to the time-difference equations in real-number-field. Some of the algorithms, for example Newton's method, have their search space in the real-number-field. Therefore, this kind of situation may lead to false localisation of the PD source. Hence, such time-delays should be considered invalid. If the time-delays are invalid, the distance error cannot be calculated for such cases and hence, the error is given as NaN (Not a Number). Identifying and discarding time-delay-groups (invalid time-delay-groups) which result in the solution of the system of non-linear equations in a complex-number-field will be advantageous in improving the accuracy of PD localisation. Methods for mathematically identifying invalid time-delay-groups are discussed in the following section.



Table 4.7 The PD source localisation results for the PD source position PD-1 with six time-delay-groups

Time-delay-group	PD source coordinates (m)			Acoustic signal arrival time, T (s)	Distance error (%)
	x	y	z		
TD-1	0.4000	0.5500	0.6000	$4.53 \times 10^{-4}$	0.00
TD-2	0.4423	0.6628	0.6141	$4.49 \times 10^{-4}$	7.01
TD-3	0.4895	0.7887	0.6298	$4.63 \times 10^{-4}$	14.8
TD-4	0.5499	0.9499	0.6500	$5.08 \times 10^{-4}$	24.8
TD-5	0.6479	1.2111	0.6826	$6.26 \times 10^{-4}$	41.0
TD-6	0.9654	2.0576	0.7885	$1.17 \times 10^{-4}$	93.6

Table 4.8 The PD source localisation results for the PD source position PD-2 with six time-delay-groups

Time-delay-group	PD source coordinates (m)			Acoustic signal arrival time, T (m)	Distance error (%)
	x	y	z		
TD-1	0.5500	0.9500	0.6500	$5.08 \times 10^{-4}$	0.00
TD-2	0.6480	1.2114	0.6827	$6.26 \times 10^{-4}$	16.2
TD-3	0.9660	2.0593	0.7887	$1.17 \times 10^{-3}$	68.8
TD-4*	0.40+ 0.49i	0.55+ 1.31i	0.60+ 0.16i	$-7.35 \times 10^{-5} + 8.95 \times 10^{-4}i$	NaN
TD-5*	0.40+ 0.34i	0.55 + 0.91i	0.60 + 0.11i	$-8.58 \times 10^{-5} + 5.31 \times 10^{-4}i$	NaN
TD-6*	0.40 + 0.29i	0.55 + 0.78i	0.60 + 0.09i	$-9.80 \times 10^{-5} + 4.00 \times 10^{-4}i$	NaN

\* The PD source localisation results of time-delay-groups that localised PD source in complex-number-field are highlighted.

## 4.2.2 Proposed methods for identification of invalid time-delay-groups

The error in time measurement is sometimes so significant that there is no solution to the non-linear sphere equations in real-number-field. Such time measurements should be considered invalid. Two mathematical methods for the identification of erroneous time (invalid time) measurements are proposed: (i) using discriminant; and (ii) using Jacobian-determinant. These methods are explained in the subsequent sub-sections.

### 4.2.2.1 Method-1: using Discriminant

In the existing non-iterative algorithm for an all-acoustic system given in Section 2.4.1, the intersection of two spheres form a plane. The PD source can be located on this

Table 4.9 The PD source localisation results for the PD source position PD-3 with six time-delay-groups

Time-delay-group	PD source coordinates (m)			Acoustic signal arrival time, T (m)	Distance error (%)
	$x$	$y$	$z$		
TD-1	0.8500	0.6000	0.7500	$2.90 \times 10^{-4}$	0.00
TD-2	0.7753	0.3782	0.6537	$2.45 \times 10^{-4}$	14.6
TD-3	0.7794	0.2138	0.5989	$2.69 \times 10^{-4}$	24.2
TD-4	0.8238	0.0461	0.5544	$3.30 \times 10^{-4}$	33.9
TD-5	0.9126	-0.1523	0.5118	$4.38 \times 10^{-4}$	45.7
TD-6	1.0697	-0.4182	0.4655	$6.18 \times 10^{-4}$	62.3

Table 4.10 The PD source localisation results for the PD source position PD-4 with six time-delay-groups

Time-delay-group	PD source coordinates (m)			Acoustic signal arrival time, T (m)	Distance error (%)
	$x$	$y$	$z$		
TD-1	0.2500	0.6500	0.4500	$2.87 \times 10^{-4}$	0.00
TD-2	0.3072	0.8064	0.4688	$2.91 \times 10^{-4}$	9.67
TD-3	0.3598	1.0130	0.4809	$3.43 \times 10^{-4}$	21.9
TD-4	0.4170	1.3941	0.4812	$5.24 \times 10^{-4}$	44.0
TD-5	0.5567	3.7119	0.3685	$2.07 \times 10^{-4}$	177
TD-6*	0.45 - 0.08i	0.13 - 1.08i	0.60+ 0.04i	$-5.55 \times 10^{-4} \sim 6.80 \times 10^{-4}i$	NaN

\* The PD source localisation results of time-delay-groups that localised PD source in complex-number-field are highlighted.

intersecting plane. Two such planes intersect in a line. The PD source can be located on this line. The line intersects any one of the spheres in two points. This results in a quadratic equation given in (2.49). One of the solutions of this quadratic equation is the PD source location. If the quadratic equation does not have a real root, it implies either the sensor detected the structure-borne-path wave or there is a significant error in the time measurement. The nature of the roots of the quadratic equation can be identified from the discriminant value. The discriminant of the quadratic equation (2.49) is given in equation (4.2).

$$Discriminant = \sigma_{21}^2 - 4\sigma_{20}\sigma_{22}, \quad (4.2)$$

A negative value for the discriminant implies that the quadratic equation have complex roots. Thus, by checking the sign of the discriminant value, it is possible to identify whether the time-delay group located the PD source in the real-number-field or in the complex-number-field. Therefore, such time-delay-group should be considered invalid and cannot be used for all-acoustic PD source localisation.

In some special cases, when the PD source is equidistant from the sensors (i.e. when one or more of the time-delays ( $t_{12}$ ,  $t_{13}$ , and  $t_{14}$ ) are zero) or when all x, all y, or all z coordinates of the sensors are the same, some constants ( $\sigma_1$  to  $\sigma_{22}$ ) given in Section 2.4.1 cannot be found (NaN). Hence, the discriminant value given in equation (4.2) cannot be determined. In such cases, the invalid time-delay-groups can be identified by using an alternative method.

#### **4.2.2.2 Method-2: using Jacobian determinant**

An alternative method to identify the invalid time-delay-groups is by solving the system of non-linear equations using Newton's method. When a system has complex roots, a straight line solution no longer exists. The solution either spiral toward or spiral away from the origin (Hirsch *et al.* 2004). Any sign transition of the eigenvalues is reflected in the sign change of the Jacobian-determinant. From a computational point of view, monitoring the sign changes of all the eigenvalues are quite difficult. Therefore, an alternative and efficient method is to monitor the sign changes of Jacobian-determinant (Padovan and Arechaga 1982). A generalised flowchart for the identification of the invalid time-delay-group by using Newton's method (including the proposed extension of Newton's method for the identification of invalid time-delay-groups) is shown in Figure 4.1. In the present study, the sign of the Jacobian-determinant is checked for all iterations of Newton's method. This is indicated in Figure 4.1 by highlighting this part in the flowchart. If the sign (+ve or -ve) of the determinant value changes from one iteration to the next, multiple times, it shows a clear case of oscillation. These oscillations are attributed to the non-convergence of Newton's method, due to an unavailability of a real

solution.

### **4.2.3 Verification of the proposed methods using numerical experiments**

In numerical experiments, for all the four PD source positions (PD-1 to PD-4) with all the six time-delay-groups (TD-1 to TD-6), the discriminant value is calculated and the sign of the Jacobian-determinant is checked for ten iterations of Newton's method. For the three PD source positions PD-1, PD-2, and PD-3, the discriminant value cannot be determined as one or more of the time-delays are zero. However, whether the solution is in real-number-field or complex-number-field can be identified by checking the sign changes of the Jacobian-determinant.

The discriminant value calculated for the PD source position PD-4 is given in Table 4.11. From Table 4.11, for the time-delay-groups TD-1 to TD-5, the discriminant value is positive and the corresponding PD source localisation results in Table 4.10 shows that the algorithm localise the PD source position in real-number-field. For the time-delay-group TD-6, the discriminant value is negative and the corresponding PD source localisation results in Table 4.10 shows that the algorithm localise the PD source position in complex-number-field. This result is highlighted in Table 4.11. Thus, whether the PD source is located in the real-number-field or in the complex-number-field can be identified by checking the sign of the discriminant value.

The Jacobian-determinant calculated for the PD source positions PD-1, PD-2, PD-3, and PD-4 are given in Table 4.12, Table 4.13, Table 4.14, and Table 4.15, respectively. From Table 4.12 and Table 4.14, it can be seen that the Jacobian-determinant has at most one sign change (no multiple sign changes) in ten iterations of Newton's method with all the six time-delay-groups. From the corresponding PD source localisation results in Table 4.7 and Table 4.9, the PD source is located in the real-number-field with all the six time-delay-groups.

From Table 4.13, the Jacobian-determinant has at most one sign change (no multiple sign changes) in ten iterations of Newton's method for the time-delay-group TD-1 to TD-3. From the corresponding PD source localisation results in Table 4.8, the PD source is located in the real-number-field for these time-delay-groups. For the time-delay-groups TD-4 to TD-6, the Jacobian-determinant has multiple sign changes in 10 iterations of Newton's method. These results are highlighted in Table 4.13. From the corresponding PD source localisation results in Table 4.8, the PD source is located in the complex-number-field for these time-delay-groups. From Table 4.15, the Jacobian-determinant has at most one sign change (no multiple sign changes) in ten iterations of Newton's method for the time-delay-group TD-1 to TD-5. From the corresponding PD source localisation results in Table 4.10, the PD source is located in the real-number-field for these time-delay-groups. For the time-delay-group TD-6, the Jacobian-determinant has multiple sign changes in ten iterations of Newton's method. These results are highlighted in Table 4.15. From the corresponding PD source localisation results in Table 4.10, the PD source is located in the complex-number-field for this time-delay-group. Thus, whether the PD source is located in the real-number-field or in the complex-number-field can be identified by checking the sign changes of the Jacobian-determinant in iterations of Newton's method.

#### **4.2.4 Application of proposed method to published literature**

In order to validate the proposed methods with practical data, the data from reference Lu *et al.* (2000) are taken and analysed. One of the PD source locations (of the two) with coordinates (70, 43, 52) cm, is chosen for the analysis. Table 4.16 shows the five groups of time-delays measured (TD-1 to TD-5) for the corresponding PD source location, as given in reference Lu *et al.* (2000). For each group of time-delays the discriminant value is found using equation (4.2). Newton's method is implemented to solve system of non-linear equations with random initial guess. For each time-delay-group, the discriminant

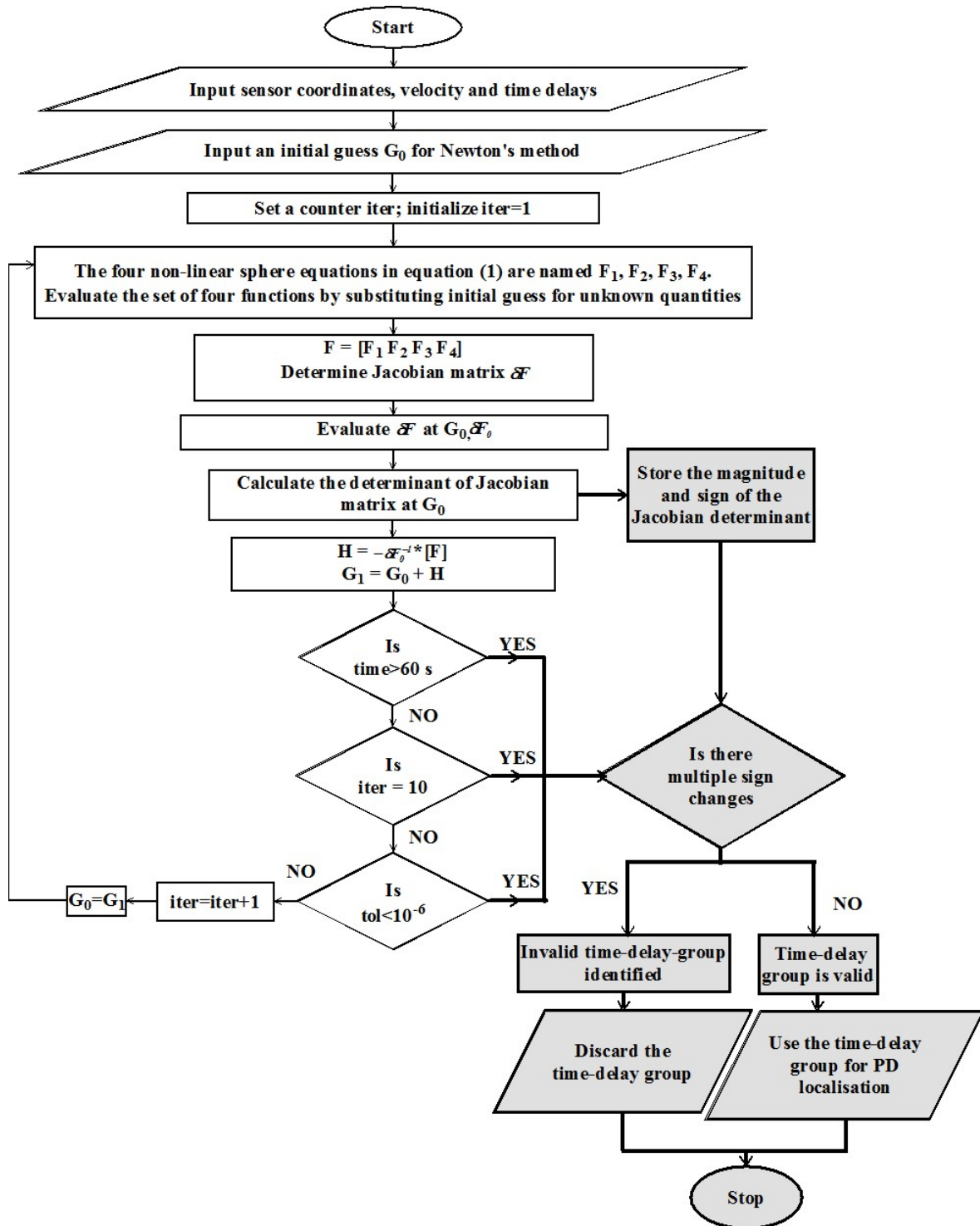


Figure 4.1 Flowchart for identification of invalid time-delay-group by using Newton's method (The highlighted portion is the proposed extension of Newton's method for the identification of invalid time-delay-group).

Table 4.11 The discriminant value computed for the PD source position PD-4 with each time-delay-group

Time-delay-group	Discriminant value ( $m^2$ )
TD-1	53.8
TD-2	63.4
TD-3	70.2
TD-4	67.4
TD-5	29.7
TD-6*	-164

\* A negative value for the discriminant implies PD source will be localised in complex-number-field with TD-6 (highlighted).

Table 4.12 Jacobian-determinants calculated for ten iterations in Newton's method for the PD source position PD-1 with each time-delay-group (TD-1 to TD-6)

Iteration number	Jacobian-determinants for the time-delay-group					
	TD-1	TD-2	TD-3	TD-4	TD-5	TD-6
1	-1867	-1245	-1749	-238	-1663	-2520
2	-871	-545	-880	-352	-634	-110
3	-928	-1032	-859	-1009	-615	-565
4	-926	-917	-859	-795	-614	-382
5	-926	-910	-859	-766	-614	-337
6	-926	-910	-859	-766	-614	-335
7	-926	-910	-859	-766	-614	-335
8	-926	-910	-859	-766	-614	-335
9	-926	-910	-859	-766	-614	-335
10	-926	-910	-859	-766	-614	-335

value and Jacobian-determinants (for ten iterations) are also shown in Table 4.16.

From Table 4.16 it is seen that whenever the discriminant value is negative, the Jacobian-determinant changes sign multiple times. This indicates the corresponding measured time-delay-group will result in complex solution for system of non-linear

Table 4.13 Jacobian-determinants calculated for ten iterations in Newton’s method for the PD source position PD-2 with each time-delay-group (TD-1 to TD-6)

Iteration number	Jacobian-determinants for the time-delay-group					
	TD-1	TD-2	TD-3	TD-4*	TD-5*	TD-6*
1	-629	-436	-2577	-339	-2035	-1842
2	-725	-212	-78	122	680	988
3	-767	-997	-757	-792	-86	-11
4	-766	-688	-452	-264	3316	43988
5	-766	-618	-350	261	1571	21982
6	-766	-614	-335	-268	601	10969
7	-766	-614	-334	255	-182	5439
8	-766	-614	-334	-280	1504	2628
9	-766	-614	-334	231	559	1124
10	-766	-614	-334	-335	-238	118

\* The multiple sign changes of Jacobian determinant in the iteration of Newton’s method implies PD source localisation in complex-number-field with TD-4, TD-5, and TD-6 (highlighted).

equations. Whenever the discriminant value is positive, the Jacobian-determinant will converge to a fixed value with at most one sign change. This indicates the system has a real solution.

From Table 4.16, it is observed that the two groups of time-delays which result in a negative discriminant value or in the oscillation of the Jacobian-determinants are TD-3 and TD-4. These results are highlighted in Table 4.16. The theoretical time-delay-group for the PD source considered is (110, 223, 334)  $\mu s$  (Lu *et al.* 2000). The percentage error in the measured time-delays for TD-3 and TD-4 are shown in Table 4.17 . From Table 4.17, it is seen that the measured time-delays have significant error.

The PD source location re-calculated for the time-delay-groups TD-3 and TD-4, using non-iterative method and iterative method (Newton’s method) are shown in Table 4.18. When the results are reproduced using non-iterative method, it is found that the solutions are complex numbers. However, in published literature Kundu *et al.* (2009),



Table 4.14 Jacobian-determinants calculated for ten iterations in Newton’s method for the PD source position PD-3 with each time-delay-group (TD-1 to TD-6)

Iteration number	Jacobian-determinants for the time-delay-group					
	TD-1	TD-2	TD-3	TD-4	TD-5	TD-6
1	1491	1860	473	1736	288	1290
2	338	701	843	988	-354	664
3	352	672	846	958	-1669	1185
4	352	671	846	958	-1151	1070
5	352	671	846	958	-1034	1064
6	352	671	846	958	-1028	1064
7	352	671	846	958	-1028	1064
8	352	671	846	958	-1028	1064
9	352	671	846	958	-1028	1064
10	352	671	846	958	-1028	1064

only the real part of the complex solution is reported as PD location. The PD source located using least square algorithm reported in reference Kundu *et al.* (2009) is also shown in Table 4.18. It is inferred from Table 4.18 that: (i) non-iterative method gives a complex solution. (ii) Newton’s method gives a false PD location, and (iii) least square algorithm gives no solution for TD-3 group and an erroneous location for TD-4 group.

### 4.3 Effect of error in absolute-time measurement on combined acoustic-electrical system

A combined acoustic-electrical system uses TOA approach for the PD source localisation. The mathematical model of a combined acoustic-electrical system is explained in Section 3.2 and the system of time difference equations is given in equation (3.1). In PD source localisation (using a fixed set of coordinates for three sensors and a specific velocity of acoustic signal), the normal practice is to acquire many groups of signals and measure the corresponding signal arrival time. The absolute acoustic signal arrival

Table 4.15 Jacobian-determinants calculated for ten iterations in Newton's method for the PD source position PD-4 with each time-delay-group (TD-1 to TD-6)

Iteration number	Jacobian-determinants for the time-delay-group					
	TD-1	TD-2	TD-3	TD-4	TD-5	TD-6*
1	-1385	-1474	-1255	-2305	-476	-359
2	-350	-599	-677	-267	72	570
3	-1098	-766	-656	-628	491	144
4	-844	-748	-656	-525	312	-489
5	-805	-748	-656	-514	261	-80
6	-804	-748	-656	-514	256	969
7	-804	-748	-656	-514	256	401
8	-804	-748	-656	-514	256	-1
9	-804	-748	-656	-514	256	135201
10	-804	-748	-656	-514	256	67600

\* The multiple sign changes of Jacobian determinant in the iteration of Newton's method implies PD source localisation in complex-number-field with TD-6 (highlighted).

time  $T_1$ ,  $T_2$ , and  $T_3$  form one group. Each such absolute-time-groups give a location of the PD source. Irrespective of the algorithm used for PD source localisation, if measured absolute-time-group is inaccurate, the estimated PD source location will have significant error.

### 4.3.1 Numerical experiments to study the effect of error in absolute-time measurement

Numerical experiment are carried out to study the effect of error in absolute-time measurement on accuracy of the PD source localisation. The appropriate computer codes are developed for carrying out these numerical experiments.

Table 4.16 (A) Five groups of time-delays given in reference Lu *et al.* (2000) (B) Discriminant value ( $m^2$ ) for each group of time-delays (C) Jacobian-determinants calculated for 10 iterations in Newton's method for each group of time-delays

(A) Time-delays ( $\mu s$ )					
Group	TD-1	TD-2	TD-3	TD-4	TD-5
$t_{12}$	82	131	145	93	206
$t_{13}$	250	200	207	191	358
$t_{14}$	374	321	351	345	253
(B) Discriminant value					
	TD-1	TD-2	TD-3*	TD-4*	TD-5
	3.02E-01	2.84E-01	-1.54E-01	-4.01E-02	2.12E+03
(C) Jacobian-determinants for 10 iterations					
Iteration number	TD-1	TD-2	TD-3	TD-4	TD-5
1	-1399.6	-1717.9	-1957.4	-1640.1	-952.38
2	-1600.7	-2120.1	-2234.5	-1922.8	-929.33
3	-956.80	-1238.4	-991.42	-932.15	-3060.5
4	-740.15	-924.57	-212.17	-405.75	-2318.5
5	-708.44	-871.30	1218.82	-64.290	-2199.8
6	-707.73	-869.67	378.77	842.45	-2196.6
7	-707.73	-869.67	-552.77	354.48	-2196.6
8	-707.73	-869.67	232.16	18.610	-2196.6
9	-707.73	-869.67	-1094.8	-3011.9	-2196.6
10	-707.73	-869.67	-290.59	-1487.3	-2196.6

\* A negative discriminant value and multiple sign changes of Jacobian determinant in the iteration of Newton's method implies PD source localisation in complex-number-field with TD-3 and TD-4 (highlighted).

#### 4.3.1.1 Data for numerical experiments

The data used in Section 3.4 for the performance analysis of the algorithms for combined acoustic-electrical system is used for studying the effect of absolute-time measurement error. A transformer tank of size 3 m  $\times$  3 m  $\times$  3 m is considered for the

Table 4.17 Percentage error in time-delay-groups TD-3 and TD-4

Group	Percentage error		
	$t_{12}$	$t_{13}$	$t_{14}$
TD-3	31.82	-7.175	5.089
TD-4	-15.45	-14.35	3.293

Table 4.18 PD source located using different algorithms with time-delay-groups TD-3 and TD-4

Group	TD-3			TD-4		
	X (cm)	Y (cm)	Z (cm)	X (cm)	Y (cm)	Z (cm)
Non-iterative method	69+5i	42-i	59+25i	73+3i	35-i	67+14i
Newton's method	656	-5	259	88	30	125
Least square algorithm	*	*	*	69.1	41.8	59.6

\* The method failed to locate the PD source position.

analysis. The coordinate of three sensors that are used for the numerical experiment are given in Table 4.19 (the first three sensors given in Table 3.3). Three randomly chosen PD source positions (PD-1 to PD-3) are given in Table 4.20 (same PD positions chosen for numerical experiments in Section 3.4.1.1). The velocity of the acoustic signal in transformer oil is taken as 1413 m/s (IEEE Std C57.127 2007).

Table 4.19 Coordinates of the sensors used for numerical experiment

Sensor number (Sn)	Sensor coordinates		
	$x_n$ (m)	$y_n$ (m)	$z_n$ (m)
S1	0.40	0.24	0.00
S2	0.60	1.76	0.00
S3	0.50	2.75	0.00

Table 4.20 PD source coordinates used for numerical experiment

PD position	PD source coordinates (m)		
	$x$	$y$	$z$
PD-1	2.8	0.9	1.7
PD-2	1.3	1.4	0.7
PD-3	1.6	2.2	0.4

#### 4.3.1.2 Procedure for numerical experiments

- Step-1: Choose one of the PD source positions
- Step-2: Calculate the theoretical absolute signal arrival time ( $T_1$ ,  $T_2$ , and  $T_3$ ) from the PD source to various sensors
- Step-3: Calculate the time ( $t_{ref}$ ) taken by the signal to travel the maximum tank dimension. The  $t_{ref}$  is given in equation 4.1. The  $t_{ref}$  is further used as the reference time in adding the absolute-time errors to one of the signal arrival time, namely  $T_3$ . The error is systematically increased in  $T_3$  by adding 0.2% to 1% (in steps of 0.2%) of  $t_{ref}$  (0.2% to 1% of  $t_{ref}$  is chosen (instead of 2% to 10% of  $t_{ref}$ ) because of the larger tank dimension (3 m  $\times$  3 m  $\times$  3 m)).
- Step-4: Six absolute-time-groups (AT-1 to AT-6) are formed for the PD source position. In these six groups, the first absolute-time-group has the theoretically calculated absolute-time values. The error is systematically increased in  $T_3$  by adding 0.2% to 1% (in steps of 0.2%) of  $t_{ref}$ . Other groups are formed by replacing  $T_3$  in the first group with the erroneous absolute-times.
- Step-5: The PD source is located by using the proposed non-iterative method for a combined acoustic-electrical system with all the absolute-time-groups.
- Step-6: The distance percentage error is calculated (using equation (2.124)) for the located PD source position, in a tank with maximum tank dimension given in

equation (2.123).

- Step-7: Repeat Step-2 to Step-6 for each PD source positions.
- Step-8: The results are analysed for understanding the effects of error in absolute-time measurement on the accuracy of PD source localisation.

The six absolute-time-groups (AT-1 to AT-6) formed for each PD position PD-1, PD-2, and PD-3 are given in Table 4.21, Table 4.22, and Table 4.23, respectively.

Table 4.21 The six absolute-time-groups (AT-1 to AT-6) for the PD source position PD-1

Absolute-time-group	Absolute-time (ms)		
	$T_1$	$T_2$	$T_3$
AT-1	2.133	2.060	$T_3 = 2.411$
AT-2	2.133	2.060	$T_3 + 0.2\%$ of $t_{ref} = 2.418$
AT-3	2.133	2.060	$T_3 + 0.4\%$ of $t_{ref} = 2.425$
AT-4	2.133	2.060	$T_3 + 0.6\%$ of $t_{ref} = 2.433$
AT-5	2.133	2.060	$T_3 + 0.8\%$ of $t_{ref} = 2.440$
AT-6	2.133	2.060	$T_3 + 1.0\%$ of $t_{ref} = 2.447$

Table 4.22 The six absolute-time-groups (AT-1 to AT-6) for the PD source position PD-2

Absolute-time-group	Absolute-time (ms)		
	$T_1$	$T_2$	$T_3$
AT-1	1.151	7.455	$T_3 = 1.216$
AT-2	1.151	7.455	$T_3 + 0.2\%$ of $t_{ref} = 1.223$
AT-3	1.151	7.455	$T_3 + 0.4\%$ of $t_{ref} = 1.231$
AT-4	1.151	7.455	$T_3 + 0.6\%$ of $t_{ref} = 1.238$
AT-5	1.151	7.455	$T_3 + 0.8\%$ of $t_{ref} = 1.245$
AT-6	1.151	7.455	$T_3 + 1.0\%$ of $t_{ref} = 1.253$

### 4.3.1.3 Results of numerical experiments

The PD source localisation results for the three PD source position PD-1, PD-2, and PD-3, with the six absolute-time-groups, are given in Table 4.24, Table 4.25, and Table 4.26, respectively. From Table 4.24, Table 4.25, and Table 4.26, as the error in absolute-time increases the PD source is located in the complex-number-field. These results are highlighted in Table 4.24, Table 4.25, and Table 4.26. The error in time measurement is sometimes so significant that there is no solution to the time-difference equations in real-number-field. Some of the algorithms, for example Newton's method, have their search space in the real-number-field. Therefore, this kind of situation may lead to false localisation of the PD source. Hence, such absolute-time-groups should be considered invalid. Identifying and discarding absolute-time-groups (invalid time-delay-groups) which result in the solution of the system of non-linear equations in a complex-number-field will be advantageous in improving the accuracy of PD localisation. Method for mathematically identifying invalid absolute-time-groups is discussed in the following section.

Table 4.23 The six absolute-time-groups (AT-1 to AT-6) for the PD source position PD-3

Absolute-time-group	Absolute-time (ms)		
	$T_1$	$T_2$	$T_3$
AT-1	1.650	0.823	$T_3 = 0.915$
AT-2	1.650	0.823	$T_3 + 0.2\%$ of $t_{ref} = 0.923$
AT-3	1.650	0.823	$T_3 + 0.4\%$ of $t_{ref} = 0.930$
AT-4	1.650	0.823	$T_3 + 0.6\%$ of $t_{ref} = 0.937$
AT-5	1.650	0.823	$T_3 + 0.8\%$ of $t_{ref} = 0.945$
AT-6	1.650	0.823	$T_3 + 1.0\%$ of $t_{ref} = 0.952$

### **4.3.2 Proposed method for identification of invalid absolute-time-groups**

In the proposed non-iterative algorithm for a combined acoustic-electrical system given in Section 3.3, the intersection of two spheres form a plane. The PD source can be located on this intersecting plane. Two such planes intersect in a line. The PD source can be located on this line. The line intersects any one of the spheres in two points. This results in a quadratic equation given in (3.24) . One of the solutions of this quadratic equation is the PD source location. If the quadratic equation does not have a real root, it implies either the sensor detected the structure-borne-path wave or there is a significant error in the time measurement. The nature of the roots of the quadratic equation can be identified from the discriminant value. The discriminant of the quadratic equation (3.24) is given in equation (4.3).

$$Discriminant = k_{15}^2 - 4k_{14}k_{16}, \quad (4.3)$$

A negative value for the discriminant implies the quadratic equation have complex roots. Thus, by checking the sign of the discriminant value, it is possible to identify whether the absolute-time-group located the PD source in the real-number-field or in the complex-number-field. Therefore, such absolute-time-group should be considered invalid and cannot be used for combined acoustic-electrical PD source localisation.

### **4.3.3 Verification of the proposed method using numerical experiments**

In numerical experiments, the discriminant value is calculated for all the three PD source positions with all the six absolute-time-groups. The discriminant value calculated for all the PD source positions are given in Table 4.27. From Table 4.27, for the PD source position PD-1, the discriminant value is positive for the absolute-time-



Table 4.24 The PD source localisation results for the PD source position PD-1 with six absolute-time-groups

Absolute-time-group	PD source coordinates (m)			Distance error (%)
	$x$	$y$	$z$	
AT-1	2.8000	0.9000	1.7000	0.00
AT-2	2.9540	0.8797	1.4675	5.38
AT-3	3.1084	0.8594	1.1690	11.80
AT-4	3.2633	0.8390	0.7268	20.70
AT-5*	3.4187	0.8186	0.00 + 0.60i	NaN
AT-6*	3.5745	0.7981	0.00 + 1.14i	NaN

\* The PD source localisation results of absolute-time-groups that localised PD source in complex-number-field are highlighted.

Table 4.25 The PD source localisation results for the PD source position PD-2 with six absolute-time-groups

Absolute-time-group	PD source coordinates (m)			Distance error (%)
	$x$	$y$	$z$	
AT-1	1.3000	1.4000	0.7000	0.00
AT-2	1.3778	1.3898	0.6063	2.35
AT-3	1.4560	1.3795	0.4817	5.18
AT-4	1.5348	1.3691	0.2881	9.14
AT-5*	1.6139	1.3587	0.00 + 0.28i	NaN
AT-6*	1.6936	1.3482	0.00 + 0.50i	NaN

\* The PD source localisation results of absolute-time-groups that localised PD source in complex-number-field are highlighted.

groups AT-1 to AT-4, and the corresponding PD source localisation results in Table 4.24 shows that the algorithm localise the PD source position in real-number-field. For the absolute-time-groups AT-5 and AT-6, the discriminant value is negative and the corresponding PD source localisation results in Table 4.24 shows that the algorithm localise the PD source position in complex-number-field. For the PD source position PD-2, the discriminant value is positive for the absolute-time-groups AT-1 to AT-4, and the

Table 4.26 The PD source localisation results for the PD source position PD-3 with six absolute-time-groups

Absolute-time-group	PD source coordinates (m)			Distance error (%)
	$x$	$y$	$z$	
AT-1	1.6000	2.2000	0.4000	0.00
AT-2	1.6586	2.1923	0.2147	3.74
AT-3*	1.7177	2.1845	0.00+ 0.27i	NaN
AT-4*	1.7772	2.1767	0.00 + 0.45i	NaN
AT-5*	1.8372	2.1688	0.00 + 0.58i	NaN
AT-6*	1.8976	2.1608	0.00 + 0.70i	NaN

\* The PD source localisation results of absolute-time-groups that localised PD source in complex-number-field are highlighted.

corresponding PD source localisation results in Table 4.25 shows that the algorithm localise the PD source position in real-number-field. For the absolute-time-groups AT-5 and AT-6, the discriminant value is negative and the corresponding PD source localisation results in Table 4.25 shows that the algorithm localise the PD source position in complex-number-field. For the PD source position PD-3, the discriminant value is positive for the absolute-time-groups AT-1 and AT-2, and the corresponding PD source localisation results in Table 4.26 shows that the algorithm localise the PD source position in real-number-field. For the absolute-time-groups AT-3 to AT-6, the discriminant value is negative and the corresponding PD source localisation results in Table 4.26 shows that the algorithm localise the PD source position in complex-number-field. The negative discriminant values are highlighted in Table 4.27. Thus, whether the PD source is located in the real-number-field or complex-number-field can be identified by checking the sign of the discriminant value.

#### 4.3.4 Application of proposed method to published literature

The efficacy of the proposed method to identify the structure-borne-path waves (or the significant error in time-measurement) using discriminant value is verified by applying

Table 4.27 Discriminant value computed for the PD source position with all the absolute-time-groups

Absolute-time-group	Discriminant value ( $m^2$ )*		
	PD-1	PD-2	PD-3
AT-1	22.7	3.84	1.25
AT-2	16.9	2.88	0.36
AT-3	10.7	1.82	-0.59
AT-4	4.14	0.65	-1.61
AT-5	-2.83	-0.62	-2.70
AT-6	-10.2	-2.01	-3.85

\* A negative value for the discriminant implies PD source will be localised in complex-number-field with the corresponding absolute-time-group (highlighted).

it to the experimental data published in Phung *et al.* (2001). The three locations of the sensor, the location of the source of the PD, and the absolute signal arrival times (from the source to the sensors) that are reported in Phung *et al.* (2001) have been used to verify the proposed method. The related data that are reported in Phung *et al.* (2001) are as follows. A transformer tank of size  $0.9 \text{ m} \times 1.1 \text{ m} \times 0.6 \text{ m}$  ((z-axis)  $\times$  (x-axis)  $\times$  (y-axis)) is used. The AE sensor used for the experiment is the PAC (type R15I) resonant sensor. It has a built-in 40 dB pre-amplifier. The typical operation range of the sensor is from 100 kHz to 450 kHz and the resonant frequency is  $\sim 160$  kHz. The coordinates of the PD source used for the experiment is (0.75, 0.30, 0.35) m. To detect the acoustic signals from the PD source, the sensor is placed at three different locations (point A, point B, and point C) on the transformer tank wall. The coordinates of the sensor when placed at point A, point B, and point C are  $SA(0.75, 0.60, 0.35)$ ,  $SB(0.25, 0.60, 0.35)$ , and  $SC(1.10, 0.30, 0.35)$ , respectively. The velocity of the acoustic signal in oil is taken as 1400 m/s.

When the sensor is placed at point A and point C, the sensor is placed normal to the PD source and the direct-path-wave is the quickest. At point A and point C the

sensor first detects the direct-path wave. As stated in Phung *et al.* (2001), point B is outside the critical incidence angle. Therefore, for the sensor placed at point B, the structure-borne-path wave is the quickest. At point B, the sensor first detects the structure-borne-path wave. The attenuation of the AE signals in the metal is larger than in transformer oil (Harrold 1979b). Therefore, the higher magnitude oscillations in the received signal correspond to the signal arrival time of direct-path wave. The signals detected by sensor at point A and point C have a sharp wavefront with the magnitude reaching its maximum almost at the beginning. On the contrary, the signal detected by sensor at point B is relatively small in the beginning (for some time) and then the magnitude increases suddenly.

In Phung *et al.* (2001), the arrival time of the direct-path-wave is identified from the signal received by the sensor at point B by applying two corrections.

- Correction-1: the time measurement based on ignoring the smaller oscillation (that are present before the sudden change in amplitude of the oscillation) in the wavefront.
- Correction-2: the time measurement based on the oscillation with largest amplitude.

The signal arrival time from PD source to AE sensor, with sensor placed at the three locations (point A, point B, and point C) are estimated in four different ways in Phung *et al.* (2001):

1. Calculated theoretically (predicted)
2. Mesuared based on first detected signal (measured)
3. Identified by applying Correction-1
4. Identified by applying Correction-2

$T_A$ ,  $T_B$ , and  $T_C$  are the absolute signal arrival time from PD source to AE sensor placed at point A, point B, and point C, respectively. The four groups of absolute signal arrival time from source to sensor reported in Phung *et al.* (2001), the corresponding discriminant value computed, and the PD source coordinates estimated for each absolute-time group are given in Table 4.28.

Table 4.28 Absolute signal arrival time given in Phung *et al.* (2001) with the corresponding discriminant value computed and PD source coordinates estimated for each absolute-time group

Estimation method	Absolute signal arrival time ( $\mu s$ )			Discriminant value ( $m^2$ )	PD source coordinates (m)		
	$T_A$	$T_B$	$T_C$		x	y	z
Predicted	214.29	416.50	250.00	$2.03 \times 10^{-6}$	0.75	0.30	0.35
Measured*	216	300	250	-0.26	0.58	0.11	0.35+0.43i
Correction-1*	216	380	250	-0.07	0.69	0.22	0.35+0.22i
Correction-2	216	450	250	0.04	0.80	0.36	0.53

\* The PD source localisation results of estimation methods that localised PD source in complex-number-field are highlighted.

From Table 4.28, when using the predicted value (with no error) of signal arrival time, the discriminant value is positive and the non-iterative algorithm located the PD source accurately. When the measured (structure-borne-path wave) signal arrival time is used, the discriminant value is negative and the non-iterative algorithm located the PD source in the complex-number-field. When the signal arrival time after applying Correction-1 is used, the discriminant value is still negative and the PD source is located in the complex-number-field. When the signal arrival time after applying Correction-2 is used, the discriminant value became positive and the PD source is located in the vicinity of the actual PD location. The PD source localisation results of estimation methods that gives a negative discriminant value is highlighted in Table 4.28.

Even though to some extent, it is possible to identify the signal arrival time of direct-path wave by examining the amplitude of the measured signal, it is not a foolproof method. The attenuation of AE signals can also happen because of barriers or other physical obstacles present in the path of acoustic wave propagation. It is possible to identify whether the sensor detected the direct-path-wave or the structure-borne-path

wave by checking the discriminant value in the proposed non-iterative algorithm. The discriminant value also indicates whether there is a significant error in time measurement. The structure-borne-path waves results in incorrect localisation of the PD source. Therefore, IEEE Std C57.127 (2007) suggests that the estimated PD source location should be confirmed by using multiple sensor locations (IEEE Std C57.127 2007).

The real-number-field is the only search space for iterative (Newton's method) and search (Genetic Algorithm) algorithms. Therefore, any significant error in time measurement may lead to false localisation of the PD source. The possibility of identifying the structure-borne-path wave or significant error in time measurement by checking the discriminant value is advantageous in PD source localisation using AE technique.

## 4.4 Summary

The errors in time measurement are sometimes so significant that there is 'no-solution' to the time-difference equations (given in equation 2.1 and equation 3.1) in the real-number-field. Hence, by identifying and discarding such time measurements, which result in a solution of the system of non-linear equations in the complex-number-field, would be advantageous in improving the accuracy of PD source localisation. Therefore, the methods for mathematically identifying the invalid time measurements for both the all-acoustic system and the combined acoustic-electrical system is presented in this chapter. The proposed methods are also applicable to UHF signals in a PD source localisation. The proposed methods will have an even greater significance with an UHF-based PD source localisation where estimated time measurements are in the range of nanoseconds.

When these invalid groups of time-delays are used for PD localisation,

- (i) non-iterative method will give a complex solution.
- (ii) iterative methods will fail to converge and give no solution as the tolerance in stopping criteria cannot be satisfied. When tolerance is not the only stopping criteria, so-

lutions are obtained when other criteria such as time limit or maximum number of iterations are reached. This results in false localisation of the PD source.

Two methods to identify the time-delay-groups which result in a complex solution for PD location are reported and analysed in this chapter,

- (i) checking the sign of the discriminant value.
- (ii) checking the multiple sign changes of the Jacobian-determinant in the iterations of Newton's method.

A method to identify the absolute-time group which result in a complex solution for PD location in a combined acoustic-electrical system is reported and analysed in this chapter. Invalid absolute-time-group can be identified by checking the sign of the discriminant value. The combined acoustic-electrical system works independent of the relative distance between the sensor and PD source. Therefore, the identification of any invalid absolute-time-group is possible by using the discriminant method alone. No alternative methods are required.

From the present study, it is not possible to identify at what percentage of error in time measurement, the solution moves from real-number-field to complex-number-field. Also, the error is added only to one time measurement in a time-delay-group or an absolute-time-group. A study can also be carried out considering error in all the time measurements in a time-delay-group or an absolute-time-group. Further study is required to arrive at a generalised conclusion on the effect of error in time measurement on accuracy of PD source localisation. However, the contribution of the present study is the development of mathematical methods to identify invalid time measurements. The proposed initial check on time measurements is important to avoid false location detection of PD and also significantly improves the accuracy in statistical PD localisation.





# Chapter 5

## Conclusions and scope for further study

### 5.1 Summary of the work

In the present study, AE detection technique is adopted to study the localisation of PDs in power transformers. The algorithms for PD localisation using the two types of acoustic location systems: (i) all-acoustic system and (ii) combined acoustic-electrical system, are studied. The laboratory experimental studies, carried out on a tank model (without barriers), to capture the AE signals from the PDs are reported. The effect of error in time measurement on the accuracy of PD localisation is also studied.

#### 5.1.1 Algorithms for PD localisation using all-acoustic system

The implementation of Newton's method and non-iterative method for the AEPD source localisation are analysed (Chapter 2). The conditions for which these methods fail to locate the position of the PD source are identified. The improvements are proposed, in implementing these methods, for a precise PD source localisation. The numerical experiments and the laboratory experiments are conducted to verify the efficacy of these methods in AEPD source localisation.

## **5.1.2 Algorithms for PD localisation using combined acoustic-electrical system**

A non-iterative method is devised for PD source localisation using the combined acoustic-electrical system, which can overcome some lacunae identified in the existing algorithms (Chapter 3). The guidelines for the sensor placement, for the reliable implementation of this newly proposed method, are also suggested. In addition, the effect of the PD source position on the performance of the proposed method is analysed. The efficacy of the proposed method is verified by applying it to the experimental data published in Al-Masri *et al.* (2016a). The performance of the proposed non-iterative method is compared with that of Newton's method and hybrid method (iterative methods).

## **5.1.3 Effect of error in time measurement on PD source localisation**

The effect of error in time-delay measurement on all-acoustic system and the effect of error in absolute-time measurement on combined acoustic-electrical system are analysed (Chapter 4). The methods for mathematically identifying the invalid time-delay and absolute-time measurements are formulated. The efficacy of these proposed methods are verified by applying it to the experimental data published in literature (Lu *et al.* 2000; Phung *et al.* 2001).

## **5.2 Important conclusions of the present study**

### **5.2.1 Conclusions from the study of algorithms used for an all-acoustic system**

- When using Newton's method for AEPD source localisation in an all-acoustic system,
  - The difficulty in identifying an efficient initial guess is solved by proposing

a hybrid method. In the hybrid method, an efficient initial guess is identified for Newton's method using the GA.

- The occurrence of a singular Jacobian matrix is prevented by proper acoustic sensor positioning on the tank wall and a careful initial guess selection.
  - The efficacy of the proposed improvements are demonstrated via numerical and laboratory experiments. In numerical experiments, when localising the PD source using Newton's method, the distance error observed in one of the trials is 243.68% (worst case error) for one of the PD source position. Whereas, the worst case error in PD source localisation is 7.94% when using hybrid method. In laboratory experiments, when localising the PD source using Newton's method, the worst case error is 23.00%. Whereas, the worst case error in PD source localisation is 0.45% when using hybrid method. The Jacobian matrix does not become singular in any of the trials, as the sensors are placed based on the proposed sensor positioning guidelines.
- An extension is proposed for the existing non-iterative method, used for AEPD source localisation in an all-acoustic system, which works for any time-delays (including zero time-delay).
    - The efficacy of the proposed extension is demonstrated via numerical and laboratory experiments.
    - In numerical experiments, when theoretically estimated time-delays are used, the proposed non-iterative method has zero distance error. Whereas, it goes more than 1% for Newton's method and hybrid method. The computational time required for the proposed non-iterative method (in the range of tens of ms) is significantly less compared to Newton's method (in the order of seconds) and hybrid method (in the order of tens of seconds).
    - In laboratory experiments, conducted on a tank model (without barriers), the proposed non-iterative method has less than 1% distance error. Whereas, it

goes more than 1% for Newton's method. The computational time required for the proposed non-iterative method (less than 1 s) is significantly less compared to Newton's method (in the order of seconds) and hybrid method (in the order of tens of seconds).

Thus, the proposed non-iterative method has better performance in terms of accuracy and computational time.

### **5.2.2 Conclusions from the study of proposed non-iterative algorithm used for a combined acoustic-electrical system**

- A non-iterative method for the PD source localisation in a power transformer using a combined acoustic-electrical system is devised and tested.
  - The non-iterative method presented is independent of the relative distances between the sensors and the PD source.
  - The devised method being non-iterative does not have any convergence problem and does not require any initial guesses. When applied to data from published literature, Newton's method does not converge for one of the absolute-time-group. Whereas, the hybrid method and proposed non-iterative method had no convergence problem and resulted in same localisation accuracy.
  - The computational time required for the non-iterative method (in the range of ms) is significantly less compared to Newton's method (in the order of seconds) and hybrid method (in the order of tens of seconds).

Thus, the proposed non-iterative method has better performance in terms of accuracy and computational time.

### **5.2.3 Conclusions from the study of effect of error in time measurement**

- The effect of error in time measurement on the accuracy of the AEPD source localisation is studied and it is found that:
  - When invalid time measurements are used for PD localisation,
    - (i) Non-iterative method will give a complex solution.
    - (ii) Iterative methods will fail to converge and give no solution as the tolerance in stopping criteria cannot be satisfied. When tolerance is not the only stopping criteria, solutions are obtained when other criteria such as time limit or maximum number of iterations are reached, resulting in false PD localisation.
  - Therefore, two methods, to identify such invalid time measurements which result in a complex solution for PD location, are devised and proposed,
    - (i) Checking the sign of the discriminant value.
    - (ii) Checking the multiple sign changes of the Jacobian-determinant in the iterations of Newton's method.

## **5.3 Contributions**

The contributions of the present study reported in the thesis are as follows:

- A hybrid method is proposed combining both the GA and the Newton's method for AEPD source localisation.
- An extension to the time-difference approach based non-iterative method for an all-acoustic system is proposed, so that it works even for the cases with zero time-differences.

- A non-iterative method for the combined acoustic-electrical PD-locator-system is devised and presented for the first time.
- The methods for mathematically identifying the invalid time measurements are developed for the first time.

## **5.4 Scope for further study**

- Developing a method to identify actual PD location from the two available solutions, in the case of non-iterative method for all-acoustic system, when both the solutions are within the tank and all the unknown quantities are positive.
- To quantify the percentage error in time measurement at which the solution moves from real-number-field to complex-number-field.
- To identify erroneous time-measurement, although the solution is in real-number-field.
- To localise the PD source positions, using the existing algorithms and also the proposed non-iterative algorithm, when there are multiple PDs present in the transformer.
- To estimate AEPD source location using other algorithms like PSO, pattern recognition method, etc., and to compare it with the proposed non-iterative methods.
- To test the proposed AEPD source localisation methods on laboratory transformer models with barriers and on actual transformers.

## References

Akbari, A., Werle, P., Akbari, M., and Mirzaei, H. R. (2016). "Challenges in calibration of the measurement of partial discharges at ultrahigh frequencies in power transformers." *IEEE Electr. Insul. Mag.*, 32(2), 27 - 34.

Al-Masri, W. M. F., Abdel-Hafez, M. F., and El-Hag, A. H. (2016a). "A novel bias detection technique for partial discharge localization in oil insulation system." *IEEE Trans. Instrum. Meas.*, 65(2), 448 - 457.

Al-Masri, W. M. F., Abdel-Hafez, M. F., and El-Hag, A. H. (2016b). "Toward high accuracy estimation of partial discharge location." *IEEE Trans. Instrum. Meas.*, 65(9), 2145 - 2153.

Ariastina, W. G. and Blackburn, T. R. (2001). "Comparison of measured PDs in oil-impregnated insulation using different sensor bandwidths." *Proc., Int. Symp. on Electrical and Insulating Materials (ISEIM)*, Himeji, Japan, 864 - 867.

Arvind, D., Khushdeep, S., and Deepak, K. (2008). "Condition monitoring of power transformer: A review." *Proc., IEEE/PES Transmission and Distribution Conference and Exposition*, Chicago, IL, USA, 1 - 6.

Aschenbrenner, D. and Kranz, H. G. (2005). "Online PD measurements and diagnosis on power transformers." *IEEE Trans. Dielectr. Electr. Insul.*, 12(2), 216 - 222.

Bartnikas, R. (2002). "Partial discharges. their mechanism, detection and measurement." *IEEE Trans. Dielectr. Electr. Insul.*, 9(5), 763 - 808.

Bengtsson, C. (1996). "Status and trends in transformer monitoring." *IEEE Trans. Power Del.*, 11(3), 1379 - 1384.

Birlasekaran, S., Choi, S. S., and Liew, A. C. (1998). "Overview of diagnostic and condition monitoring techniques for in-service power apparatus." *Proc., Int. Conf. on Energy Management and Power Delivery (EMPD)*, Singapore, 673 - 678.

Biswas, S., Dey, D., Chatterjee, B., and Chakravorti, S. (2016). "Cross-spectrum analysis based methodology for discrimination and localization of partial discharge source using acoustic sensors." *IEEE Trans. Dielectr. Electr. Insul.*, 23(6), 3556 - 3565.

Biswas, S., Koley, C., Chatterjee, B., and Chakravorti, S. (2012). "A methodology for identification and localization of partial discharge sources using optical sensors." *IEEE Trans. Dielectr. Electr. Insul.*, 19(1), 18 - 28.

Blackburn, T. R., James, R. E., Su, Q., Phung, T., Tychsen, R., and Simpson, J. (1991). "An improved electric/acoustic method for the location of partial discharges in power transformers." *Proc., 3<sup>rd</sup> Int. Conf. on Properties and Applications of Dielectric Materials*, Tokyo, Japan, 1132 - 1135.

Boczar, T. (2001). "Identification of a specific type of PD from acoustic emission frequency spectra." *IEEE Trans. Dielectr. Electr. Insul.*, 8(4), 598 - 606.

Boczar, T. (2005). "Time-frequency analysis of the acoustic emission pulses generated by multi-source partial discharges in oil." *Proc., IEEE Int. Conf. on Dielectric Liquids (ICDL)*, Coimbra, Portugal, 265 - 268.

Boczar, T., Borucki, S., Cichon, A., and Zmarzly, D. (2009). "Application possibilities of artificial neural networks for recognizing partial discharges measured by the



acoustic emission method.” *IEEE Trans. Dielectr. Electr. Insul.*, 16(1), 214 - 223.

Boczar, T. and Zmarzly, D. (2004). “Application of wavelet analysis to acoustic emission pulses generated by partial discharges.” *IEEE Trans. Dielectr. Electr. Insul.*, 11(3), 433 - 449.

Boya, C., Ruiz-Llata, M., Posada, J., and Garcia-Souto, J. A. (2015). “Identification of multiple partial discharge sources using acoustic emission technique and blind source separation.” *IEEE Trans. Dielectr. Electr. Insul.*, 22(3), 1663 - 1673.

Búa-Núñez, I., Posada-Román, J. E., Rubio-Serrano, J., and Garcia-Souto, J. A. (2014). “Instrumentation system for location of partial discharges using acoustic detection with piezoelectric transducers and optical fiber sensors.” *IEEE Trans. Instrum. Meas.*, 63(5), 1002 - 1013.

Cavallini, A., Chen, X., Montanari, G. C., and Ciani, F. (2010). “Diagnosis of EHV and HV transformers through an innovative partial-discharge-based technique.” *IEEE Trans. Power Del.*, 25(2), 814 - 824.

Chan, J. C., Ma, H., and Saha, T. K. (2014). “Automatic blind equalization and thresholding for partial discharge measurement in power transformer.” *IEEE Trans. Power Del.*, 29(4), 1927 - 1938.

Chan, J. C., Ma, H., and Saha, T. K. (2015). “Hybrid method on signal de-noising and representation for online partial discharge monitoring of power transformers at substations.” *IET- Sci. Meas. Technol.*, 9(7), 890 - 899.

Chen, L. J., Lin, W. M., Tsao, T. P., and Lin, Y. H. (2007). “Study of partial discharge measurement in power equipment using acoustic technique and wavelet transform.” *IEEE Trans. Power Del.*, 22(3), 1575 - 1580.

Cheney, E. and Kincaid, D. (2007). *Numerical Mathematics and Computing*, Thomson Higher Education, Belmont, CA, USA .

Coenen, S. and Tenbohlen, S. (2012). "Location of PD sources in power transformers by UHF and acoustic measurements." *IEEE Trans. Dielectr. Electr. Insul.*, 19(6), 1934 - 1940.

Olivieri, M. M., Mannheimer, W. A., and Ripper-Neto, A. P. (2000). "On the use of acoustic signals for detection and location of partial discharges in power transformers." *Proc., IEEE Int. Symp. on Electrical Insulation*, Anaheim, CA, USA, 259 - 262.

Castro, B. A., de Melo Brunini, D., Baptista, F. G., Andreoli, A. L., and Ulson, J. A. C. (2017). "Assessment of macro fiber composite sensors for measurement of acoustic partial discharge signals in power transformers." *IEEE Sensors J.*, 17(18), 6090 - 6099.

Dhole, P., Sinha, T., Nayak, S., Kundu, P., and Kishore, N. (2008). "Analysis of propagation paths of partial discharge acoustic emission signals." *Proc., 15<sup>th</sup> Nat. Power Syst. Conference (NPSC)*, IIT-Bombay, Mumbai, India.

Eleftherion, P. M. (1995). "Partial discharge. XXI. acoustic emission based PD source location in transformers." *IEEE Electr. Insul. Mag.*, 11(6), 22 - 26.

Fabiani, D. and Montanari, G. C. (2001). "The effect of voltage distortion on ageing acceleration of insulation systems under partial discharge activity." *IEEE Electr. Insul. Mag.*, 17(3), 24 - 33.

Fuhr, J., Haessig, M., Boss, P., Tschudi, D., and King, R. A. (1993). "Detection and location of internal defects in the insulation of power transformers." *IEEE Trans. Electr. Insul.*, 28(6), 1057 - 1067.

Ghosh, R., Chatterjee, B., and Dalai, S. (2017). "A method for the localization of partial discharge sources using partial discharge pulse information from acoustic emissions." *IEEE Trans. Dielectr. Electr. Insul.*, 24(1), 237 - 245.

Grossmann, E. and Feser, K. (2005). "Sensitive online PD-measurements of onsite oil/paper-insulated devices by means of optimized acoustic emission techniques (aet)." *IEEE Trans. Power Del.*, 20(1), 158 - 162.

Han, Y. and Song, Y. H. (2003). "Condition monitoring techniques for electrical equipment- a literature survey." *IEEE Trans. Power Del.*, 18(1), 4-13.

Harbaji, M., Shaban, K., and El-Hag, A. (2015). "Classification of common partial discharge types in oil-paper insulation system using acoustic signals." *IEEE Trans. Dielectr. Electr. Insul.*, 22(3), 1674 - 1683.

Harrold, R. T. (1979a). "Acoustic waveguides for sensing and locating electrical discharges in high voltage power transformers and other apparatus." *IEEE Trans. Power App. Syst.*, PAS-98(2), 449 - 457.

Harrold, R. T. (1979b). "Acoustical techniques for detecting and locating electrical discharges." *Corona Measurement and Interpretation*, ASTM, PA, USA, 327 - 408.

Harrold, R. T. (1985). "Acoustical technology applications in electrical insulation and dielectrics." *IEEE Trans. Electr. Insul.*, EI-20(1), 3 - 19.

Harrold, R. T. (1986). "Acoustic theory applied to the physics of electrical breakdown in dielectrics." *IEEE Trans. Electr. Insul.*, EI-21(5), 781 - 792.

Hekmati, A. and Hekmati, R. (2017). "Optimum acoustic sensor placement for par-

tial discharge allocation in transformers.” *IET - Sci. Meas. Technol.*, 11(5), 581 - 589.

Hirsch, M., Smale, S., and Devaney, R. (2004). “Differential Equations, Dynamical Syst., and an Introduction to Chaos.” *Differential equations, dynamical systems, and an introduction to chaos*. Academic Press, California, USA.

Homaei, M., Moosavian, S. M., and Illias, H. A. (2014). “Partial discharge localization in power transformers using neuro-fuzzy technique.” *IEEE Trans. Power Del.*, 29(5), 2066 - 2076.

Hooshmand, R. A., Parastegari, M., and Yazdanpanah, M. (2013). “Simultaneous location of two partial discharge sources in power transformers based on acoustic emission using the modified binary partial swarm optimisation algorithm.” *IET - Sci. Meas. Technol.*, 7(2), 112 - 118.

Howells, E. and Norton, E. T. (1981). “Location of partial discharge sites in on-line transformers.” *IEEE Trans. Power App. Syst.*, PAS-100(1), 158–162.

Howells, E. and Norton, E. T. (1984). “Parameters affecting the velocity of sound in transformer oil.” *IEEE Trans. Power App. Syst.*, PAS-103(5), 1111 - 1115.

Huang, Y., Benesty, J., Elko, G. W., and Mersereati, R. M. (2001). “Real-time passive source localization: a practical linear-correction least-squares approach.” *IEEE Trans. Speech Audio Process.*, 9(8), 943 - 956.

Hucker, T. and Krantz, H. G. (1995). “Requirements of automated PD diagnosis systems for fault identification in noisy conditions.” *IEEE Trans. Dielectr. Electr. Insul.*, 2(4), 544 - 556.

Hussein, R., Shaban, K. B., and El-Hag, A. H. (2016). “Denoising of acoustic partial

discharge signals corrupted with random noise.” *IEEE Trans. Dielectr. Electr. Insul.*, 23(3), 1453 - 1459.

Hussein, R., Shaban, K. B., and El-Hag, A. H. (2017). “Robust feature extraction and classification of acoustic partial discharge signals corrupted with noise.” *IEEE Trans. Instrum. Meas.*, 66(3), 405 - 413.

Hussein, R., Shaban, K. B., and El-Hag, A. H. (2018). “Denoising different types of acoustic partial discharge signals using power spectral subtraction.” *High Voltage*, 3(1), 44–50.

IEC 60270 (2000). “*High-voltage test techniques - partial discharge measurements.*” 1 - 45.

IEEE Std C57.104 (2009). “*IEEE guide for the interpretation of gases generated in oil-immersed transformers.*” 1 - 36.

IEEE Std C57.127 (2007). “*IEEE guide for the detection and location of acoustic emissions from partial discharges in oil-immersed power transformers and reactors.*” 1 - 47.

IEEE Std C57.143 (2012). “*IEEE guide for application for monitoring equipment to liquid-immersed transformers and components.*” 1 - 83.

Jacob, N. D., McDermid W. M., and Kordi, B. (2012). “On-line monitoring of partial discharges in a HVDC station environment.” *IEEE Trans. Dielectr. Electr. Insul.*, 19(3), 925 -935.

Janani, H., Kordi, B., and Jozani, M. J. (2017). “Classification of simultaneous multiple partial discharge sources based on probabilistic interpretation using a two-step logistic regression algorithm.” *IEEE Trans. Dielectr. Electr. Insul.*, 24(1), 54 - 65.

Kanakambaran, S., Sarathi, R., and Srinivasan, B. (2017). "Identification and localization of partial discharge in transformer insulation adopting cross recurrence plot analysis of acoustic signals detected using fiber bragg gratings." *IEEE Trans. Dielectr. Electr. Insul.*, 24(3), 1773 - 1780.

Karr, C. L., Weck, B., and Freeman, L. M. (1998). "Solutions to systems of nonlinear equations via a genetic algorithm." *Eng. Appl. of Artificial Intell.*, 11(3), 369 - 375.

Khanali, M., Jayaram, S., and Cheng, J. (2013). "Effects of voltages with high-frequency contents on the transformer insulation properties." *Proc., IEEE Electrical Insulation Conference (EIC)*, Ottawa, Ontario, Canada, 235 - 238.

Kraetge, A., Hoek, S., Koch, M., and Koltunowicz, W. (2013). "Robust measurement, monitoring and analysis of partial discharges in transformers and other HV apparatus." *IEEE Trans. Dielectr. Electr. Insul.*, 20(6), 2043 - 2051.

Kruger, T. and Patsch, R. (2003). "Active noise reduction for partial discharge measurement in the frequency domain." *Proc., IEEE Bologna Power Tech Conference*, Bologna, Italy, 3 - 8.

Kumar, A. S., Gupta, R. P., Udayakumar, K., and Venkatasami, A. (2008). "Online partial discharge detection and location techniques for condition monitoring of power transformers: A review." *Proc., Int. Conf. on Condition Monitoring and Diagnosis*, Beijing, China, 927 - 931.

Kundu, P., Kishore, N. K, and Sinha, A. K. (2012). "Identification of two simultaneous partial discharge sources in an oil-pressboard insulation system using acoustic emission techniques." *Appl. Acoust.*, 73(4), 395 - 401.

Kundu, P., Kishore, N. K., and Sinha, A. K. (2007). "Wavelet based fractal analyzing method of partial discharge acoustic emission signal." *Proc., Int. Conf. on Industrial and Information Systems*, Penadeniya, Sri Lanka, 357 - 360.

Kundu, P., Kishore, N. K., and Sinha, A. K. (2009). "A non-iterative partial discharge source location method for transformers employing acoustic emission techniques." *Appl. Acoust.*, 70(11), 1378 - 1383.

Kurz, J., Markalous, S., Grosse, C., and Reinhardt, H. (2005). "New approaches for three dimensional source location-examples from acoustic emission analysis." *In European Geosciences Union-General Assembly*, 7.

Kweon, D. J., Chin, S. B., Kwak, H. R., Kim, J. C., and Song, K. B. (2005). "The analysis of ultrasonic signals by partial discharge and noise from the transformer." *IEEE Trans. Power Del.*, 20(3), 1976 - 1983.

Lalitha, E. M. and Satish, L. (2000). "Wavelet analysis for classification of multi-source PD patterns." *IEEE Trans. Dielectr. Electr. Insul.*, 7(1), 40 - 47.

Lee, C. H., Chiu, M. Y., Huang, C. H., Yen, S. S., and Fan, C. L. (2008). "Characteristics analysis of sensors for on-line partial discharge measurement." *Int. Conf. on Condition Monitoring and Diagnosis*, Beijing, China, 1275 - 1278.

Leibfried, T. (1998). "Online monitors keep transformers in service." *IEEE Comput. Appl. Power*, 11(3), 36 -42.

Li, J., Xutao, H., Liu, Z., and Yao, X. (2016). "A novel GIS partial discharge detection sensor with integrated optical and UHF methods." *IEEE Trans. Power Del.*, 33(4), 2047 - 2049.

Li, X., Deng, Z. D., Rauchenstein, L. T., and Carlson, T. J. (2016b). “Contributed review: Source-localization algorithms and applications using time of arrival and time difference of arrival measurements.” *Review of Scientific Instruments*, 87(4), 041502: 1 - 12.

Liu, H.-L. (2016). “Acoustic partial discharge localization methodology in power transformers employing the quantum genetic algorithm.” *Appl. Acoust.*, 102, 71–78.

Lu, Y., Tan, X., and Hu, X. (2000). “PD detection and localisation by acoustic measurements in an oil-filled transformer.” *IEE Proc., Sci. Meas. Technol.*, 147(2), 81 - 85.

Lundgaard, L. E. (1992a). “Partial discharge. XIII. acoustic partial discharge detection fundamental considerations.” *IEEE Electr. Insul. Mag.*, 8(4), 25 - 31.

Lundgaard, L. E. (1992b). “Partial discharge. XIV. acoustic partial discharge detection practical application.” *IEEE Electr. Insul. Mag.*, 8(5), 34 - 43.

Lundgaard, L. E., Hansen, W., and Dursun, K. (1989). “Location of discharges in power transformers using external acoustic sensors.” *Proc., 6<sup>th</sup> Int. Symp. on High Voltage Engineering*, New Orleans, LA, USA, 1 - 4

Lundgaard, L. E., Hansen, W., Linhjell, D., and Painter, T. J. (2004). “Aging of oil-impregnated paper in power transformers.” *IEEE Trans. Power Del.*, 19(1), 230 - 239.

Ma, G. M., Zhou, H. Y., Shi, C., Li, Y. B., Zhang, Q., Li, C. R., and Zheng, Q. (2018). “Distributed partial discharge detection in a power transformer based on phase-shifted fbg.” *IEEE Sensors J.*, 18(7), 2788 - 2795.

Ma, X., Zhou, C., and Kemp, I. J. (2002). “Interpretation of wavelet analysis and its application in partial discharge detection.” *IEEE Trans. Dielectr. Electr. Insul.*, 9(3),



446 - 457.

Mondal, M., Kumbhar, G. B., and Kulkarni, S. V. (2018). "Localization of partial discharges inside a transformer winding using a ladder network constructed from terminal measurements." *IEEE Trans. Power Del.*, 33(3), 1035 - 1043.

Markalous, S. M. and Feser, K. (2004). "All-acoustic PD measurements of oil/paper-insulated transformers for PD-localization." *Proc., 2<sup>nd</sup> Int. Conf. on Advances in Processing, Testing and Application of Dielectric Materials*, Wroclaw, Poland.

Markalous, S. M., Tenbohlen, S., and Feser, K. (2005). "New robust non-iterative algorithms for acoustic PD-localization in oil/paper-insulated transformers." *Proc., 14<sup>th</sup> Int. Symp. on high voltage engineering*, Beijing, China, 29.

Markalous, S. M., Tenbohlen, S., and Feser, K. (2008). "Detection and location of partial discharges in power transformers using acoustic and electromagnetic signals." *IEEE Trans. Dielectr. Electr. Insul.*, 15(6), 1576 - 1583.

Mathworks (2011). *Global optimization toolbox: User's guide* (R2010b).

Meunier, R. and Vaillancourt, G. H. (1996). "Propagation behaviour of acoustic partial discharge signals in oil-filled transformers." *proc., Int. Conf. on Conduction and Breakdown in Dielectric Liquids*, Roma, Italy, 401 - 404.

Mirzaei, H. R., Akbari, A., Gockenbach, E., and Miralikhani, K. (2015). "Advancing new techniques for UHF PD detection and localization in the power transformers in the factory tests." *IEEE Trans. Dielectr. Electr. Insul.*, 22(1), 448 - 455.

Mirzaei, H. R., Akbari, A., Gockenbach, E., Zanjani, M., and Miralikhani, K. (2013). "A novel method for ultra-high-frequency partial discharge localization in power trans-

formers using the particle swarm optimization algorithm.” *IEEE Electr. Insul. Mag.*, 29(2), 26 - 39.

Mohammadi, E., Niroomand, M., Rezaeian, M., and Amini, Z. (2009). “Partial discharge localization and classification using acoustic emission analysis in power transformer.” *Proc., 31<sup>st</sup> Int. Telecommunications Energy Conference*, Incheon, South Korea, 1 - 6.

Montanari, G. C., Morshuis, P., and Cervi, A. (2015). “Monitoring HV transformer conditions: The strength of combining various diagnostic property observations.” *Proc., IEEE Electr. Insul. Conf. (EIC)*, Seattle, WA, USA, 141 - 144.

Muthanna, K. T., Sarkar, A., Das, K., and Waldner, K. (2006). “Transformer insulation life assessment.” *IEEE Trans. Power Del.*, 21(1), 150 - 156.

Nagamani, H. N., Shanker, T. B., Vaidhyathan, V., and Neelakantan, S. (2005). “Acoustic emission technique for detection and location of simulated defects in power transformers.” *IEEE Russia Power Tech*, 1 - 7.

Nattrass, D. A. (1988). “Partial discharge measurement and interpretation.” *IEEE Electr. Insul. Mag.*, 4(3), 10 - 23.

Niemeyer, L. (1995). “A generalized approach to partial discharge modeling.” *IEEE Trans. Dielectr. Electr. Insul.*, 2(4), 510 - 528.

Novak, J. P. and Bartnikas, R. (2000). “Effect of dielectric surfaces on the nature of partial discharges.” *IEEE Trans. Dielectr. Electr. Insul.*, 7(1), 146 - 151.

Okubo, H., Hayakawa, N., and Matsushita, A. (2002). “The relationship between partial discharge current pulse waveforms and physical mechanisms.” *IEEE Electr. Insul.*

*Mag.*, 18(3), 38 - 45.

Padovan, J. and Arechaga, T. (1982). "Formal convergence characteristics of elliptically constrained incremental newton-raphson algorithms." *Int. J. of Engineering Sci.*, 20(10), 1077 - 1097.

Park, D. W., Cho, H. E., Cha, S. W., and Kil, G. S. (2012). "Positioning of partial discharge origin by acoustic signal detection in insulation oil." *J. of Int. Council Electr. Eng.*, 2(1), 28 - 32.

Peyraque, L., Boisdon, C., Beroual, A., and Buret, F. (1995). "Static electrification and partial discharges induced by oil flow in power transformers." *IEEE Trans. Dielectr. Electr. Insul.*, 2(1), 40 - 45.

Phung, B. T., Blackburn, T. R., and Liu, Z. (2001). "Acoustic measurements of partial discharge signals." *J. of Electr. Electron. Eng.*, Australia, 21(1), 41 - 47.

Pompili, M., Mazzetti, C., and Bartnikas, R. (2005). "Partial discharge pulse sequence patterns and cavity development times in transformer oils under AC conditions." *IEEE Trans. Dielectr. Electr. Insul.*, 12(2), 395 - 403.

Punekar, G. S., Antony, D., Bhavanishanker, T., Nagamani, H. N., and Kishore, N. K. (2013). "Genetic algorithm in location identification of AEPD source: Some aspects." *Proc., IEEE 1<sup>st</sup> Int. Conf. on Condition Assessment Techniques in Electr.Syst. (CATCON)*, kolkatta, India, 386 - 390.

Punekar, G. S., Jadhav, P., Bhavani, S. T., and Nagamani, H. N. (2012). "Some aspects of location identification of PD source using ae signals by an iterative method." *Proc., IEEE 10<sup>th</sup> Int. Conf. on the Properties and Appl. of Dielectric Materials*, Bangalore, India, 1 - 4.

Purkait, P. and Chakravorti, S. (2003). "Impulse fault classification in transformers by fractal analysis." *IEEE Trans. Dielectr. Electr. Insul.*, 10(1), 109 - 116.

Reeves, C. and Rowe, J. (2002). "Genetic Algorithms: Principles and Perspectives: A Guide to GA Theory." *Operations Research/Comput. Sci. Interfaces Series*. Springer US.

Richeng, L., Kai, B., and Xuehai, G. (2008). "Partial discharges multi-targets localization in power transformers based on spatial-estimation." *Proc., Int. Conf. on Condition Monitoring and Diagnosis*, Beijing, China, 509 - 512.

Rubio-Serrano, J., Rojas-moreno, M. V., Posada, J., Martinez-tarifa, J. M., Robles, G., and Garcia-souto, J. A. (2012). "Electro-acoustic detection, identification and location of partial discharge sources in oil-paper insulating systems." *IEEE Trans. Dielectr. Electr. Insul.*, 19(5), 1569 - 1578.

Saha, T. K. (2003). "Review of modern diagnostic techniques for assessing insulation condition in aged transformers." *IEEE Trans. Dielectr. Electr. Insul.*, 10(5), 903 - 917.

Sarkar, B., Mishra, D. K., Koley, C., Roy, N. K., and Biswas, P. (2016). "Intensity modulated fiber bragg grating sensor for detection of partial discharges inside high voltage apparatus." *IEEE Sensors J.*, 16(22), 7950 - 7957.

Satish, L. and Zaengl, W. S. (1995). "Can fractal features be used for recognizing 3-d partial discharge patterns?" *IEEE Trans. Dielectr. Electr. Insul.*, 2(3), 352 - 359.

Sharkawy, R. M., Abdel-Galil, T. K., Mangoubi, R. S., Salama, M. M., and Bartnikas, R. (2008). "Particle identification in terms of acoustic partial discharge measurements

in transformer oils." *IEEE Trans. Dielectr. Electr. Insul.*, 15(6), 1649 - 1656.

Shim, I., Soraghan, J. J., and Siew, W. H. (2000). "Digital signal processing applied to the detection of partial discharge: an overview." *IEEE Electr. Insul. Mag.*, 16(3), 6 - 12.

Sinaga, H. H., Phung, B. T., and Blackburn, T. R. (2012). "Partial discharge localization in transformers using UHF detection method." *IEEE Trans. Dielectr. Electr. Insul.*, 19(6), 1891 - 1900.

Singh, J., Sood, Y. R., and Jarial, R. K. (2008). "Condition monitoring of power transformers - bibliography survey." *IEEE Electr. Insul. Mag.*, 24(3), 11 - 25.

Stone, G. C. (1991). "Partial discharge. VII. practical techniques for measuring PD in operating equipment." *IEEE Electr. Insul. Mag.*, 7(4), 9 - 19.

Stone, G. C. (2005). "Partial discharge diagnostics and electrical equipment insulation condition assessment." *IEEE Trans. Dielectr. Electr. Insul.*, 12(5), 891 - 904.

Strang, G. (1980). "Linear Algebra and Its Applications" Cengage Learning, New Delhi, India.

Su, C. C., Tai, C. C., Chen, C. Y., Hsieh, J. C., and Chen, J. F. (2008). "Partial discharge detection using acoustic emission method for a waveguide functional high voltage cast-resin dry-type transformer." *Proc., Int. Conf. on Condition Monitoring and Diagnosis*, Beijing, China, 517 - 520.

Tanaka, T., Okamoto, T., Nakanishi, K., and Miyamoto, T. (1993). "Aging and related phenomena in modern electric power systems." *IEEE Trans. Electr. Insul.*, 28(5), 826 - 844.

Tang, J. and Xie, Y. (2011). "Partial discharge location based on time difference of energy accumulation curve of multiple signals." *IET Electric Power Appl.*, 5(1), 175 - 180.

Tang, L., Wu, Z., Li, H., and Nie, D. (1996). "Location of partial discharges in power transformers using computer-aided acoustic techniques." *Canadian J. Electr. Comput. Eng.*, 21(2), 67 - 71.

Tang, Z., Li, C., Cheng, X., Wang, W., Li, J., and Li, J. (2006). "Partial discharge location in power transformers using wideband RF detection." *IEEE Trans. Dielectr. Electr. Insul.*, 13(6), 1193 - 1199.

Veloso, G. C., da Silva, L. B., Lambert-Torres, G., and Pinto, J. (2006). "Localization of partial discharges in transformers by the analysis of the acoustic emission." *Proc., IEEE Int. Symp. on Industrial Electronics*, Montreal, Que., Canada, 537 - 541.

Venkatesh, A. S. P., Danikas, M. G., and Sarathi, R. (2011). "Understanding of partial discharge activity in transformer oil under transient voltages adopting acoustic emission technique." *Proc., 6<sup>th</sup> Int. Conf. on Industrial and Information Syst.*, Kandy, Sri Lanka, 98 - 101.

Wang, C., Jin, X., Cheng, T. C., Zhang, S., Dong, Z., Wang, Z., Lin, D., and Zhu, D. (1997). "Analysis and suppression of interference for on-line monitoring of partial discharge of power transformers." *Proc., IEEE Annual Report Conference on Electrical Insulation and Dielectric Phenomena*, Minneapolis, MN, USA, 530 - 533.

Wang, M., Vandermaar, A. J., and Srivastava, K. D. (2002). "Review of condition assessment of power transformers in service." *IEEE Electr. Insul. Mag.*, 18(6), 12 - 25.

Wang, X., Li, B., Roman, H. T., Russo, O. L., Chin, K., and Farmer, K. R. (2006).

“Acousto-optical PD detection for transformers.” *IEEE Trans. Power Del.*, 21(3), 1068 - 1073.

Wang, X., Li, B., Xiao, Z., Russo, O. L., Roman, H. T., Chin, K., and Farmer, K. R. (2005). “Acoustic energy shifting in transformer oil at different temperatures.” *IEEE Trans. Power Del.*, 20(3), 2356 - 2357.

Wang, Y. B., Chang, D. G., Fan, Y. H., Zhang, G. J., Zhan, J. Y., Shao, X. J., and He, W. L. (2017). “Acoustic localization of partial discharge sources in power transformers using a particle-swarm-optimization-route-searching algorithm.” *IEEE Trans. Dielectr. Electr. Insul.*, 24(6), 3647 - 3656.

Ward, B. H. (2001). “A survey of new techniques in insulation monitoring of power transformers.” *IEEE Electr. Insul. Mag.*, 17(3), 16 - 23.

Xie, Q., Li, T., Tao, J., Liu, X., Liu, D., and Xu, Y. (2016). “Comparison of the acoustic performance and positioning accuracy of three kinds of planar partial discharge ultrasonic array sensors.” *IET Radar, Sonar Navigation*, 10(1), 166 - 173.

Zeng, F., Tang, J., Huang, L., and Wang, W. (2015). “A semi-definite relaxation approach for partial discharge source location in transformers.” *IEEE Trans. Dielectr. Electr. Insul.*, 22(2), 1097 - 1103.

Zheng, D., Zhang, C. X., Yang, G. Q., and Sun, X. Y. (2006). “An experiment study of partial discharge pattern recognition method based on wavelet neural networks.” *Proc., IEEE Int. Symp. on Electrical Insulation*, Toronto, Ont., Canada, 230 - 233.

Zhou, X., Zhou, C., and Kemp, I. J. (2005). “An improved methodology for application of wavelet transform to partial discharge measurement denoising.” *IEEE Trans. Dielectr. Electr. Insul.*, 12(3), 586 - 594.

Zhu, D., Tan, K., and Jin, X. (1988). "The study of acoustic emission method for detection of partial discharge in power transformer." *Proc., 2<sup>nd</sup> Int. Conf. on Properties and Applications of Dielectric Materials*, Beijing, China, 614 - 617.

Zingales, G. (2000). "The requirements of a PD measuring system analyzed in the time domain." *IEEE Trans. Dielectr. Electr. Insul.*, 7(1), 2 - 5.



List of Publications based on PhD Research Work					
Sl.No.	Title of the paper	Authors (In the same order as in the paper. Underline the Research Scholar's name)	Name of the Journal/ Conference/ Symposium, Vol., No., Pages	Month & Year of Publication	Category*
1	Noniterative Method for Combined Acoustic-Electrical Partial Discharge Source Localization	Deepthi Antony, G. S. Puneekar.	IEEE Transactions on Power Delivery vol. 33, no. 4, pp. 1679-1688. <b>DOI: <a href="https://doi.org/10.1109/TPWRD.2017.2769159">10.1109/TPWRD.2017.2769159</a></b> <b>(SCI Indexed; IF: 3.218)</b>	August, 2018	1
2	Identification of invalid time-delay-groups using discriminant and Jacobian-determinant in acoustic emission PD source localisation	Deepthi Antony, G. S. Puneekar.	IET Science, Measurement & Technology vol. 11, no. 3, pp. 315-321. <b>DOI: <a href="https://doi.org/10.1049/iet-smt.2016.0362">10.1049/iet-smt.2016.0362</a></b> <b>(SCI Indexed; IF: 1.263)</b>	May, 2017	1
3	Effects of error in time-delay on AEPD source localization using Newton's method: Numerical experimentation	Deepthi Antony, G. S. Puneekar, N. K. Kishore.	IEEE International Conference on Condition Assessment Techniques in Electrical Systems (CATCON), Ropar, November 16-18, pp. 166-169. <b>DOI: <a href="https://doi.org/10.1109/CATCON.2017.8280205">10.1109/CATCON.2017.8280205</a></b>	November, 2017	3
4	On Location Identification of AEPD Source	G. S. Puneekar, Kallappu Jyosthna, Deepthi Antony.	National Conference on High Voltage Engineering & Technology (NCHVET), Bangalore, January 27-28, pp. 238-241.	January, 2017	3
5	Improvements in AEPD location identification by removing outliers and post processing	Deepthi Antony, G. S. Puneekar.	IEEE International Conference on Condition Assessment Techniques in Electrical Systems (CATCON), Bangalore, December 10-12, pp. 66-69. <b>DOI: <a href="https://doi.org/10.1109/CATCON.2015.7449510">10.1109/CATCON.2015.7449510</a></b>	December, 2015	3
6	Improvements in an Iterative Method for Localization of Partial Discharge Source in Oil Insulation	Deepthi Antony, G. S. Puneekar, N. K. Kishore.	Electrostatics Joint Conference, Boston, USA, June 18-20.	June, 2018**	3
<p>*Category: 1: Journal paper, full paper reviewed 2: Journal paper, Abstract reviewed 3: Conference/Symposium paper, full paper reviewed 4: Conference/Symposium paper, abstract reviewed 5: others (including papers in Workshops, NITK Research Bulletins, Short notes etc.)</p> <p>**Awarded 1<sup>st</sup> place in student paper competition.</p>					
<b>Research Scholar</b> Name & Signature, with Date			<b>Research Guide</b> Name & Signature, with Date		

<b>List of other Related Publications</b>					
<b>Sl.No.</b>	<b>Title of the paper</b>	<b>Authors</b> (In the same order as in the paper. Underline the Research Scholar's name)	<b>Name of the Journal/ Conference/ Symposium, Vol., No., Pages</b>	<b>Month &amp; Year of Publication</b>	<b>Category*</b>
7	Effects of Transformer-oil Temperature on Amplitude and Peak Frequency of Partial Discharge Acoustic Signals	T. B. Shanker, H. N. Nagamani, Deepthi Antony, G. S. Puneekar.	IEEE Transactions on Power Delivery <b>DOI: <a href="#">10.1109/TPWRD.2018.2799489</a></b> ( <b>SCI Indexed; IF: 3.218</b> )	In press	1
8	On choice of velocity for acoustic-emission linear-source-localization in metallic medium	Deepthi Antony, P. Sahoo, G. S. Puneekar.	The Journal of CPRI Vol. II, No.4, pp.689-696.	December, 2015	1
9	Case Studies on Transformer Fault Diagnosis using Dissolved Gas Analysis	T. B. Shanker, H. N. Nagamani, Deepthi Antony, G. S. Puneekar.	IEEE PES Asia-Pacific Power and Energy Engineering Conference (APPEEC), Bangalore, November 8-10, pp. 1-3. <b>DOI: <a href="#">10.1109/APPEEC.2017.8309010</a></b>	November, 2017	3
10	Effects of error in acoustic velocity on partial discharge localization in power transformers over its working temperature range	G. S. Puneekar, Deepthi Antony, A. Aiswarya, T. B. Shanker.	National Conference on Condition Monitoring (NCCM), Kalpakkam, October 26-27, p. 3A-D.	October, 2017	3
11	Acoustic Emission Partial Discharge Source Localization: Number of Sensors versus Accuracy	Deepthi Antony, A. Aiswarya, G. S. Puneekar.	International Engineering Symposium - IES Kumamoto University, Japan, March 7-9, p. K2-2.	March, 2018	3
<p>*Category: 1: Journal paper, full paper reviewed 2: Journal paper, Abstract reviewed 3: Conference/Symposium paper, full paper reviewed 4: Conference/Symposium paper, abstract reviewed 5: others (including papers in Workshops, NITK Research Bulletins, Short notes etc.) (If the paper has been accepted for publication but yet to be published, the supporting documents must be attached.)</p>					
<b>Research Scholar</b> Name & Signature, with Date			<b>Research Guide</b> Name & Signature, with Date		

## BIODATA

### Deepthi Antony

Research Scholar, Department of Electrical and Electronics Engineering,  
NITK Surathkal-575025, Karnataka, India.  
Emails: deepthi1717@gmail.com, ee14f06.deepthi@nitk.edu.in  
Phone: +91 8277405696

### Permanent address

Alappattu House,  
Sanathanam ward,  
Alappuzha-688001, Kerala, India

### ACADEMIC CHRONICLE

- **Doctor of Philosophy** (pursuing) in Electrical Engineering at National Institute of Technology Karnataka, Surathkal (9.69 CGPA)
- **Master of Technology** (2013) in Power & Energy Systems at National Institute of Technology Karnataka, Surathkal (8.49 CGPA)
- **Bachelor of Engineering** (2010) in Electrical & Electronics Engineering at Anna University, Chennai (83.33%)
- **Higher Secondary Education** (2006, State Board) at St. Joseph's Girls Higher Secondary School, Kerala (91.6%)
- **Secondary Education** (2004, State Board) at St. Joseph's Girls Higher Secondary School, Kerala (92.3%)

### EXPERIENCE

**Teaching:** Assistant Professor in the Department of Electrical and Electronics Engineering at SCMS School of Engineering & Technology, Kerala (1.5 years)

### RESEARCH AREA:

High voltage Engineering - Non-destructive testing (Acoustic emission testing) of power transformers

### COMPUTER PROFICIENCY:

**Packages:** MATLAB, PSpice, Latex

**Platforms Used:** Windows, Ubuntu

**Course:** Completed a course titled Swift C++ with Distinction from NIIT.

### PUBLICATIONS BASED ON DOCTORAL RESEARCH

- Given in List of Publications; Pages A and B. Number of Journal publications: 4; Number of Conference publications: 7.

### PUBLICATIONS BASED ON M.TECH RESEARCH

- Gururaj S Punekar, Deepthi Antony, T. Bhavani Shanker, H. N. Nagamani and Kishore N. K., "Genetic algorithm in location identification of AEPD source: Some aspects", **IEEE International Conference on Condition Assessment Techniques in Electrical Systems (CATCON)**, Calcutta, 2013, pp. 386-390.

### AWARDS AND RECOGNITIONS

- 1<sup>st</sup> place in paper presentation at 2018 Joint Electrostatic Conference held at Boston University, Boston, USA during July 2018.
- Granted travel funding for attending Joint Electrostatic Conference held at Boston University, Boston, USA by Government of India through SERB under International Travel Support scheme.
- GATE score: 602; All India rank: 886 (2011).
- Electrical Engineering department topper (2006-2010, Jeppiaar Engineering College, Chennai).

### **EXTRACURRICULAR ACTIVITIES**

- Represented Kerala State, Anna University and NITK in National level Basket-ball Championship.
- Awarded Best Player (women) in 2016 All-India Inter-NIT Basketball Championship held at NIT-Jaipur.
- Bagged several prizes in district level elocution competition.

### **REFERENCES**

- *Dr. Gururaj S Punekar*, Professor, Dept.of Electrical Engg., *National Institute of Technology Karnataka*, Surathkal, Karnataka (gsp@nitk.edu.in).
- *Dr. Tangella Bhavani Shanker*, Joint Director and Quality Manager, *Central Power Research Institute*, Bangalore, India. (tbs@cpri.in).

Place : Surathkal, India

Deepthi Antony